

Supporting Information

Red-emitting Boron Difluoride Complexes with Mega-large Stokes Shift and Unexpectedly High Fluorescent Quantum Yield

Xiaojie Ren,^{‡[a, b]} Fan Zhang,^{‡[a]} Hongchen Luo,^[a] Lide Liao,^[a] Xiangzhi Song^{*[a, b]} and Wenqiang Chen^{*[c]}

^a College of Chemistry & Chemical Engineering, Central South University, Changsha, 410083, P. R. China. Email: song@rowland.harvard.edu. (Xiangzhi Song).

^b Key Laboratory of Hunan Province for Water Environment and Agriculture Product Safety, Central South University, Changsha, 410083, P. R. China.

^c College of Chemistry and Materials Science, Guangxi Key Laboratory of Natural Polymer Chemistry and Physics, Nanning Normal University, Nanning, 530001, P. R. China. Email: chenwq@csu.edu.cn. (Wenqiang Chen).

‡ These authors contributed equally to this work.

Contents

1. General methods.....	- 2 -
2. Synthesis	- 3 -
3. Photophysical properties of DE-DFOB-R, Julo-DFOB-R and TQ-DFOB-R	- 8 -
4. Theoretical calculations	- 14 -
5. Photophysical properties of compounds TQ-DFOB-R in solid state	- 16 -
6. X-ray structures of compound TQ-DFOB-Br.....	- 17 -
7. Ratiometric fluorescence response to TFA/TEA vapors.....	- 26 -
8. Cell and zebrafish culture and fluorescence imaging	- 29 -
9. NMR and HRMS spectra.....	- 30 -

1. General methods

Materials and instruments: Unless otherwise stated, all reagents were purchased from commercial suppliers and used without further purification. Solvents were purified by standard methods prior to use. Twice-distilled water was used throughout all experiments. NMR spectra were recorded on a BRUKER 500 M spectrometer, using TMS as an internal standard. All accurate mass spectrometric experiments were performed on a micro TOF-Q II mass spectrometer (Bruker Daltonik, Germany). UV-Vis absorption spectra were measured using a Shimadzu UV-2450 spectrophotometer. Emission spectra were recorded at room temperature using a HITACHI F-7000 fluorescence spectrophotometer. Fluorescence lifetimes were determined on Fluo Time 100 with Pico Quant's time-resolved spectrometer. Fluorescence microscopy was performed on an Olympus IX83 inverted microscope. TLC analysis was performed on silica gel plates and column chromatography was conducted using silica gel (mesh 200-300), both of which were obtained from Qingdao Ocean Chemicals, China. Fluorescence imaging experiments in living cells and zebrafish were performed on an Opera Phenix/Operetta CLS from PerkinElmer, Inc. All the tests were conducted at room temperature.

The fluorescent quantum yields in solution were measured on a Hitachi F-7000 spectrophotometer using a standard reference and calculated from the following equation:

$$\Phi_u = \Phi_s \frac{F_u}{F_s} \frac{A_s}{A_u} \frac{n_u^2}{n_s^2}$$

Φ denotes the fluorescent quantum yield; F means the integral intensity of fluorescence, A refers to the absorbance at the excitation wavelength and n is the refraction index of solvents. u and s represent the testing and the standard samples, respectively.

Electrochemical analysis: Cyclic voltammograms of **TQ-DFOB-NMe₂**, **TQ-DFOB-Me** and **TQ-DFOB-CN** were measured in dichloromethane solution (1 mM), containing 0.1 M TBAPF₆ as the supporting electrolyte, glassy carbon electrode as a working electrode, Pt wire as a counter electrode, and Ag/AgCl as reference electrode at a scanning rate of 50 mVs⁻¹ at room temperature.

X-ray crystallography: Diffraction data of **TQ-DFOB-Br** were recorded on a Bruker CCD diffractometer with monochromatized Mo-K radiation ($\lambda = 0.71073\text{\AA}$). The collected frames were processed with the software SAINT. Data collection and reduction were carried out using CrysAlisPro program. Absorption correction was performed using SADABS built-in the CrysAlisPro program suite. The crystal structure was solved by direct methods and refined by

full-matrix least-squares on F2 using the SHELXTL software package. Atomic positions of non-hydrogen atoms were refined with anisotropic parameters. All hydrogen atoms were introduced at their geometric positions and refined as riding atoms.

2. Synthesis

2.1 Synthesis of TQ-DFOB-R.

The synthetic route of **TQ-DFOB-R** were illustrated in Scheme 1.

Synthesis of compounds 1-7. To a solution of 1,4-diethyl-7-hydroxy-1,2,3,4-tetrahydroquinoxalin-6-carboxaldehyde **A** (1 mmol) and respective anilines **B** (1 mmol) in 20 mL absolute ethanol was added a catalytic amount of *p*-TsOH (one crystal). The resulting solution was heated to reflux. TLC analysis was used to monitor the reaction. After the reaction was completed, the solvent was evaporated under a reduced pressure. The obtained residue was purified by column chromatography on silica gel to yield the corresponding pure compounds.

Compound 1: Red oil. Mass: 218.38 mg. Yield: 62%. ¹H NMR (500 MHz, CDCl₃) δ 8.32 (s, 1H), 7.21 (d, *J* = 8.9 Hz, 2H), 6.75 (d, *J* = 9.0 Hz, 2H), 6.40 (s, 1H), 6.14 (s, 1H), 3.51 – 3.43 (m, 2H), 3.38 (q, *J* = 7.1 Hz, 2H), 3.26 (dd, *J* = 13.7, 6.8 Hz, 2H), 3.14 (s, 2H), 2.96 (s, 6H), 1.20 (t, *J* = 7.1 Hz, 6H). ¹³C NMR (125 MHz, CDCl₃) δ 160.59, 155.70, 148.75, 141.83, 137.25, 127.70, 120.98, 113.28, 112.75, 108.60, 97.84, 47.51, 45.63, 45.37, 40.88, 10.65, 10.35.

Compound 2: Red oil. Mass: 278.14 mg. Yield: 82%. ¹H NMR (500 MHz, CDCl₃) δ 13.73 (s, 1H), 8.32 (s, 1H), 7.21 (d, *J* = 8.9 Hz, 2H), 6.92 (d, *J* = 8.9 Hz, 2H), 6.41 (s, 1H), 6.15 (s, 1H), 3.83 (s, 3H), 3.49 (t, *J* = 5.0 Hz, 2H), 3.39 (q, *J* = 7.1 Hz, 2H), 3.27 (q, *J* = 7.1 Hz, 2H), 3.19 – 3.13 (m, 2H), 1.21 (tt, *J* = 7.1, 4.8 Hz, 6H). ¹³C NMR (125 MHz, CDCl₃) δ 159.88, 157.92, 157.44, 141.95, 141.55, 127.83, 121.30, 114.53, 112.90, 108.42, 97.64, 55.54, 47.54, 45.63, 45.34, 10.64, 10.31.

Compound 3: Red oil. Mass: 248.86 mg. Yield: 77%. ¹H NMR (500 MHz, CDCl₃) δ 13.81 (s, 1H), 8.33 (s, 1H), 7.18 (q, *J* = 8.5 Hz, 4H), 6.40 (s, 1H), 6.14 (s, 1H), 3.48 (t, *J* = 5.6 Hz, 2H), 3.39 (q, *J* = 7.0 Hz, 2H), 3.27 (q, *J* = 7.1 Hz, 2H), 3.15 (t, *J* = 4.5 Hz, 2H), 2.37 (s, 3H), 1.21 (tt, *J* = 7.1, 4.4 Hz, 6H). ¹³C NMR (125 MHz, CDCl₃) δ 161.08, 157.89, 145.36, 142.43, 134.72, 129.90, 127.91, 120.02, 112.65, 108.47, 97.67, 47.61, 45.62, 45.29, 20.99, 10.66, 10.30.

Compound 4: Red oil. Mass: 212.40 mg. Yield: 58%. ¹H NMR (500 MHz, CDCl₃) δ 8.21 (s, 1H), 8.13 (s, 1H), 7.53 (d, *J* = 8.7 Hz, 2H), 7.14 (d, *J* = 8.7 Hz, 2H), 6.34 (s, 1H), 6.08 (s, 1H), 3.53 – 3.46 (m, 2H), 3.37 (q, *J* = 7.0 Hz, 2H), 3.26 (q, *J* = 7.0 Hz, 2H), 3.18 – 3.11 (m, 2H),

2.18 (s, 3H), 1.19 (tt, $J = 7.0, 3.9$ Hz, 6H). ^{13}C NMR (125 MHz, CDCl_3) δ 168.63, 162.80, 156.38, 143.30, 142.75, 135.41, 128.06, 121.05, 120.16, 112.26, 108.46, 97.68, 47.69, 45.75, 45.51, 45.16, 24.45, 10.65, 10.21.

Compound 5: Red oil. Mass: 181.93 mg. Yield: 47%. ^1H NMR (500 MHz, CDCl_3) δ 13.50 (s, 1H), 8.27 (s, 1H), 7.42 (d, $J = 8.7$ Hz, 2H), 7.06 (d, $J = 8.7$ Hz, 2H), 6.36 (s, 1H), 6.09 (s, 1H), 3.47 – 3.42 (m, 2H), 3.35 (q, $J = 7.1$ Hz, 2H), 3.23 (q, $J = 7.1$ Hz, 2H), 3.13 – 3.08 (m, 2H), 1.17 (q, $J = 7.2$ Hz, 6H). ^{13}C NMR (125 MHz, CDCl_3) δ 160.65, 158.85, 147.21, 142.75, 132.21, 128.12, 121.93, 117.86, 112.55, 108.36, 97.30, 47.65, 45.69, 45.48, 45.09, 10.71, 10.22.

Compound 6: Red oil. Mass: 116.96 mg. Yield: 35%. ^1H NMR (500 MHz, CDCl_3) δ 13.38 (s, 1H), 8.30 (s, 1H), 7.63 (d, $J = 8.6$ Hz, 2H), 7.26 (d, $J = 8.6$ Hz, 2H), 6.35 (s, 1H), 6.10 (s, 1H), 3.57 – 3.49 (m, 2H), 3.41 (q, $J = 7.1$ Hz, 2H), 3.28 (q, $J = 7.1$ Hz, 2H), 3.20 – 3.14 (m, 2H), 1.21 (tt, $J = 12.9, 7.1$ Hz, 6H). ^{13}C NMR (125 MHz, CDCl_3) δ 161.59, 159.19, 152.02, 143.65, 133.42, 128.49, 120.83, 119.33, 112.20, 108.61, 107.36, 97.19, 47.79, 45.85, 45.46, 45.04, 10.73, 10.16.

Compound 7: Red oil. Mass: 163.44 mg. Yield: 42%. ^1H NMR (500 MHz, $\text{DMSO}-d_6$) δ 13.29 (s, 1H), 8.63 (s, 1H), 7.62 (d, $J = 8.5$ Hz, 2H), 7.25 (d, $J = 8.2$ Hz, 2H), 6.62 (s, 1H), 6.00 (s, 1H), 3.46 (s, 2H), 3.43 – 3.29 (m, 2H), 3.23 (q, $J = 14.8, 7.9$ Hz, 2H), 3.10 (s, 2H), 1.11 (tt, $J = 7.0, 4.2$ Hz, 6H). ^{13}C NMR (125 MHz, $\text{DMSO}-d_6$) δ 159.93, 149.45, 145.38, 144.64, 128.41, 127.28, 127.17, 119.72, 112.69, 96.74, 95.70, 56.50, 49.07, 47.57, 19.02, 10.85, 10.18.

Synthesis of TQ-DFOB-R. To a solution of respective compounds **1**, **2**, **3**, **4**, **5**, **6** and **7** (0.5 mmol) in 5 mL freshly distilled dichloroethane at 80 °C was added DIEA (1.25 mmol). The resulting mixture was stirred for 10 minutes and then $\text{BF}_3\text{-OEt}_2$ was added (1.25 mmol). The reaction course was monitored by TLC analysis. After the reaction was completed, the reaction mixture was cooled to room temperature, diluted with 20 mL DCM and then washed with saturated aqueous NaHCO_3 solution. The organic layers were separated, combined and dried over anhydrous Na_2SO_4 . The solvent was evaporated under vacuum. The crude product was subjected to further purification by column chromatography.

TQ-DFOB-NMe₂. Red powder. Mass: 146.08 mg. Yield: 73%. Mp: 109–111°C. ^1H NMR (500 MHz, CDCl_3) δ 7.94 (s, 1H), 7.39 (d, $J = 7.6$ Hz, 2H), 6.73 (d, $J = 7.6$ Hz, 2H), 6.36 (s, 1H), 6.21 (s, 1H), 3.56 (s, 2H), 3.42 (d, $J = 6.2$ Hz, 2H), 3.28 (d, $J = 6.0$ Hz, 2H), 3.16 (s, 2H), 2.98 (s, 6H), 1.33 – 1.11 (m, 6H). ^{13}C NMR (125 MHz, CDCl_3) δ 156.85, 155.78, 149.70, 146.60,

133.05, 129.46, 123.68, 112.65, 109.72, 106.43, 97.21, 48.09, 46.22, 45.32, 44.60, 40.64, 10.78, 9.96. HRMS (ESI) m/z: calcd for $C_{21}H_{27}BF_2N_4O$, 400.2246; found, 400.2244.

TQ-DFOB-OMe. Red powder. Mass: 174.24 mg. Yield: 90%. Mp: 182-183 °C. 1H NMR (500 MHz, $CDCl_3$) δ 7.94 (s, 1H), 7.43 (d, J = 8.9 Hz, 2H), 6.92 (d, J = 9.0 Hz, 2H), 6.35 (s, 1H), 6.18 (s, 1H), 3.83 (s, 3H), 3.60 – 3.52 (m, 2H), 3.42 (q, J = 7.1 Hz, 2H), 3.27 (q, J = 7.1 Hz, 2H), 3.18 – 3.13 (m, 2H), 1.23 (t, J = 7.1 Hz, 3H), 1.19 (t, J = 7.1 Hz, 3H). ^{13}C NMR (125 MHz, $CDCl_3$) δ 158.71, 157.34, 156.64, 147.19, 136.77, 129.61, 124.20, 114.44, 109.66, 106.39, 97.06, 55.55, 48.14, 46.29, 45.31, 44.51, 10.79, 9.91. HRMS (ESI) m/z: calcd for $C_{20}H_{24}BF_2N_3O_2$, 387.1390; found, 387.1919.

TQ-DFOB-Me. Red powder. Mass: 163.33mg. Yield: 88%. Mp: 171-173 °C. 1H NMR (500 MHz, $CDCl_3$) δ 7.97 (s, 1H), 7.39 (d, J = 8.2 Hz, 2H), 7.21 (d, J = 8.1 Hz, 2H), 6.36 (s, 1H), 6.19 (s, 1H), 3.62 – 3.52 (m, 2H), 3.43 (q, J = 7.1 Hz, 2H), 3.27 (q, J = 7.1 Hz, 2H), 3.21 – 3.10 (m, 2H), 2.37 (s, 3H), 1.23 (t, J = 7.2 Hz, 3H), 1.20 (t, J = 7.1 Hz, 3H). ^{13}C NMR (125 MHz, $CDCl_3$) δ 157.58, 156.78, 147.35, 141.07, 137.05, 129.84, 129.69, 122.86, 109.67, 106.47, 97.03, 48.10, 46.30, 45.35, 44.50, 21.00, 10.80, 9.91. HRMS (ESI) m/z: calcd for $C_{20}H_{24}BF_2N_3O$, 371.1980; found, 371.1971.

TQ-DFOB-NHCOMe. Mass: 173.96 mg. Red powder. Yield: 84%. Mp: 235-236°C. 1H NMR (500 MHz, $DMSO-d_6$) δ 10.09 (s, 1H), 8.47 (s, 1H), 7.65 (d, J = 9.0 Hz, 2H), 7.43 (d, J = 8.8 Hz, 2H), 6.65 (s, 1H), 6.11 (s, 1H), 3.56 (t, J = 5.0 Hz, 2H), 3.47 (q, J = 7.0 Hz, 2H), 3.24 (q, J = 7.0 Hz, 2H), 3.12 (t, J = 5.0 Hz, 2H), 2.06 (s, 3H), 1.13 (m, 6H). ^{13}C NMR (125 MHz, $DMSO-d_6$) δ 168.81, 157.87, 156.91, 147.51, 138.60, 138.50, 129.71, 123.36, 119.87, 110.55, 106.53, 96.09, 48.08, 45.98, 45.12, 44.39, 24.47, 11.04, 9.85. HRMS (ESI) m/z: calcd for $C_{21}H_{25}BF_2N_4O_2$, 414.2039; found, 414.2034.

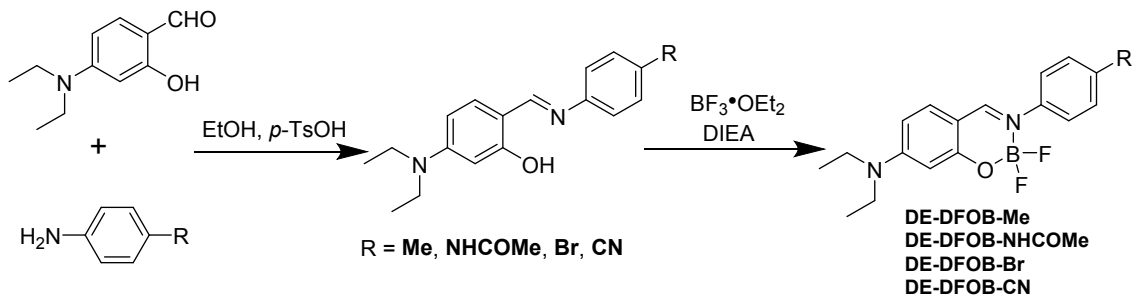
TQ-DFOB-Br. Red powder. Mass: 206.67 mg. Yield: 95%. Mp: 228-230 °C. 1H NMR (500 MHz, $CDCl_3$) δ 7.95 (s, 1H), 7.53 (d, J = 11.7 Hz, 2H), 7.39 (d, J = 8.7 Hz, 2H), 6.35 (s, 1H), 6.19 (s, 1H), 3.65 – 3.56 (m, 2H), 3.46 (q, J = 7.2 Hz, 2H), 3.29 (q, J = 7.1 Hz, 2H), 3.19 (t, J = 4.8 Hz, 2H), 1.26 (t, J = 7.2 Hz, 3H), 1.21 (t, J = 7.0 Hz, 3H). ^{13}C NMR (125 MHz, $CDCl_3$) δ 158.18, 156.29, 147.96, 142.55, 132.33, 129.92, 124.65, 120.67, 109.56, 106.74, 97.04, 48.16, 46.47, 45.40, 44.44, 10.85, 9.90. HRMS (ESI) m/z: calcd for $C_{19}H_{21}BF_2N_3Obr$, 435.0929; found, 435.0927.

TQ-DFOB-CN. Red powder. Mass: 160.52 mg. Yield: 84%. Mp: 222-223 °C. 1H NMR (500 MHz, $CDCl_3$) δ 7.97 (s, 1H), 7.63 (d, J = 8.8 Hz, 2H), 7.58 (d, J = 8.7 Hz, 2H), 6.30 (s, 1H),

6.12 (s, 1H), 3.62 (t, $J = 5.1$ Hz, 2H), 3.47 (q, $J = 7.1$ Hz, 2H), 3.27 (q, $J = 7.0$ Hz, 2H), 3.18 (s, 2H), 1.26 (t, $J = 7.2$ Hz, 3H), 1.19 (t, $J = 7.1$ Hz, 3H). ^{13}C NMR (125 MHz, CDCl_3) δ 158.87, 155.13, 148.91, 146.94, 133.19, 130.09, 123.16, 118.60, 109.69, 109.25, 107.35, 96.67, 48.30, 46.70, 45.35, 44.25, 10.93, 9.82. HRMS (ESI) m/z: calcd for $\text{C}_{20}\text{H}_{21}\text{BFN}_4\text{O}$, 363.1792; found, 363.1791.

TQ-DFOB-SO₃H. Red powder. Mass: 124.58 mg. Yield: 57%. Mp: >300°C. ^1H NMR (500 MHz, $\text{DMSO}-d_6$) δ 8.53 (s, 1H), 7.67 (d, $J = 8.5$ Hz, 2H), 7.45 (d, $J = 8.4$ Hz, 2H), 6.67 (s, 1H), 6.12 (s, 1H), 3.57 (t, $J = 4.9$ Hz, 2H), 3.48 (dd, $J = 14.0, 6.9$ Hz, 2H), 3.25 (q, $J = 6.9$ Hz, 2H), 3.13 (t, $J = 4.9$ Hz, 2H), 1.13 (m, 6H). ^{13}C NMR (125 MHz, $\text{DMSO}-d_6$) δ 158.06, 157.32, 147.95, 146.90, 143.59, 129.84, 126.94, 122.31, 110.53, 106.73, 96.04, 48.13, 46.05, 45.12, 44.36, 11.07, 9.86. HRMS (ESI) m/z: calcd for $\text{C}_{19}\text{H}_{22}\text{BF}_2\text{N}_3\text{O}_4\text{S}$, 437.1392; found, 437.1393.

2.2 Synthesis of DE-DFOB-R



Scheme S1. Synthesis of compounds **DE-DFOB-R**.

The synthetic method of **DE-DFOB-R** is the same as that of **TQ-DFOB-R**.

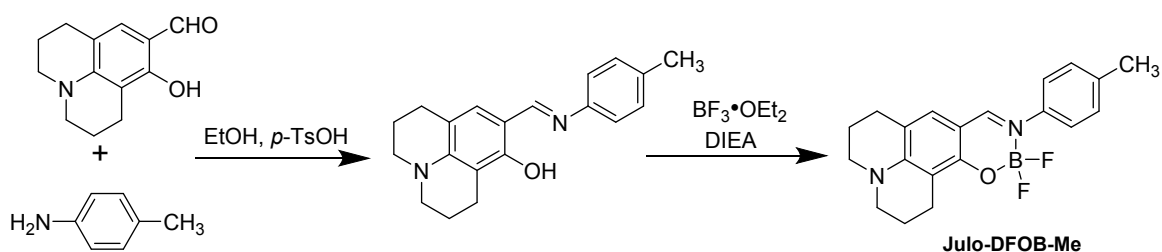
DE-DFOB-Me. Mass: 86.18 mg. Yield: 52.2%. ^1H NMR (400 MHz, CDCl_3) δ 8.03 (s, 1H), 7.40 (d, $J = 8.2$ Hz, 2H), 7.23 (d, $J = 9.0$ Hz, 3H), 6.37 (dd, $J = 9.0, 2.4$ Hz, 1H), 6.25 (d, $J = 2.2$ Hz, 1H), 3.56 – 3.27 (m, 4H), 2.39 (s, 3H), 1.25 (t, $J = 7.1$ Hz, 6H). ^{13}C NMR (100 MHz, CDCl_3) δ 161.7, 158.0, 156.0, 140.7, 137.6, 133.7, 129.9, 122.9, 106.8, 106.4, 98.1, 45.1, 21.0, 12.6.

DE-DFOB-NHCOMe. Mass: 89.94 mg. Yield: 48.2%. ^1H NMR (400 MHz, CDCl_3) δ 9.62 (s, 1H), 8.14 (s, 1H), 7.67 (s, 2H), 7.59 – 7.49 (m, 1H), 7.36 (d, $J = 27.6$ Hz, 2H), 6.38 (s, 1H), 6.17 (s, 1H), 3.46 (d, $J = 3.4$ Hz, 4H), 2.14 (d, $J = 10.1$ Hz, 3H), 1.30 – 1.16 (m, 6H). ^{13}C NMR (100 MHz, CDCl_3) δ 168.64, 161.61, 158.17, 155.98, 138.27, 138.01, 133.44, 123.24, 120.16, 106.33, 97.53, 45.05, 23.86, 12.58.

DE-DFOB-Br. Mass: 97.53 mg. Yield: 49.5%. ¹H NMR (500 MHz, CDCl₃) δ 8.02 (s, 1H), 7.54 (d, *J* = 8.8 Hz, 2H), 7.39 (d, *J* = 8.7 Hz, 2H), 7.24 (d, *J* = 9.1 Hz, 1H), 6.38 (dd, *J* = 9.1, 2.4 Hz, 1H), 6.23 (d, *J* = 2.3 Hz, 1H), 3.47 (q, *J* = 7.1 Hz, 4H), 1.26 (t, *J* = 7.1 Hz, 6H). ¹³C NMR (125 MHz, CDCl₃) δ 161.9, 157.8, 156.5, 142.2, 134.0, 132.4, 124.7, 121.2, 107.0, 106.9, 98.0, 45.2, 12.6.

DE-DFOB-CN. Mass: 114.80 mg. Yield: 67.3%. ¹H NMR (400 MHz, CDCl₃) δ 8.06 (s, 1H), 7.68 (dd, *J* = 33.2, 8.6 Hz, 4H), 7.25 (d, *J* = 9.1 Hz, 2H), 6.41 (dd, *J* = 9.1, 2.2 Hz, 1H), 6.23 (s, 1H), 3.50 (q, *J* = 7.1 Hz, 4H), 1.28 (t, *J* = 7.1 Hz, 6H). ¹³C NMR (100 MHz, CDCl₃) δ 162.3, 157.4, 157.0, 146.6, 134.4, 133.3, 123.6, 118.3, 110.7, 107.5, 107.3, 97.9, 45.4, 12.6.

2.3 Synthesis of Julo-DFOB-R



Scheme S2. Synthesis of compounds **Julo-DFOB-Me**.

The synthetic method of **Julo-DFOB-Me** is the same as that of **TQ-DFOB-R**.

Julo-DFOB-Me. Mass: 80.57 mg. Yield: 45.5%. ¹H NMR (400 MHz, DMSO-*d*₆) δ 8.44 (s, 1H), 7.37 (d, *J* = 8.2 Hz, 2H), 7.26 (d, *J* = 8.3 Hz, 2H), 7.05 (s, 1H), 3.36 – 3.32 (m, 3H), 2.62 (dt, *J* = 12.0, 6.2 Hz, 3H), 2.33 (s, 2H), 1.85 (s, 3H). ¹³C NMR (100 MHz, DMSO-*d*₆) δ 158.7, 156.0, 151.6, 141.0, 136.7, 130.2, 130.0, 123.0, 115.9, 106.2, 105.3, 50.2, 49.8, 27.0, 21.4, 20.9, 20.3, 20.0.

3. Photophysical properties of DE-DFOB-R, Julo-DFOB-R and TQ-DFOB-R

Table S1. Photophysical data of **DE-DFOB-R** in different solvents.

R	Solvent	$\lambda_{\text{abs}}/\text{nm}$	$\epsilon_{\text{max}}/\text{M}^{-1}\text{cm}^{-1}$	$\lambda_{\text{em}}/\text{nm}$	τ/ns	Φ_f^{a}	Stokes shift/nm
Me	DCM	399	75000	456	0.18	0.07	57
	THF	395	86000	454	0.17	0.06	59
	CH ₃ CN	396	69000	456	0.13	0.02	60
	CH ₃ OH	395	58000	454	0.13	0.02	59
NHCOMe	DCM	406	73000	481	0.17	0.07	75
	THF	401	57000	483	0.14	0.04	82
	CH ₃ CN	402	125000	481	0.12	0.04	79
	CH ₃ OH	401	91000	482	0.17	0.04	81
Br	DCM	405	55000	460	0.42	0.17	55
	THF	402	73000	459	0.22	0.09	57
	CH ₃ CN	402	55000	459	0.12	0.01	57
	CH ₃ OH	399	67000	458	0.16	0.02	59
CN	DCM	419	47000	468	0.25	0.08	49
	THF	415	88000	468	0.13	0.04	53
	CH ₃ CN	414	48000	468	0.11	0.01	54
	CH ₃ OH	413	84000	466	0.10	0.01	53

^a Using coumarin 102 as a reference $\Phi_f = 0.93$ in ethanol.

Table S2. Photophysical data of **Julo-DFOB-Me** in different solvents.

R	Solvent	$\lambda_{\text{abs}}/\text{nm}$	$\epsilon_{\text{max}}/\text{M}^{-1}\text{cm}^{-1}$	$\lambda_{\text{em}}/\text{nm}$	τ/ns	Φ_f^{a}	Stokes shift/nm
Me	DCM	416	59000	469	0.60	0.20	53
	THF	411	58000	468	0.49	0.19	57
	CH ₃ CN	413	53000	467	0.80	0.23	54
	CH ₃ OH	412	61000	467	0.64	0.23	55

^a Using coumarin 153 as a reference ($\Phi_f = 0.38$ in ethanol).

Table S3. Photophysical data of **TQ-DFOB-R** in different solvents.

R	Solvent	$\lambda_{\text{abs}}/\text{nm}$	$\epsilon/\text{M}^{-1}\cdot\text{cm}^{-1}$	$\lambda_{\text{em}}/\text{nm}$	τ/ns	Φ_f^{a}	Stokes shift/ nm
NMe₂	DCM	469	33300	609	3.55	0.68	140
	THF	460	33600	604	3.66	0.60	144
	CH ₃ CN	464	32800	620	2.52	0.27	156
	CH ₃ OH	461	42000	618	2.13	0.27	157
OMe	DCM	456	18000	615	3.95	0.30	159
	THF	453	23900	617	3.73	0.44	164
	CH ₃ CN	452	22100	642	2.09	0.13	190
	CH ₃ OH	450	27700	626	1.94	0.15	176
Me	DCM	455	14100	617	3.88	0.49	162
	THF	452	25300	618	3.49	0.40	166
	CH ₃ CN	453	25200	643	1.96	0.11	190
	CH ₃ OH	451	17700	641	1.82	0.16	190
NHCOMe	DCM	465	34200	626	3.48	0.40	161
	THF	475	39100	618	3.30	0.44	161
	CH ₃ CN	459	40900	642	1.83	0.17	183
	CH ₃ OH	456	24600	642	1.62	0.14	186
Br	DCM	464	27600	633	3.07	0.36	169
	THF	461	20200	640	2.47	0.28	179
	CH ₃ CN	461	18300	666	1.40	0.07	205
	CH ₃ OH	458	33700	656	1.33	0.10	198
CN	DCM	478	26100	656	2.12	0.24	178
	THF	477	31700	666	1.55	0.19	189
	CH ₃ CN	476	30200	682	0.89	0.05	206
	CH ₃ OH	475	33800	684	0.74	0.06	209

^aUsing fluorescein as a reference ($\Phi_f=0.91$ in basic ethanol).

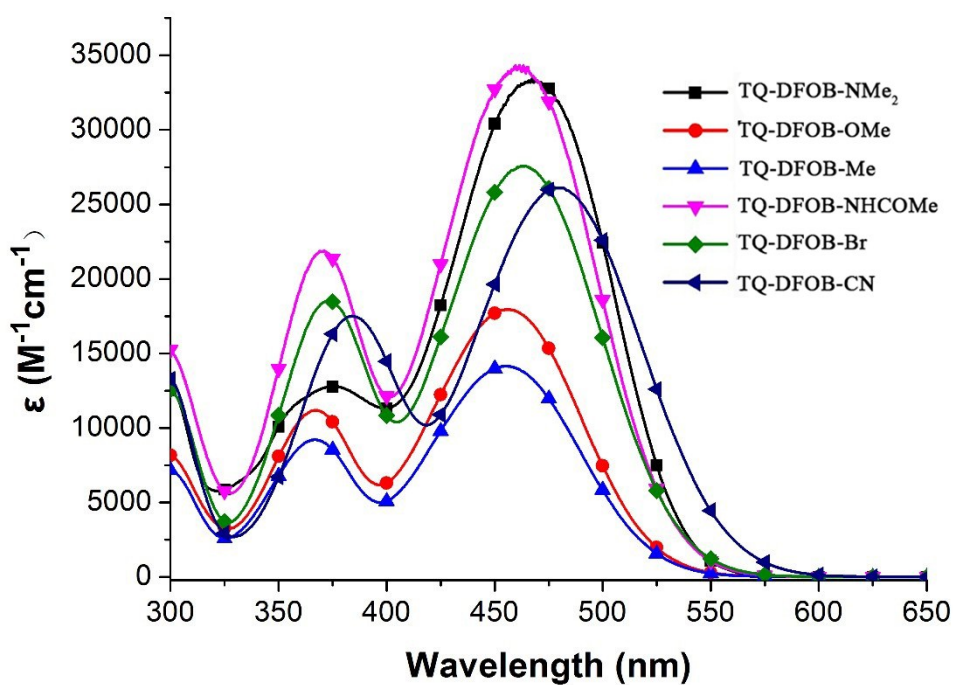


Figure S1. UV-vis absorption spectra of compounds **TQ-DFOB-R** in DCM.

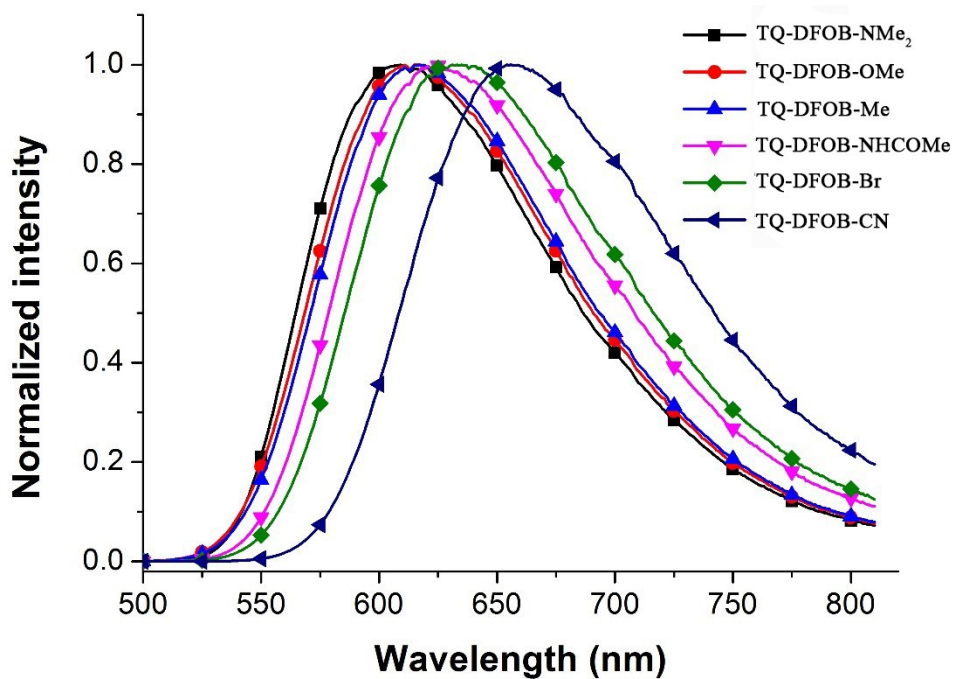


Figure S2. Normalized fluorescence spectra of compounds **TQ-DFOB-R** in DCM.

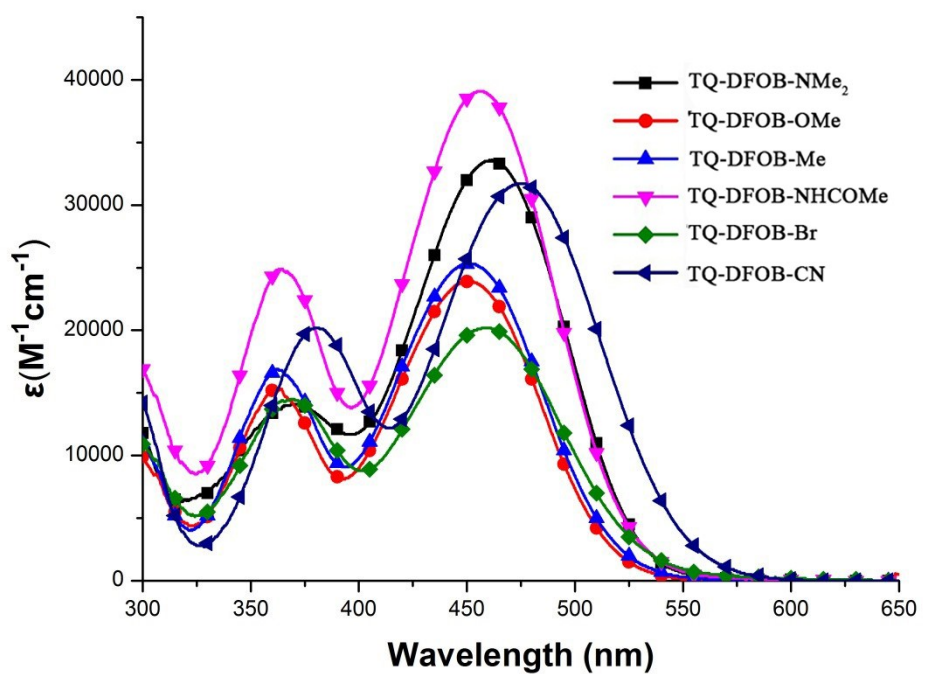


Figure S3. UV-vis absorption spectra of compounds **TQ-DFOB-R** in THF.

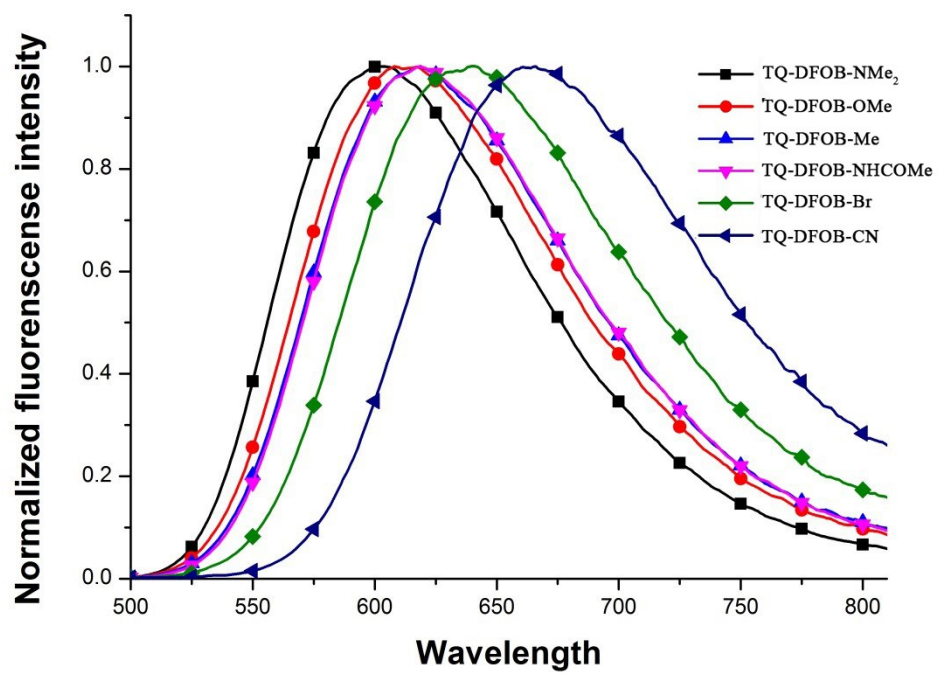


Figure S4. Normalized fluorescence spectra of compounds **TQ-DFOB-R** in THF.

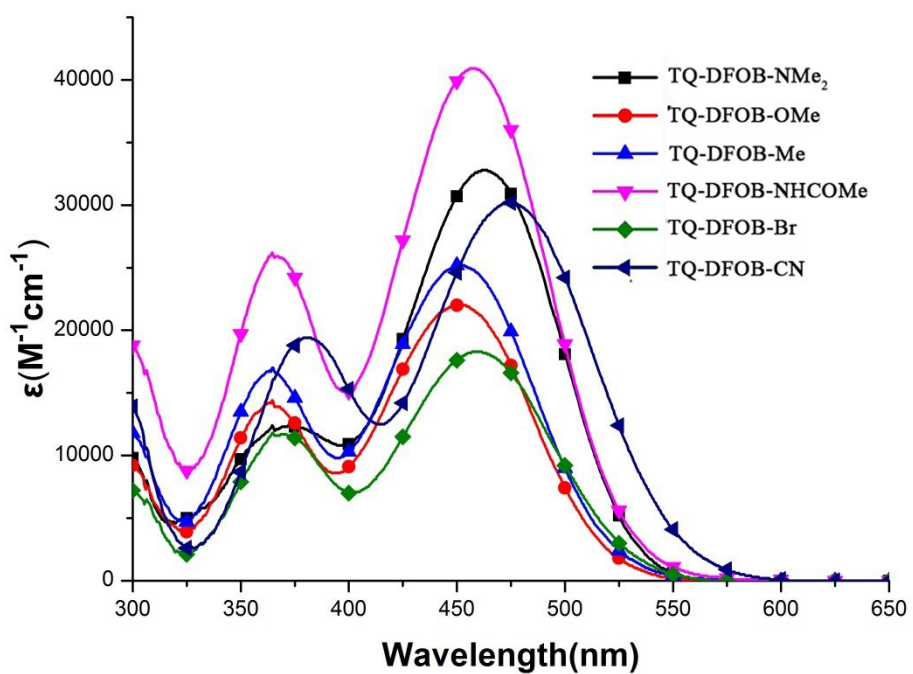


Figure S5. UV-vis absorption spectra of compounds **TQ-DFOB-R** in CH_3CN .

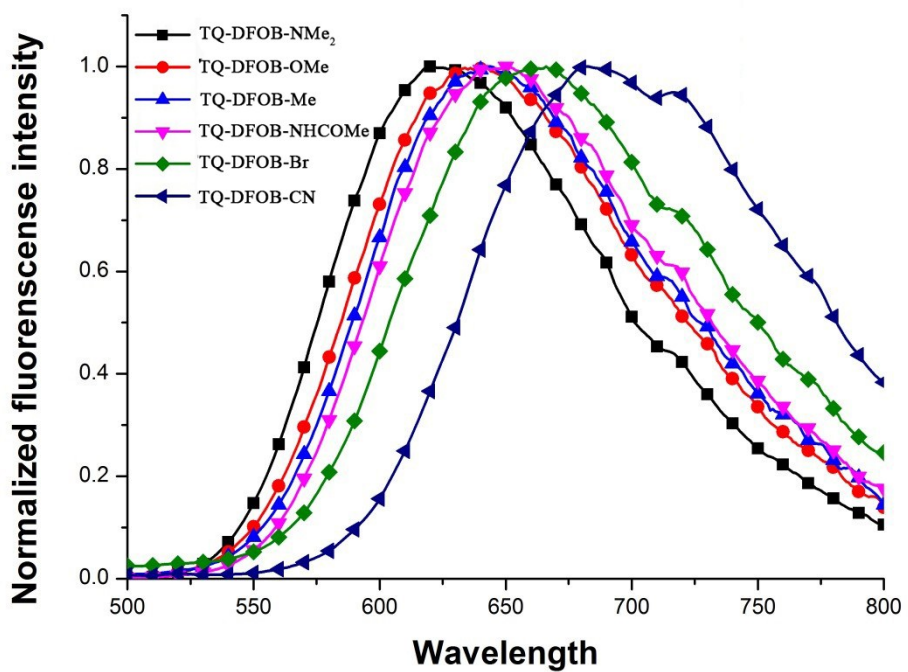


Figure S6. Normalized fluorescence spectra of compounds **TQ-DFOB-R** in CH_3CN .

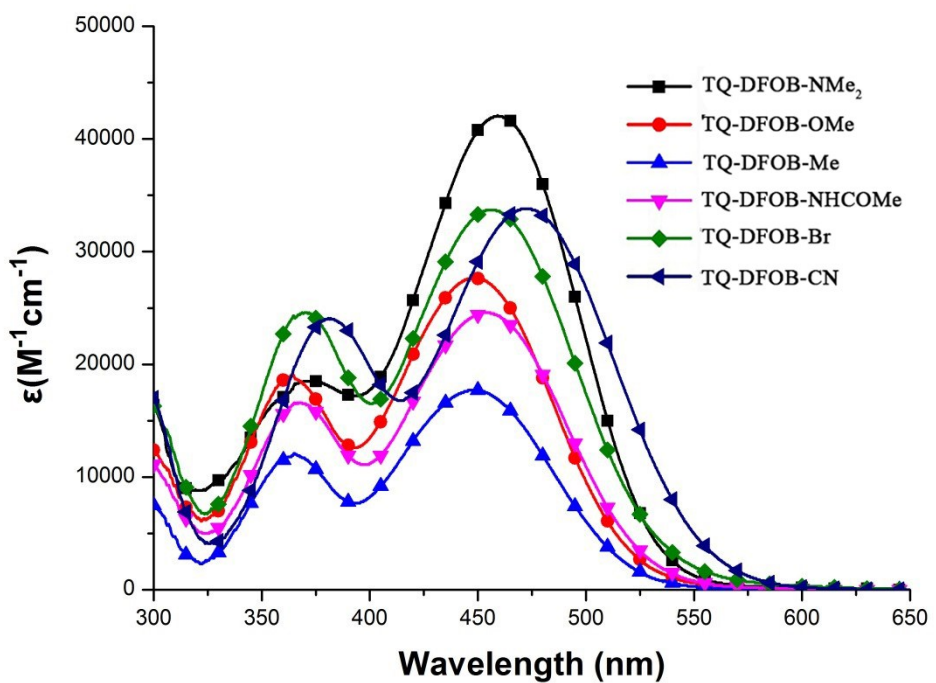


Figure S7. UV-vis absorption spectra of compounds **TQ-DFOB-R** in CH₃OH.

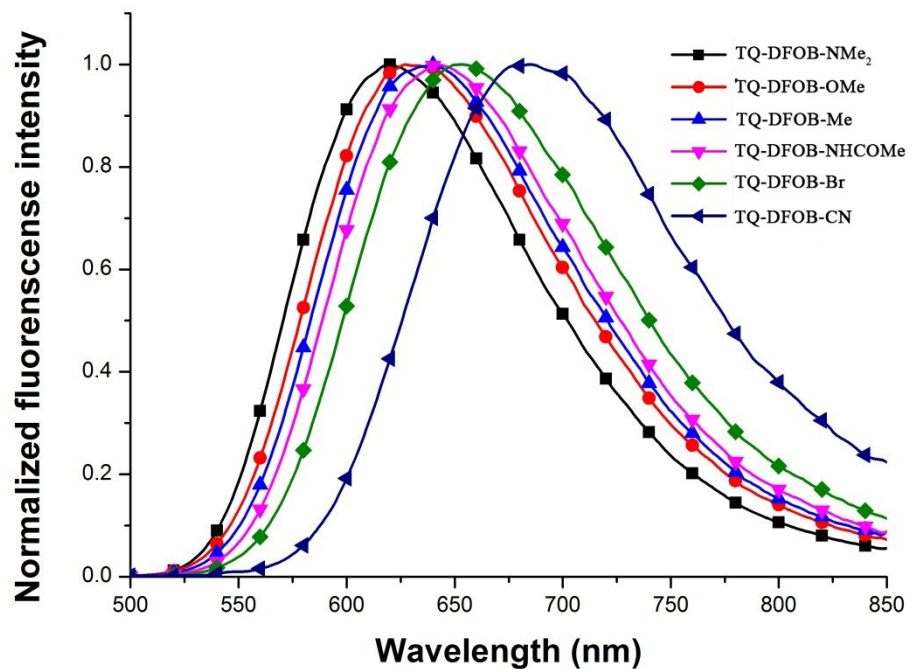


Figure S8. Normalized fluorescence spectra of compounds **TQ-DFOB-R** in CH₃OH.

4. Theoretical calculations

In general, the Stokes shift is dependent on the geometry difference of fluorescent dyes between the energy-minimized ground state (S_0) and the energy-minimized first excited state (S_1) (*Dyes Pigm.*, 2016, **126**, 232-238.). In principle, unsymmetric fluorescent dyes possess energetically and structurally distinct S_0 and S_1 states because of the larger electron transfer through the whole molecule than their symmetric analogues (*J. Am. Chem. Soc.*, 2009, **131**, 6099-6101.; *J. Am. Chem. Soc.*, 2005, **127**, 4170-4171.; *J. Am. Chem. Soc.*, 2018, **140**, 7716-7722.; *Angew. Chem., Int. Ed.*, 2011, **50**, 12214-12217), which can result in large Stokes shift. To gain better insight into the geometries of these dyes, density functional theory (DFT) and time-dependent (TD)-DFT calculations were performed on **TQ-DFOB-Me** using Gaussian 09. Geometry optimizations for S_0 and S_1 states of **TQ-DFOB-Me** in dichloromethane were conducted using B3LYP functional with 6-31G (d, p) basis sets, as shown in Figure S9. It's seen that the three dihedral angles: d_1 between the two planes of the end benzene ring and BF_2 -core; and d_2 (C5-C6-C7-C8) and d_3 (C5'-C6'-C7'-C8') between tetrahydroquinoxaline moiety and BF_2 -core were 41.352° , 176.61° and 152.483° at S_0 state, which were 26.022° , -158.539° and 144.757° at S_1 state, respectively. In other words, the molecular structure conformation of **TQ-DFOB-Me** changed a lot when going from S_0 state to S_1 state upon excitation. We also compared the extent of electron transfer between LUMO and HOMO in **TQ-DFOB-Me**, **DEA-DFOB-Me** and **Julo-DFOB-Me**, shown in Figure S10. A greater electron transfer was seen for **TQ-DFOB-Me**, which can result in a larger structural conformation change and thereby leading to a larger Stokes shift.

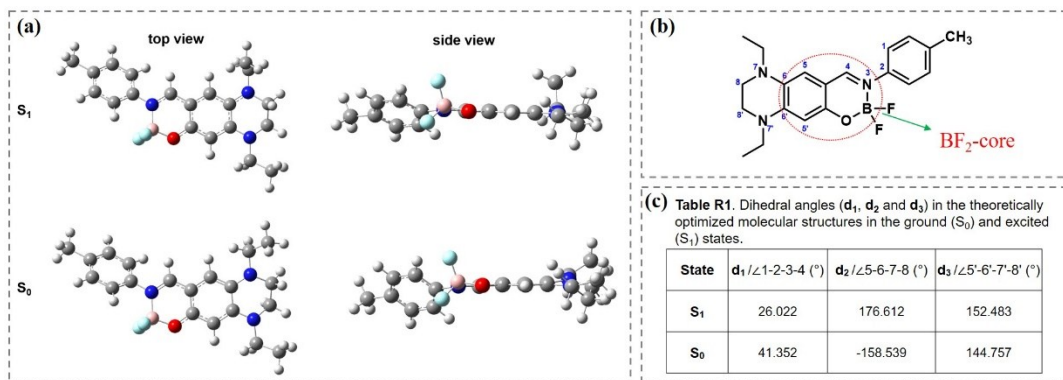


Figure S9. (a) Theoretically optimized molecular structures of **TQ-DFOB-Me** in S_0 and S_1 state in dichloromethane; (b) atom and bond labeling of **TQ-DFOB-Me**; (c) dihedral angles in the theoretically optimized molecular structure.

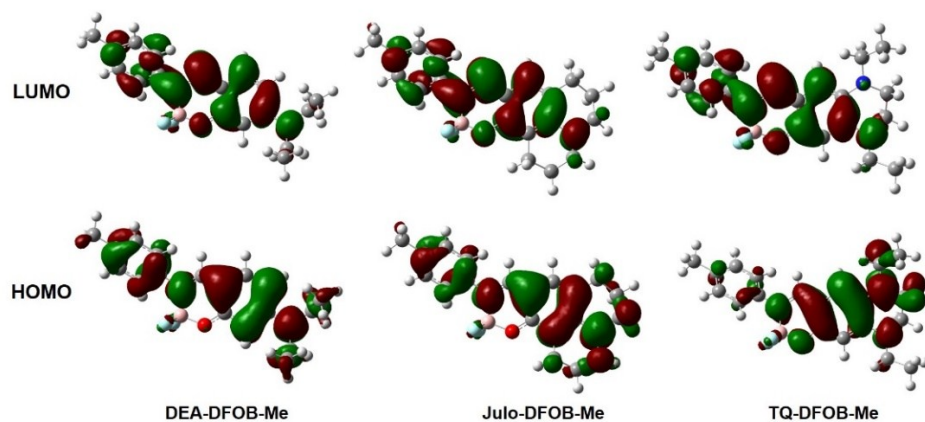


Figure S10. LUMOs and HOMOs of **DEA-DFOB-Me**, **Julo-DFOB-Me** and **TQ-DFOB-Me** in dichloromethane (red: positive; green: negative).

5. Photophysical properties of compounds TQ-DFOB-R in solid state

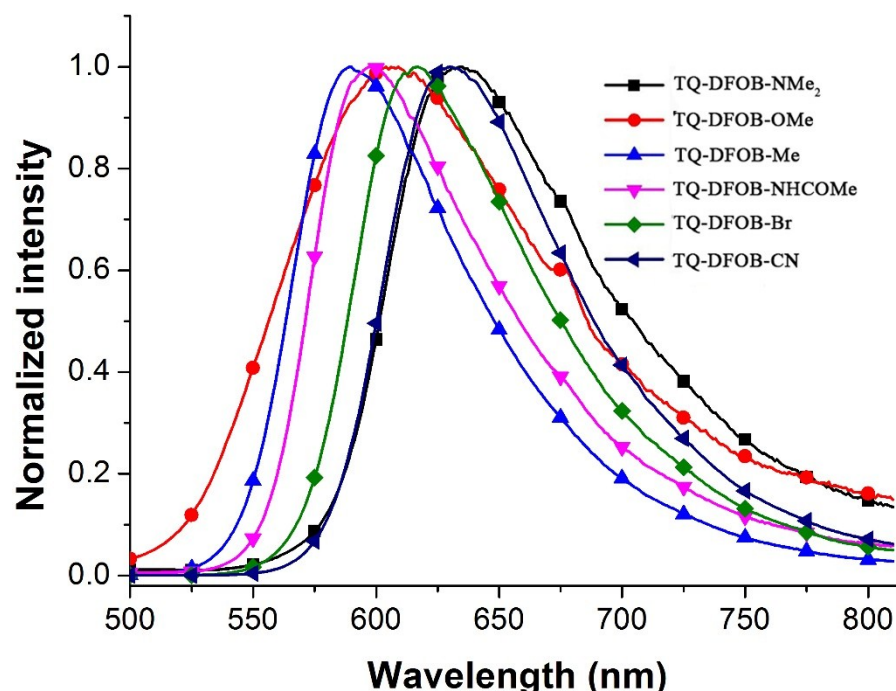


Figure S11. Normalized fluorescence of compounds **TQ-DFOB-R** in solid state.

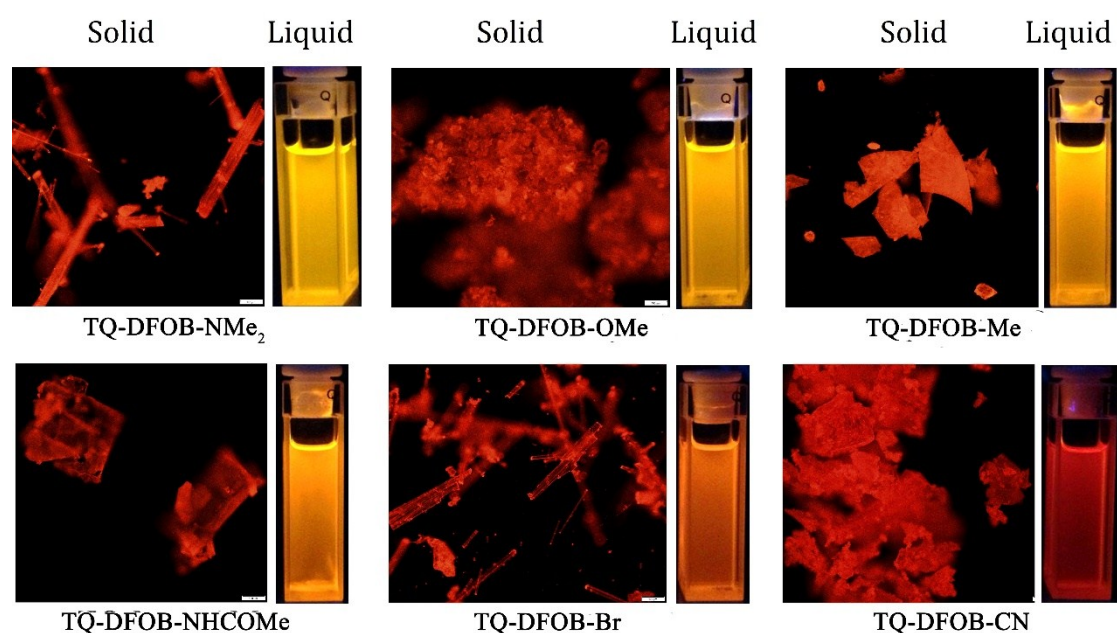


Figure S12. Photographs of compounds **TQ-DFOB-R** in dichloromethane and in solid state.

6. X-ray structures of compound TQ-DFOB-Br

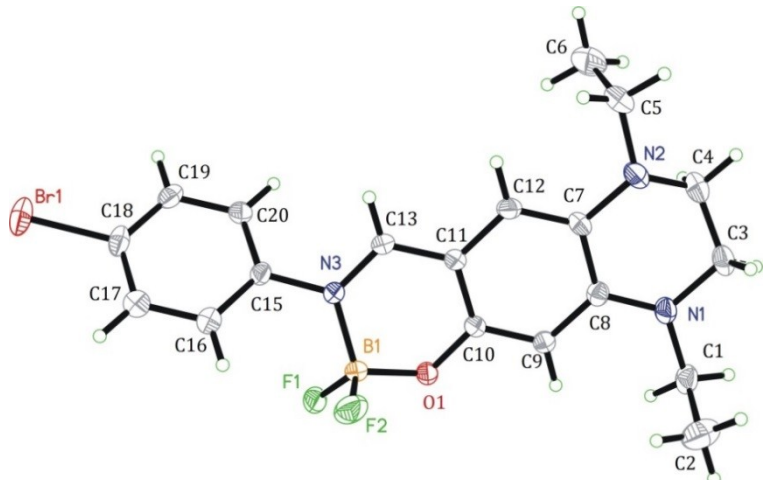


Figure S13. ORTEP view of compound **TQ-DFOB-Br** with 50% probability.

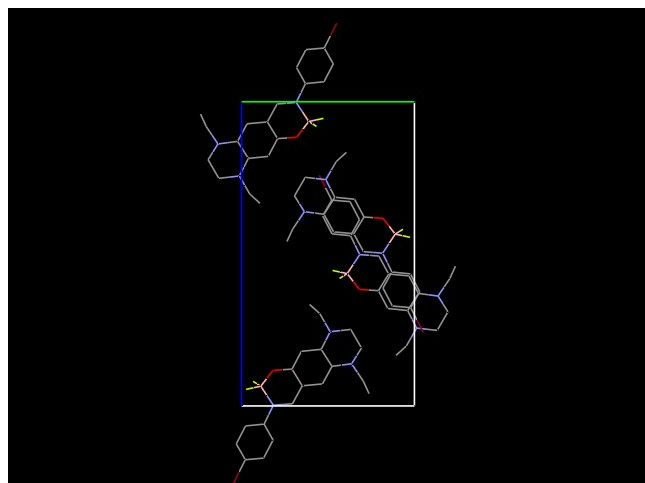


Figure S14. Part of a crystal-packing pattern of compound **TQ-DFOB-Br** along with the a axis.

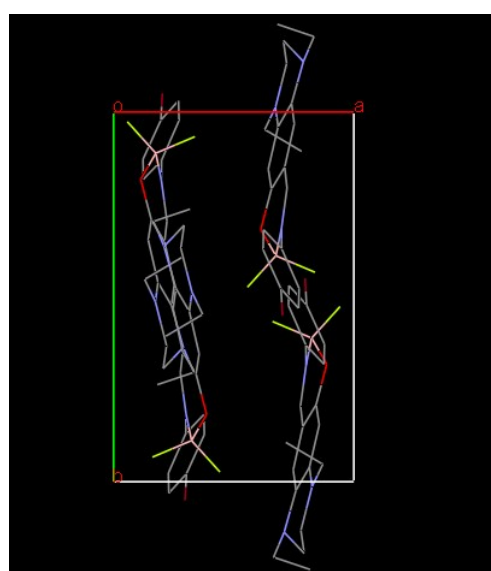


Figure S15. Part of a crystal-packing pattern of compound **TQ-DFOB-Br** along with the c axis.

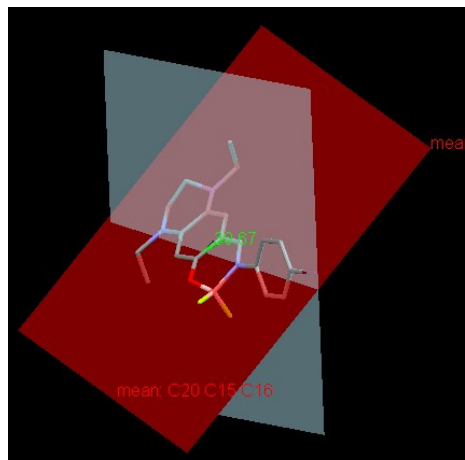


Figure S16. Determination of the dihedral angle of compound **TQ-DFOB-Br**.

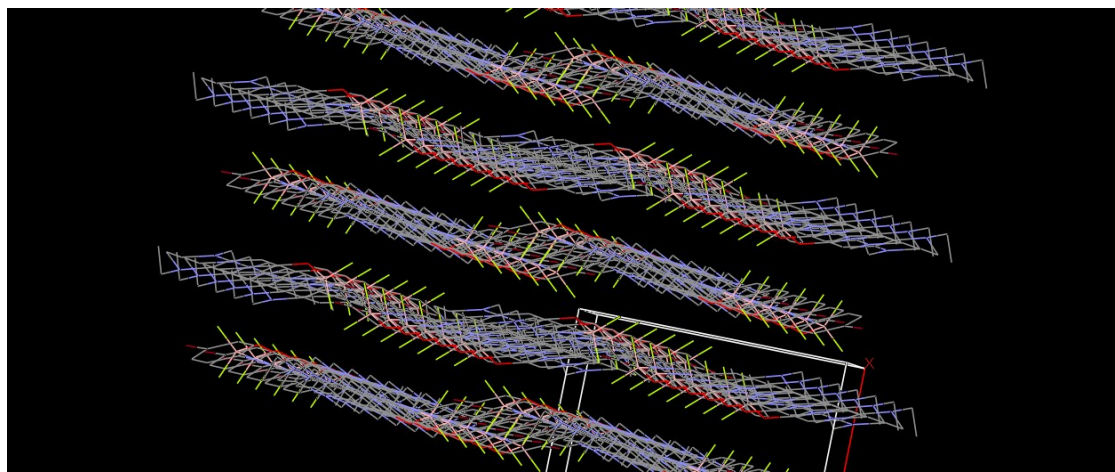


Figure S17. Packing diagram view of compound **TQ-DFOB-Br**.

Table S4. Crystal data and structure refinement for compound **TQ-DFOB-Br**.

Empirical formula	C ₁₉ H ₂₁ BBrF ₂ N ₃ O
Formula weight	436.11
Temperature/K	293 K
Wavelength	0.71073 Å
Crystal system	Orthorhombic
space group	P2(1)/C
a/Å	7.65210
b/Å	11.7979
c/Å	20.7618
α/°	90
β/°	90
γ/°	90
V/Å ³	1874.35
Z	4
ρ _{calc} mg/m ³	1.545
Absorption coefficient	2.226 mm ⁻¹

F(000)	888
Theta range for data collection	1.99 to 27.64°
Limiting indices	-8≤ h ≤ 9, -14≤ k ≤ 15, -27≤ l ≤ 25
Reflections collected	9639
Independent reflections	4316 [R(int) = 0.0192]
Data / restraints / parameters	4316 / 0 / 240
Goodness-of-fit on F ²	1.009
Final R indices [I>2σ (I)]	R ₁ = 0.0295, wR ₂ = 0.0647
Final R indexes [all data]	R ₁ = 0.0402, wR ₂ = 0.0674
Absolute structure parameter	1.001
Largest diff. peak /hole/e Å ⁻³	0.241/ -0.381

Table S5. Atomic coordinates (x 10⁴) and equivalent isotropic displacement parameters (Å² x 10³) for compound **TQ-DFOB-Br**. U(eq) is defined as one third of the trace of the orthogonalized U^{ij} tensor.

	x	y	z	U(eq)
Br(1)	7030(1)	5507(1)	-2584(1)	61(1)
F(1)	5570(2)	4739(1)	546(1)	59(1)
F(2)	8386(2)	4335(1)	809(1)	68(1)
N(1)	6737(2)	-127(1)	2441(1)	41(1)
N(2)	7900(3)	-1367(1)	1387(1)	51(1)
N(3)	6985(3)	3164(1)	23(1)	34(1)
O(1)	6127(2)	3181(1)	1170(1)	46(1)
B(1)	6756(4)	3887(2)	649(1)	39(1)
C(1)	6291(4)	473(2)	3033(1)	49(1)
C(2)	7830(5)	1064(3)	3338(1)	79(1)
C(3)	7203(4)	-1316(2)	2516(1)	50(1)
C(4)	7065(5)	-1939(2)	1905(1)	58(1)
C(5)	8342(4)	-2041(2)	817(1)	62(1)
C(6)	6816(6)	-2375(2)	405(1)	87(1)
C(7)	7408(3)	-233(2)	1302(1)	35(1)
C(8)	6848(3)	393(2)	1862(1)	34(1)
C(9)	6439(3)	1539(2)	1796(1)	36(1)
C(10)	6570(3)	2084(2)	1211(1)	33(1)
C(11)	7122(3)	1491(2)	663(1)	33(1)
C(12)	7522(3)	321(2)	724(1)	36(1)
C(13)	7220(3)	2057(2)	72(1)	35(1)
C(15)	6996(3)	3696(2)	-597(1)	33(1)
C(16)	7721(3)	4767(2)	-658(1)	42(1)
C(17)	7702(3)	5308(2)	-1247(1)	44(1)
C(18)	6968(3)	4783(2)	-1768(1)	42(1)
C(19)	6224(3)	3725(2)	-1715(1)	40(1)
C(20)	6240(3)	3180(2)	-1124(1)	36(1)

Table S6. Bond lengths [Å] and angles [°] for compound **TQ-DFOB-Br**.

Br(1)-C(18)	1.8989(18)
F(1)-B(1)	1.371(3)
F(2)-B(1)	1.395(3)
N(1)-C(8)	1.352(2)
N(1)-C(3)	1.456(3)
N(1)-C(1)	1.459(3)
N(2)-C(7)	1.400(3)
N(2)-C(4)	1.422(3)
N(2)-C(5)	1.464(3)
N(3)-C(13)	1.322(2)
N(3)-C(15)	1.433(2)
N(3)-B(1)	1.565(3)
O(1)-C(10)	1.341(2)
O(1)-B(1)	1.447(3)
C(1)-C(2)	1.507(4)
C(1)-H(1A)	0.9700
C(1)-H(1B)	0.9700
C(2)-H(2A)	0.9600
C(2)-H(2B)	0.9600
C(2)-H(2C)	0.9600
C(3)-C(4)	1.470(3)
C(3)-H(3A)	0.9700
C(3)-H(3B)	0.9700
C(4)-H(4A)	0.9700
C(4)-H(4B)	0.9700
C(5)-C(6)	1.501(4)
C(5)-H(5A)	0.9700
C(5)-H(5B)	0.9700
C(6)-H(6A)	0.9600
C(6)-H(6B)	0.9600
C(6)-H(6C)	0.9600
C(7)-C(12)	1.370(3)
C(7)-C(8)	1.443(3)
C(8)-C(9)	1.395(3)
C(9)-C(10)	1.377(3)
C(9)-H(9A)	0.9300
C(10)-C(11)	1.401(3)
C(11)-C(13)	1.399(2)
C(11)-C(12)	1.419(3)
C(12)-H(12A)	0.9300
C(13)-H(13A)	0.9300
C(15)-C(20)	1.379(3)
C(15)-C(16)	1.385(3)

C(16)-C(17)	1.379(3)
C(16)-H(16A)	0.9300
C(17)-C(18)	1.367(3)
C(17)-H(17A)	0.9300
C(18)-C(19)	1.377(3)
C(19)-C(20)	1.386(3)
C(19)-H(19A)	0.9300
C(20)-H(20A)	0.9300
C(8)-N(1)-C(3)	121.16(17)
C(8)-N(1)-C(1)	122.93(17)
C(3)-N(1)-C(1)	115.72(16)
C(7)-N(2)-C(4)	115.3(2)
C(7)-N(2)-C(5)	118.67(17)
C(4)-N(2)-C(5)	117.20(19)
C(13)-N(3)-C(15)	120.04(15)
C(13)-N(3)-B(1)	119.39(15)
C(15)-N(3)-B(1)	120.54(14)
C(10)-O(1)-B(1)	121.29(17)
F(1)-B(1)-F(2)	110.58(18)
F(1)-B(1)-O(1)	108.6(2)
F(2)-B(1)-O(1)	109.78(19)
F(1)-B(1)-N(3)	110.10(17)
F(2)-B(1)-N(3)	107.7(2)
O(1)-B(1)-N(3)	110.08(16)
N(1)-C(1)-C(2)	113.3(2)
N(1)-C(1)-H(1A)	108.9
C(2)-C(1)-H(1A)	108.9
N(1)-C(1)-H(1B)	108.9
C(2)-C(1)-H(1B)	108.9
H(1A)-C(1)-H(1B)	107.7
C(1)-C(2)-H(2A)	109.5
C(1)-C(2)-H(2B)	109.5
H(2A)-C(2)-H(2B)	109.5
C(1)-C(2)-H(2C)	109.5
H(2A)-C(2)-H(2C)	109.5
H(2B)-C(2)-H(2C)	109.5
N(1)-C(3)-C(4)	111.81(17)
N(1)-C(3)-H(3A)	109.3
C(4)-C(3)-H(3A)	109.3
N(1)-C(3)-H(3B)	109.3
C(4)-C(3)-H(3B)	109.3
H(3A)-C(3)-H(3B)	107.9
N(2)-C(4)-C(3)	112.6(2)

N(2)-C(4)-H(4A)	109.1
C(3)-C(4)-H(4A)	109.1
N(2)-C(4)-H(4B)	109.1
C(3)-C(4)-H(4B)	109.1
H(4A)-C(4)-H(4B)	107.8
N(2)-C(5)-C(6)	115.0(3)
N(2)-C(5)-H(5A)	108.5
C(6)-C(5)-H(5A)	108.5
N(2)-C(5)-H(5B)	108.5
C(6)-C(5)-H(5B)	108.5
H(5A)-C(5)-H(5B)	107.5
C(5)-C(6)-H(6A)	109.5
C(5)-C(6)-H(6B)	109.5
H(6A)-C(6)-H(6B)	109.5
C(5)-C(6)-H(6C)	109.5
H(6A)-C(6)-H(6C)	109.5
H(6B)-C(6)-H(6C)	109.5
C(12)-C(7)-N(2)	123.29(18)
C(12)-C(7)-C(8)	118.71(17)
N(2)-C(7)-C(8)	117.90(16)
N(1)-C(8)-C(9)	120.89(18)
N(1)-C(8)-C(7)	120.16(17)
C(9)-C(8)-C(7)	118.95(16)
C(10)-C(9)-C(8)	121.50(17)
C(10)-C(9)-H(9A)	119.3
C(8)-C(9)-H(9A)	119.3
O(1)-C(10)-C(9)	119.21(17)
O(1)-C(10)-C(11)	120.42(16)
C(9)-C(10)-C(11)	120.35(17)
C(13)-C(11)-C(10)	119.35(17)
C(13)-C(11)-C(12)	122.08(17)
C(10)-C(11)-C(12)	118.55(16)
C(7)-C(12)-C(11)	121.94(17)
C(7)-C(12)-H(12A)	119.0
C(11)-C(12)-H(12A)	119.0
N(3)-C(13)-C(11)	122.08(16)
N(3)-C(13)-H(13A)	119.0
C(11)-C(13)-H(13A)	119.0
C(20)-C(15)-C(16)	119.92(17)
C(20)-C(15)-N(3)	121.10(18)
C(16)-C(15)-N(3)	118.93(18)
C(17)-C(16)-C(15)	119.9(2)
C(17)-C(16)-H(16A)	120.1
C(15)-C(16)-H(16A)	120.1

C(18)-C(17)-C(16)	119.8(2)
C(18)-C(17)-H(17A)	120.1
C(16)-C(17)-H(17A)	120.1
C(17)-C(18)-C(19)	121.19(17)
C(17)-C(18)-Br(1)	119.51(17)
C(19)-C(18)-Br(1)	119.28(16)
C(18)-C(19)-C(20)	119.17(19)
C(18)-C(19)-H(19A)	120.4
C(20)-C(19)-H(19A)	120.4
C(15)-C(20)-C(19)	120.07(19)
C(15)-C(20)-H(20A)	120.0
C(19)-C(20)-H(20A)	120.0

Table S7. Anisotropic displacement parameters ($\text{\AA}^2 \times 10^3$) for compound **TQ-DFOB-Br**. Formula for the anisotropic displacement factor exponent: $-2\pi^2 [h^2 a^{*2} U^{11} + \dots + 2 h k a^* b^* U^{12}]$.

	U11	U22	U33	U23	U13	U12
Br(1)	61(1)	79(1)	43(1)	28(1)	10(1)	12(1)
F(1)	100(1)	38(1)	38(1)	3(1)	10(1)	26(1)
F(2)	86(1)	73(1)	45(1)	-8(1)	-8(1)	-29(1)
N(1)	50(1)	36(1)	37(1)	9(1)	5(1)	0(1)
N(2)	72(2)	30(1)	50(1)	3(1)	8(1)	8(1)
N(3)	45(1)	30(1)	26(1)	0(1)	3(1)	2(1)
O(1)	78(1)	30(1)	30(1)	1(1)	13(1)	13(1)
B(1)	58(2)	30(1)	29(1)	-4(1)	3(1)	0(1)
C(1)	61(2)	50(1)	35(1)	12(1)	10(1)	3(1)
C(2)	86(2)	92(2)	58(2)	-22(2)	-4(2)	3(2)
C(3)	59(2)	38(1)	51(1)	16(1)	-1(1)	-1(1)
C(4)	80(2)	36(1)	60(1)	13(1)	-5(2)	2(1)
C(5)	85(2)	35(1)	66(2)	-2(1)	0(2)	15(1)
C(6)	131(3)	47(2)	84(2)	-15(1)	-15(2)	-9(2)
C(7)	38(1)	25(1)	42(1)	3(1)	2(1)	-1(1)
C(8)	32(1)	36(1)	33(1)	3(1)	0(1)	-4(1)
C(9)	47(2)	32(1)	30(1)	-1(1)	5(1)	4(1)
C(10)	40(1)	27(1)	32(1)	-1(1)	2(1)	0(1)
C(11)	43(1)	27(1)	30(1)	-1(1)	2(1)	-1(1)
C(12)	42(1)	33(1)	34(1)	-6(1)	4(1)	0(1)
C(13)	44(1)	32(1)	28(1)	-4(1)	1(1)	1(1)
C(15)	39(1)	34(1)	27(1)	2(1)	6(1)	5(1)
C(16)	48(1)	44(1)	35(1)	2(1)	1(1)	-1(1)
C(18)	40(1)	52(1)	35(1)	15(1)	11(1)	13(1)
C(19)	43(1)	49(1)	29(1)	-3(1)	3(1)	7(1)
C(20)	41(1)	32(1)	36(1)	-2(1)	5(1)	5(1)

Table S8. Hydrogen coordinates ($\times 10^4$) and isotropic displacement parameters ($\text{\AA}^2 \times 103$) for compound **TQ-DFOB-Br**.

	x	y	z	U(eq)
H(1A)	5810	-64	3339	59
H(1B)	5393	1029	2939	59
H(2A)	7455	1448	3721	118
H(2B)	8304	1606	3040	118
H(2C)	8709	516	3445	118
H(3A)	6436	-1662	2832	59
H(3B)	8391	-1370	2676	59
H(4A)	7589	-2682	1957	70
H(4B)	5840	-2046	1801	70
H(5A)	8936	-2724	958	74
H(5B)	9157	-1612	555	74
H(6A)	7223	-2804	42	131
H(6B)	6227	-1706	256	131
H(6C)	6021	-2828	653	131
H(9A)	6069	1945	2155	44
H(12A)	7872	-80	361	43
H(13A)	7459	1641	-299	42
H(16A)	8219	5121	-302	51
H(17A)	8187	6027	-1289	53
H(19A)	5717	3380	-2072	48
H(20A)	5739	2465	-1082	44

Table S9. Torsion angles [$^\circ$] for compound **TQ-DFOB-Br**.

C(10)-O(1)-B(1)-F(1)	152.67(19)
C(10)-O(1)-B(1)-F(2)	-86.3(2)
C(10)-O(1)-B(1)-N(3)	32.1(3)
C(13)-N(3)-B(1)-F(1)	-143.5(2)
C(15)-N(3)-B(1)-F(1)	38.5(3)
C(13)-N(3)-B(1)-F(2)	95.9(2)
C(15)-N(3)-B(1)-F(2)	-82.1(3)
C(13)-N(3)-B(1)-O(1)	-23.8(3)
C(15)-N(3)-B(1)-O(1)	158.2(2)
C(8)-N(1)-C(1)-C(2)	-82.5(3)
C(3)-N(1)-C(1)-C(2)	92.6(3)
C(8)-N(1)-C(3)-C(4)	-23.6(3)
C(1)-N(1)-C(3)-C(4)	161.2(2)
C(7)-N(2)-C(4)-C(3)	-52.0(3)
C(5)-N(2)-C(4)-C(3)	160.9(2)
N(1)-C(3)-C(4)-N(2)	48.2(3)
C(7)-N(2)-C(5)-C(6)	-72.9(3)
C(4)-N(2)-C(5)-C(6)	73.0(3)

C(4)-N(2)-C(7)-C(12)	-154.9(2)
C(5)-N(2)-C(7)-C(12)	-8.3(3)
C(4)-N(2)-C(7)-C(8)	28.8(3)
C(5)-N(2)-C(7)-C(8)	175.3(2)
C(3)-N(1)-C(8)-C(9)	-178.5(2)
C(1)-N(1)-C(8)-C(9)	-3.6(3)
C(3)-N(1)-C(8)-C(7)	1.0(3)
C(1)-N(1)-C(8)-C(7)	175.9(2)
C(12)-C(7)-C(8)-N(1)	-179.4(2)
N(2)-C(7)-C(8)-N(1)	-2.8(3)
C(12)-C(7)-C(8)-C(9)	0.1(3)
N(2)-C(7)-C(8)-C(9)	176.7(2)
N(1)-C(8)-C(9)-C(10)	179.0(2)
C(7)-C(8)-C(9)-C(10)	-0.5(3)
B(1)-O(1)-C(10)-C(9)	159.3(2)
B(1)-O(1)-C(10)-C(11)	-22.2(3)
C(8)-C(9)-C(10)-O(1)	178.6(2)
C(8)-C(9)-C(10)-C(11)	0.1(3)
O(1)-C(10)-C(11)-C(13)	0.5(3)
C(9)-C(10)-C(11)-C(13)	179.0(2)
O(1)-C(10)-C(11)-C(12)	-177.9(2)
C(9)-C(10)-C(11)-C(12)	0.6(3)
N(2)-C(7)-C(12)-C(11)	-175.8(2)
C(8)-C(7)-C(12)-C(11)	0.6(3)
C(13)-C(11)-C(12)-C(7)	-179.3(2)
C(10)-C(11)-C(12)-C(7)	-1.0(3)
C(15)-N(3)-C(13)-C(11)	-176.3(2)
B(1)-N(3)-C(13)-C(11)	5.6(4)
C(10)-C(11)-C(13)-N(3)	7.2(4)
C(12)-C(11)-C(13)-N(3)	-174.5(2)
C(13)-N(3)-C(15)-C(20)	38.9(3)
B(1)-N(3)-C(15)-C(20)	-143.1(2)
C(13)-N(3)-C(15)-C(16)	-143.8(2)
B(1)-N(3)-C(15)-C(16)	34.2(3)
C(20)-C(15)-C(16)-C(17)	-0.8(3)
N(3)-C(15)-C(16)-C(17)	-178.2(2)
C(15)-C(16)-C(17)-C(18)	0.0(3)
C(16)-C(17)-C(18)-C(19)	0.8(4)
C(16)-C(17)-C(18)-Br(1)	-177.49(18)
C(17)-C(18)-C(19)-C(20)	-0.7(3)
Br(1)-C(18)-C(19)-C(20)	177.56(18)
C(16)-C(15)-C(20)-C(19)	0.9(3)
N(3)-C(15)-C(20)-C(19)	178.2(2)
C(18)-C(19)-C(20)-C(15)	-0.1(3)

7. Ratiometric fluorescence response to TFA/TEA vapors

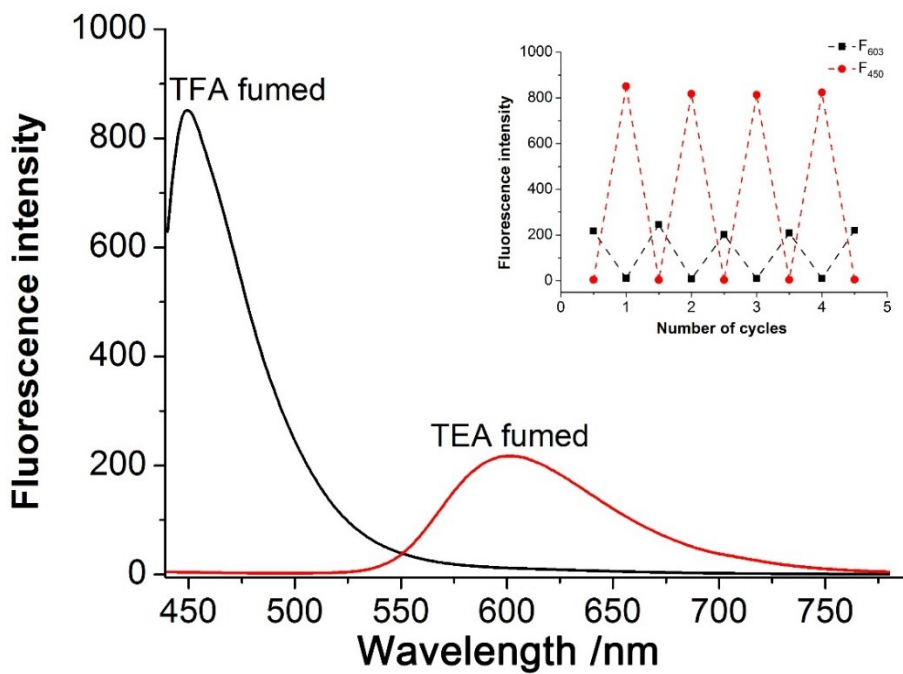


Figure S18. Fluorescence spectra of test trips containing compound **TQ-DFOB-NMe₂** fumed with TFA/TEA vapors. Inset: fluorescence switching by observing the intensity at 603 nm and 450 nm.

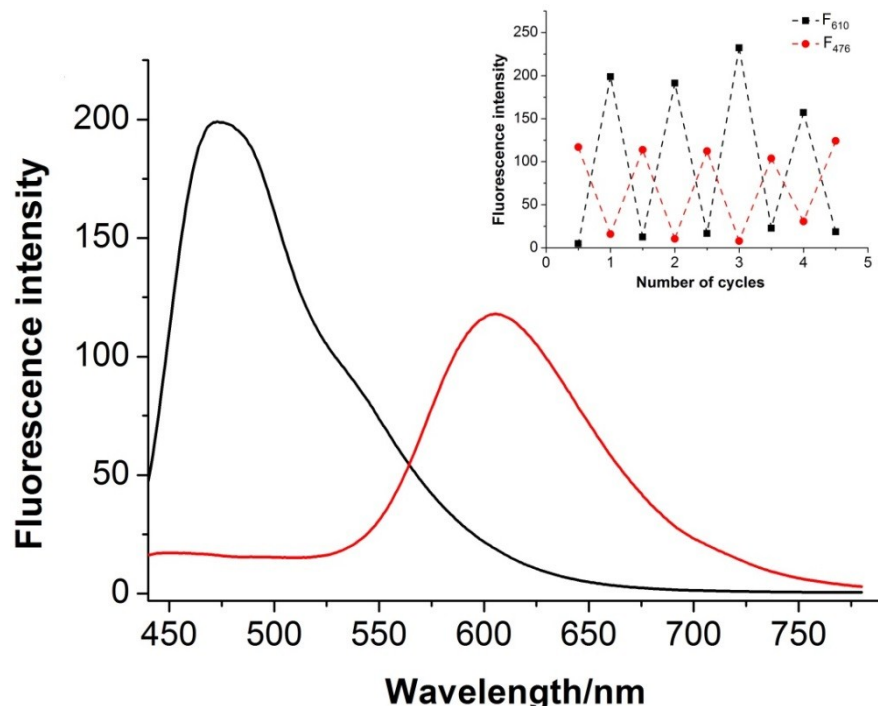


Figure S19. Fluorescence spectra of test trips containing compound **TQ-DFOB-OMe** fumed with TFA/TEA vapors. Inset: fluorescence switching by observing the intensity at 610 nm and 476 nm.

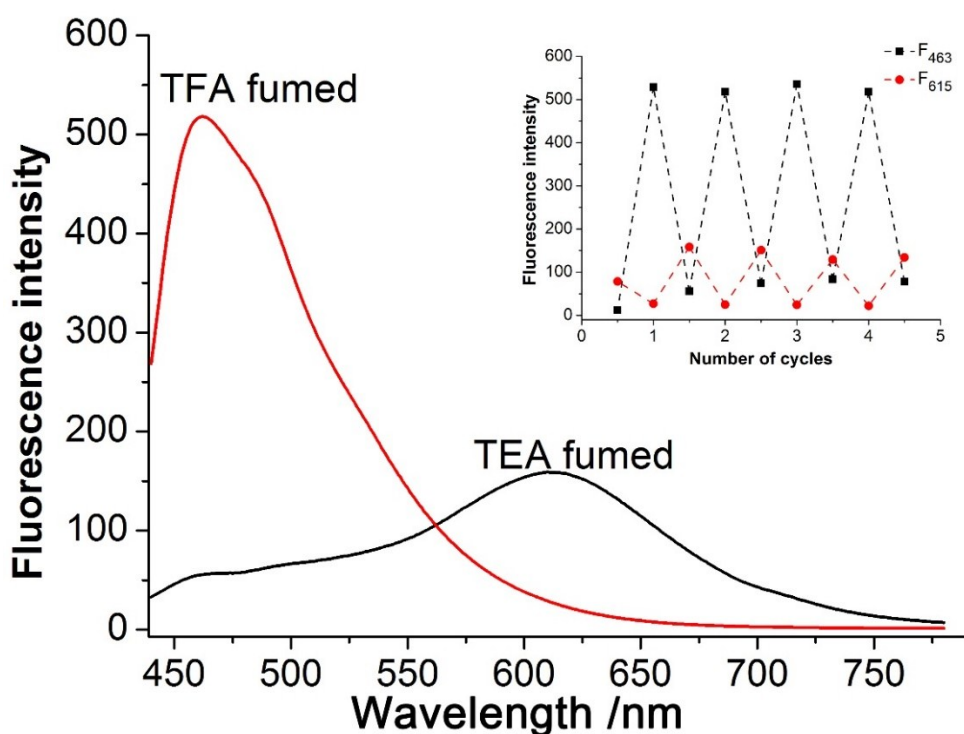


Figure S20. Fluorescence spectra of test trips containing compound **TQ-DFOB-NHCOMe** fumed with TFA/TEA vapors. Inset: fluorescence switching by observing the intensity at 615 nm and 463 nm.

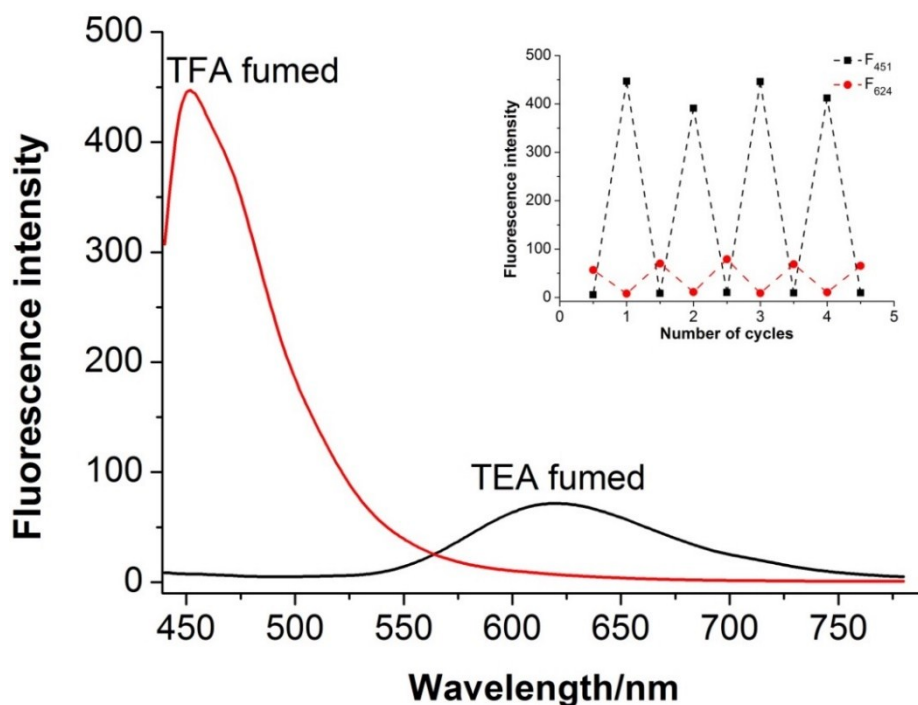


Figure S21. Fluorescence spectra of test trips containing compound **TQ-DFOB-Br** fumed with TFA/TEA vapors. Inset: fluorescence switching by observing the intensity at 624 nm and 451 nm.

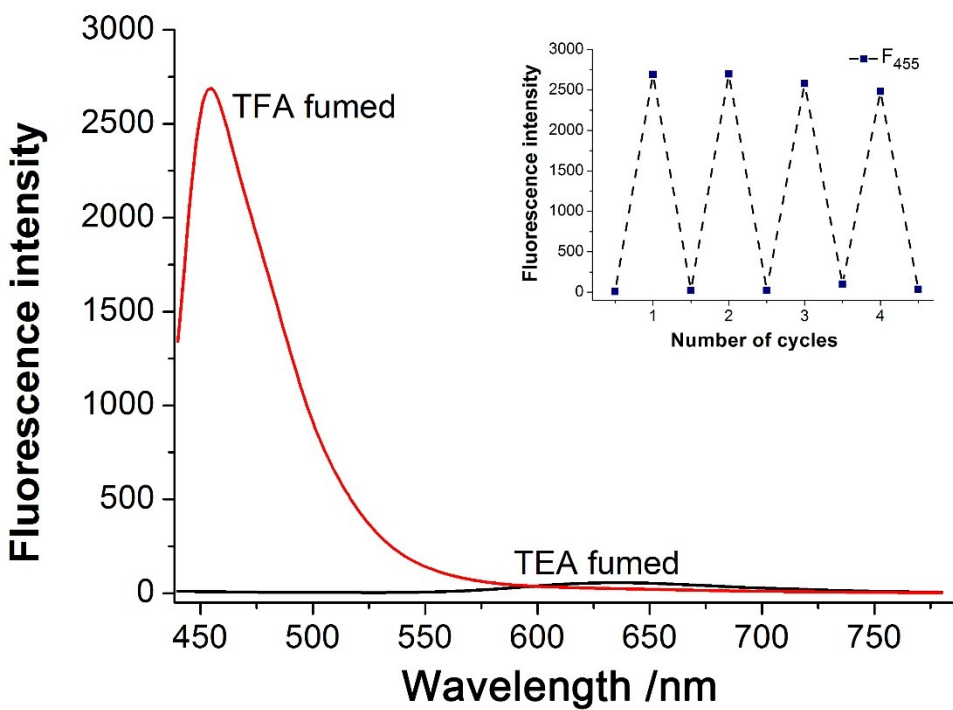


Figure S22. Fluorescence spectra of test trips containing compound **TQ-DFOB-CN** fumed with TFA/TEA vapors. Inset: fluorescence switching by observing the intensity at 455 nm.

8. Cell and zebrafish culture and fluorescence imaging

Hela cells were used for imaging and toxicity experiments. HeLa cells were cultured using DMEM (GIBCO, Invitrogen) medium with 10% fetal bovine and 1% dual antibody (streptomycin and penicillin) at 37 °C in a humidified 5% CO₂ incubator. When the number of adherent cells grow steadily in the culture bottle reaches 85-95%, the digestion is passed on. Discard the original culture medium, wash the adhered cells three times with phosphate buffer solution (PBS), add trypsin to digest the cells for three minutes, and then add culture medium containing 10% serum to stop digestion. The digested cell suspension was transferred to the centrifugal tube for centrifugation (800 r/min, 3min), the supernatant was discarded, and cells were suspended and precipitated by a mixture of serum and dual antibody media. The cell concentration (about 2*10⁵ cells/mL) was adjusted and transferred to 96 orifice plate and co-focusing plate for MTT and bioimaging experiment, respectively.

Zebrafish was cultured at 28 °C in E3 embryo media, consisting of 15 mM NaCl, 0.5 mM MgSO₄, 1 mM CaCl₂, 0.15 mM KH₂PO₄, 0.05 mM Na₂HPO₄, 0.7 mM NaHCO₃ and 1% methylene blue, whose pH = 7.5. Three-day old zebrafish was selected for the imaging experiments.

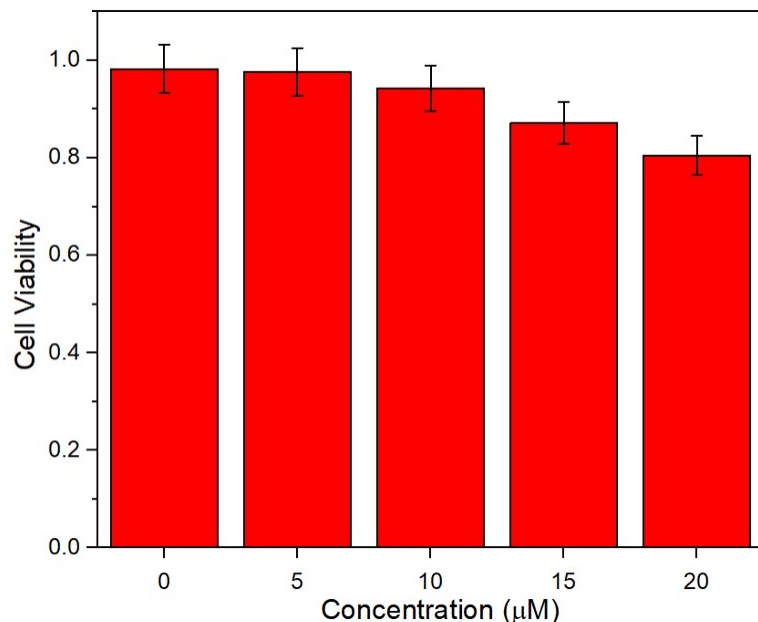


Figure S23. Cytotoxicity assay of **TQ-DFOB-SO₃H** at different concentrations in HeLa cells.

9. NMR and HRMS spectra

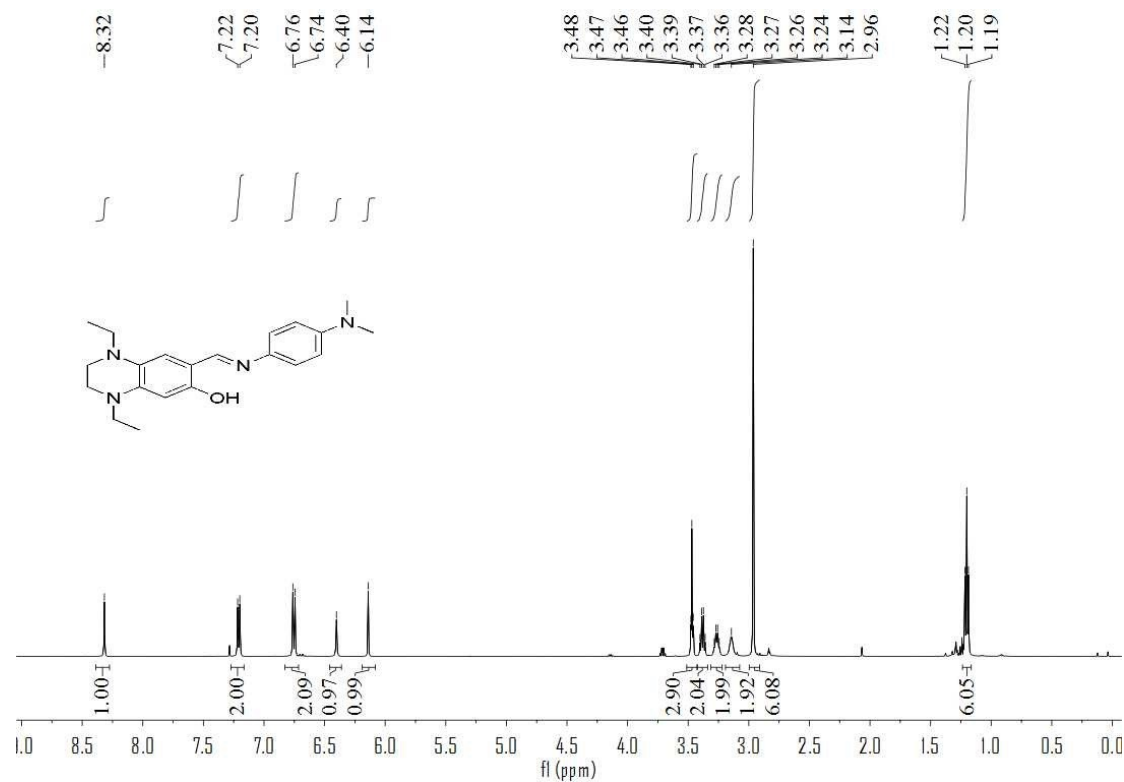


Figure S24. ^1H NMR spectrum of compound **1** in CDCl_3 .

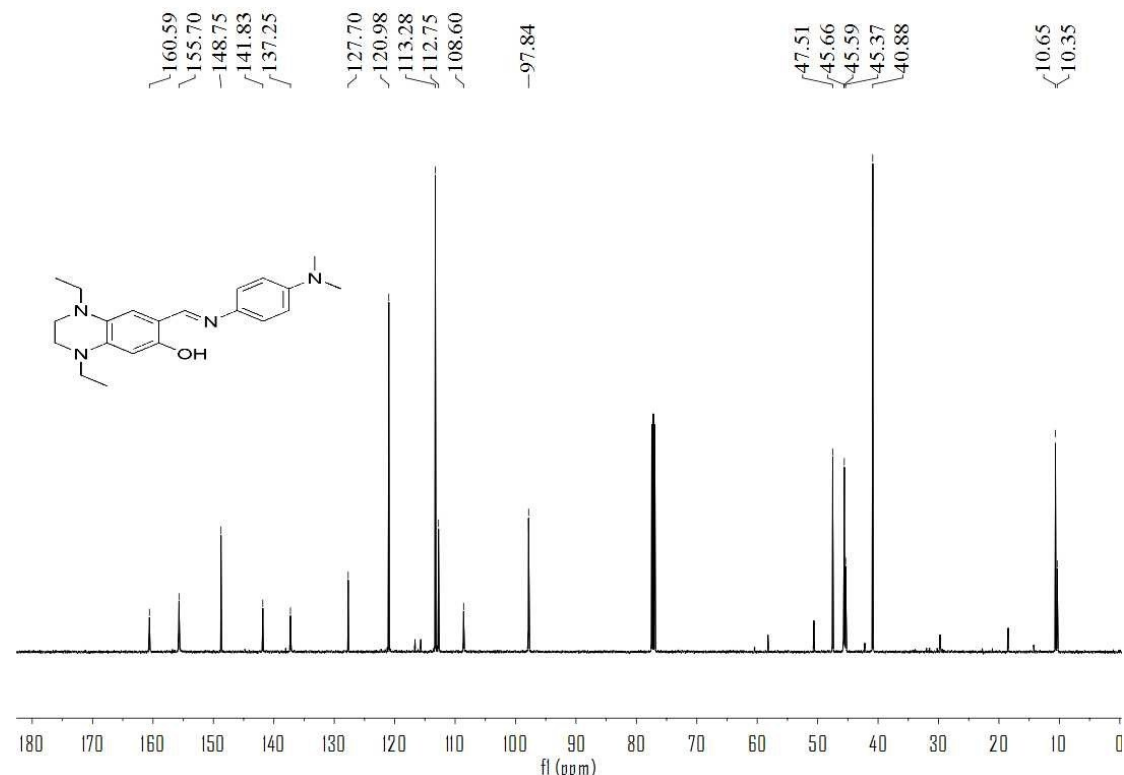


Figure S25. ^{13}C NMR spectrum of compound **1** in CDCl_3 .

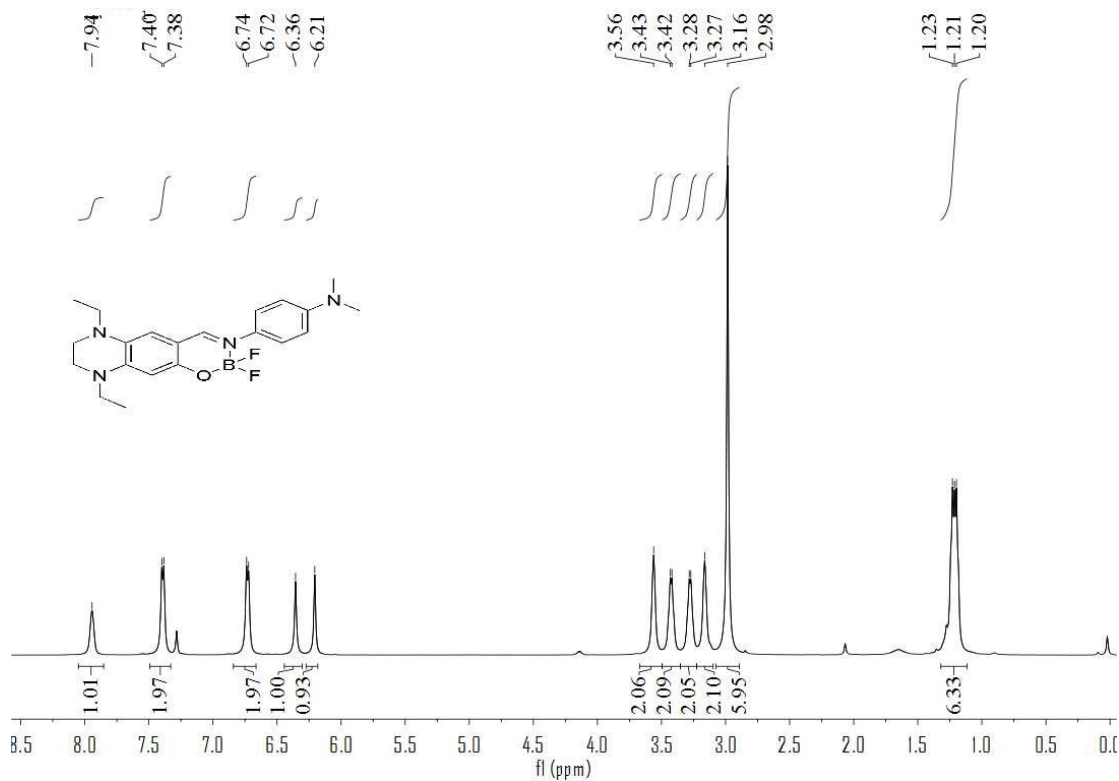


Figure S26. ¹H NMR spectrum of compound TQ-DFOB-NMe₂ in CDCl₃.

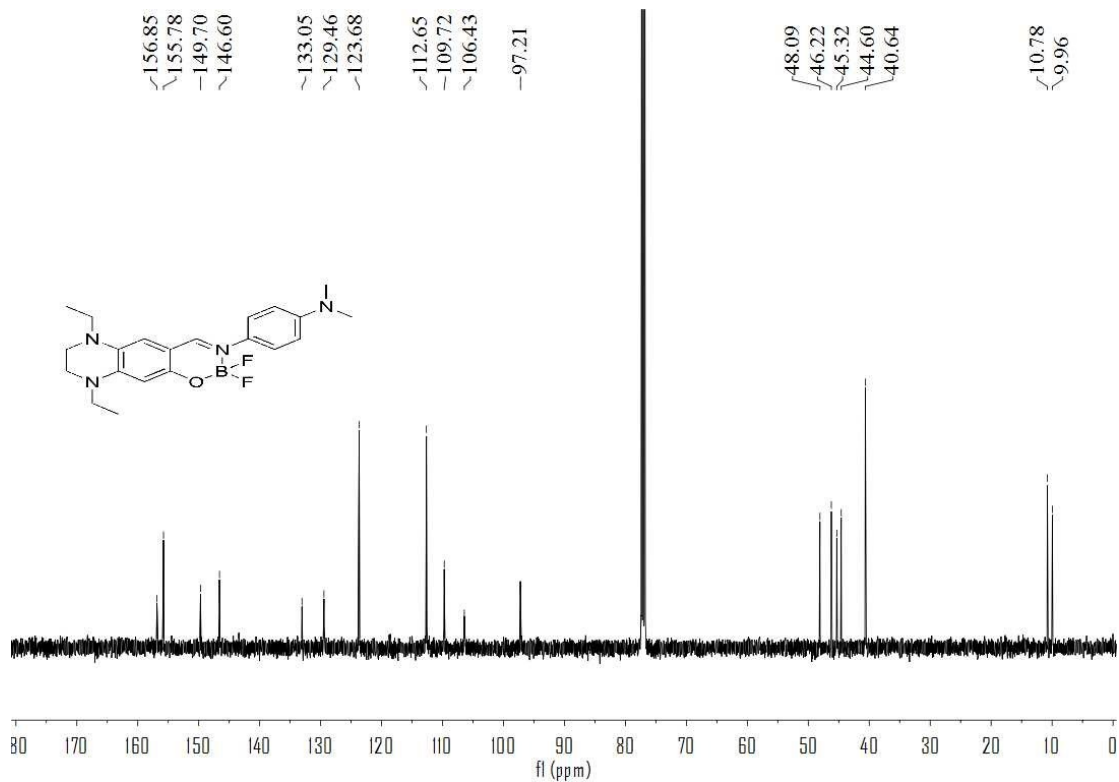


Figure S27. ¹³C NMR spectrum of compound TQ-DFOB-NMe₂ in CDCl₃.

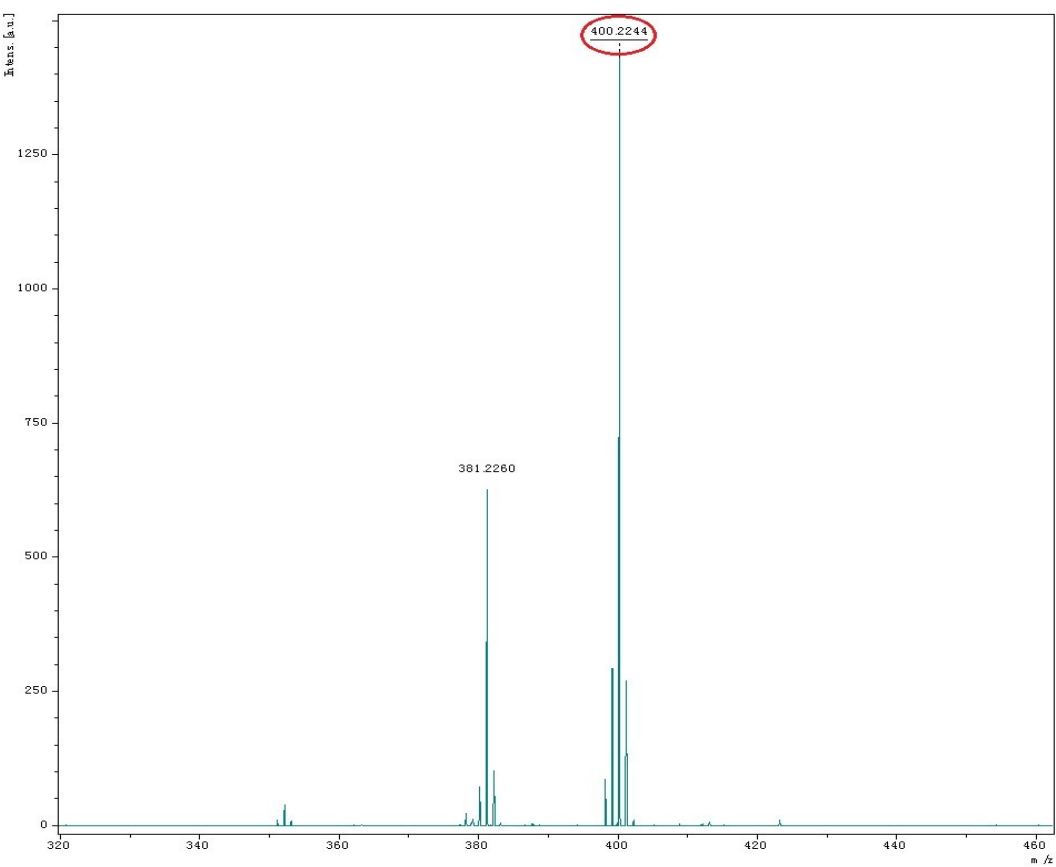


Figure S28. HRMS spectrum of **TQ-DFOB-NMe₂**.

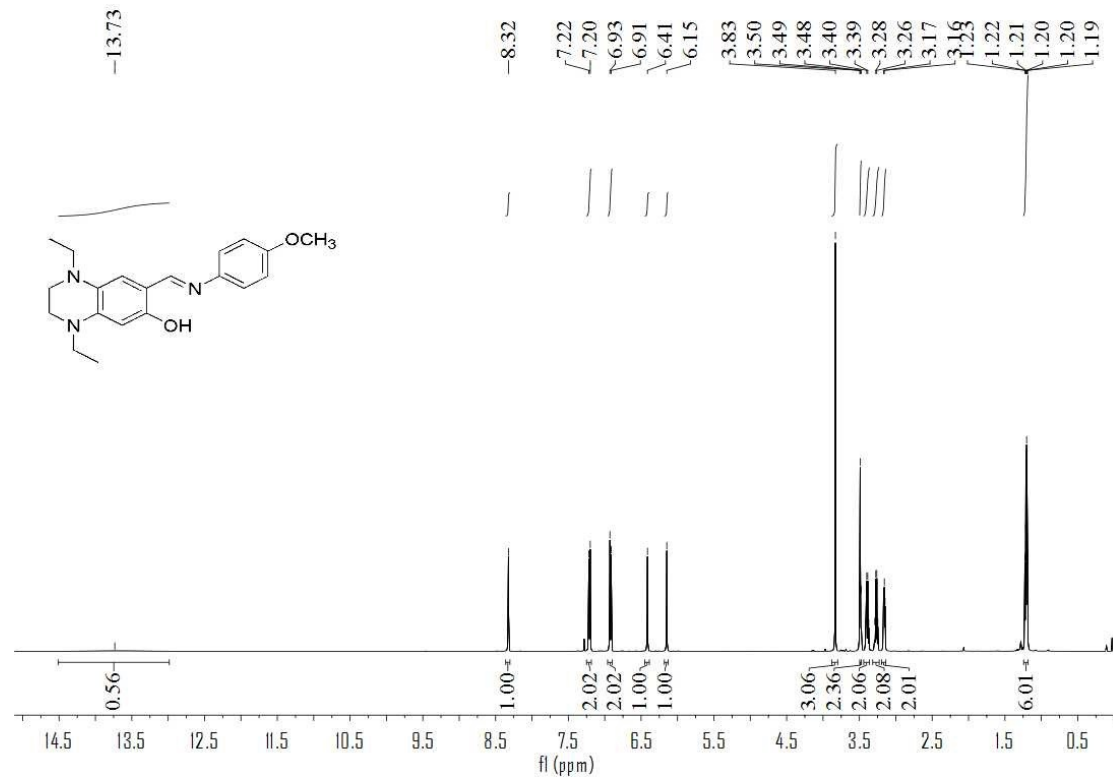


Figure S29. ¹H NMR spectrum of compound **2** in CDCl₃.

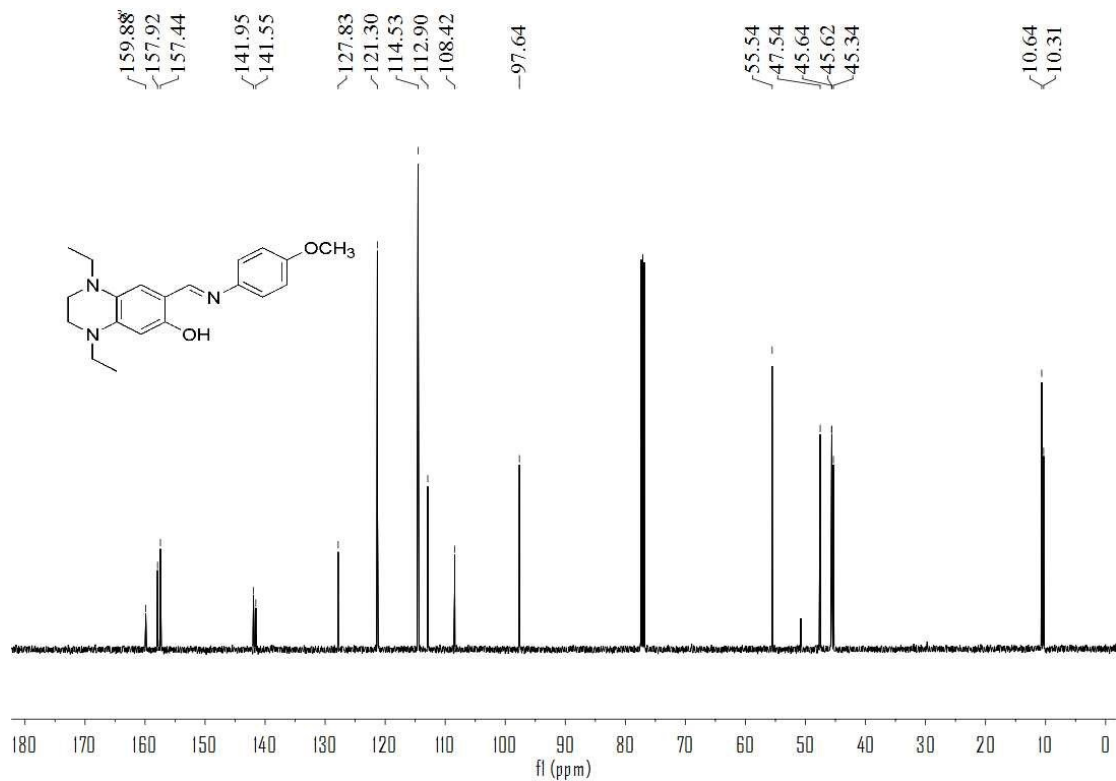


Figure S30. ^{13}C NMR spectrum of compound **2** in CDCl_3 .

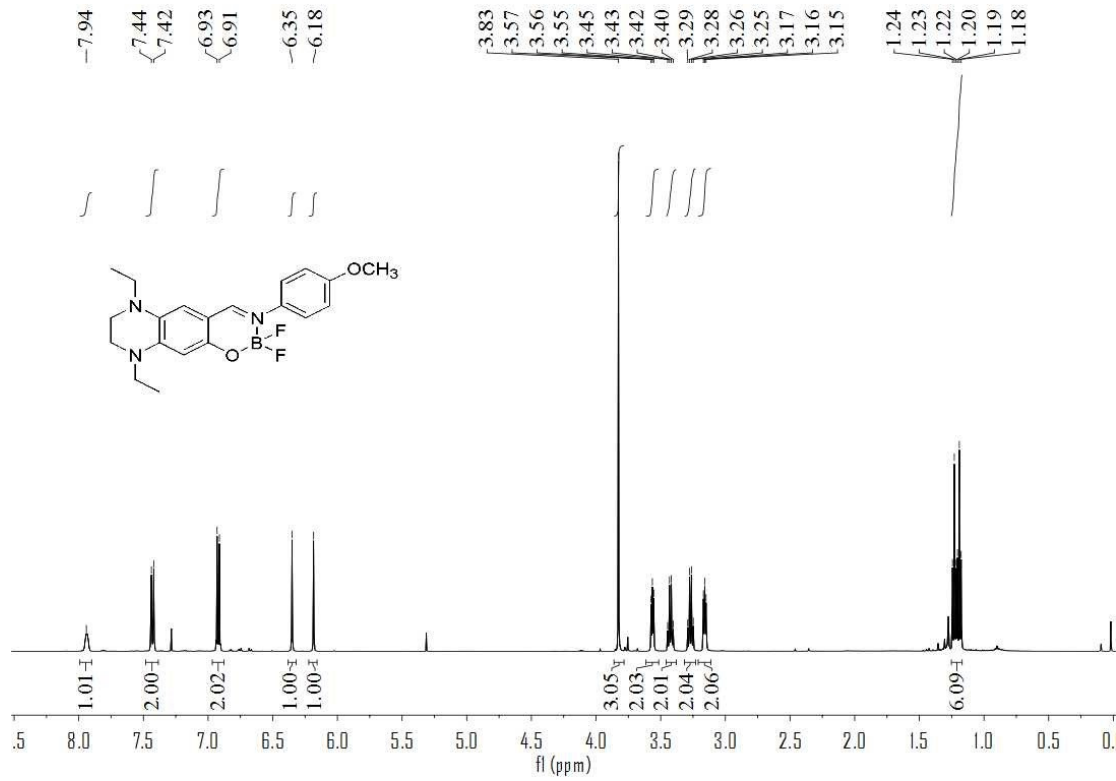


Figure S31. ^1H NMR spectrum of compound **TQ-DFOB-OMe** in CDCl_3 .

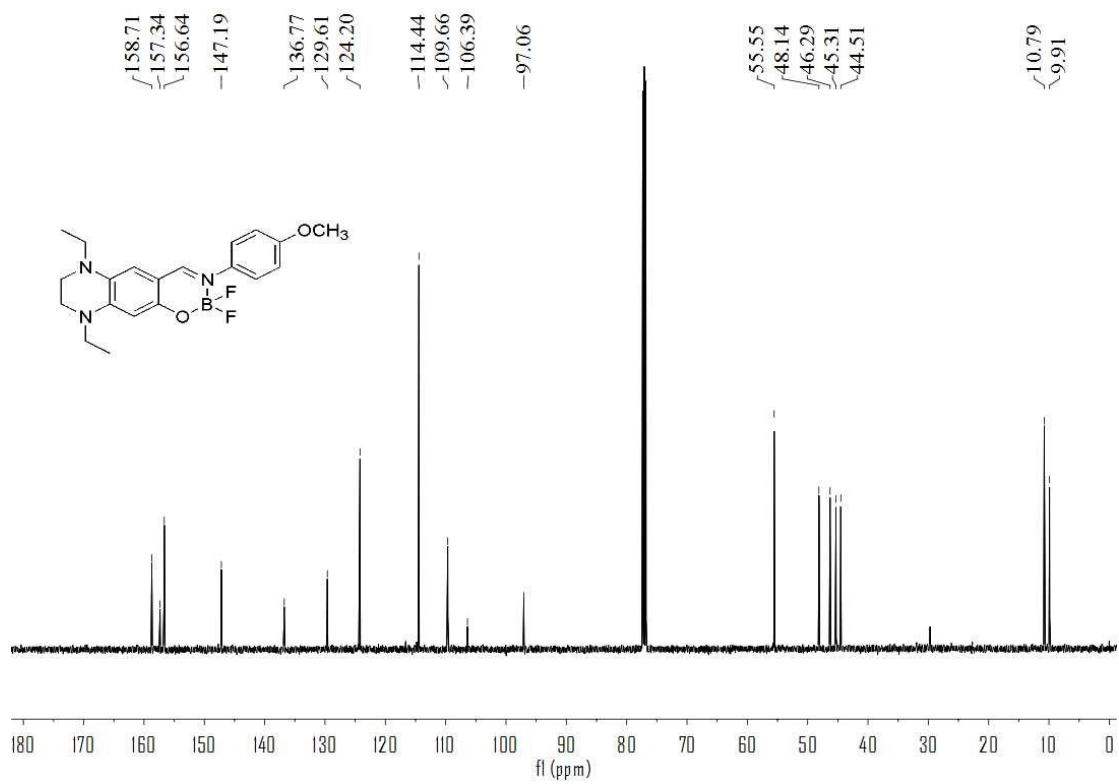


Figure S32. ^{13}C NMR spectrum of TQ-DFOB-OMe in CDCl_3 .

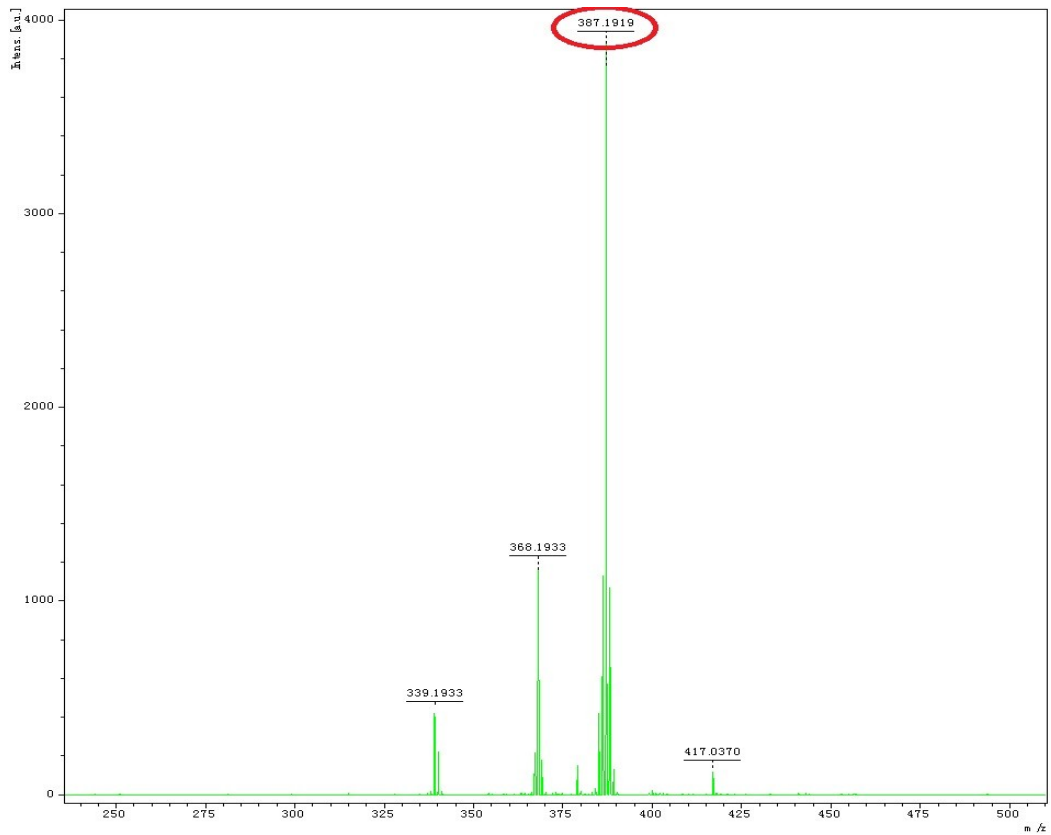


Figure S33. HRMS spectrum of TQ-DFOB-OMe.

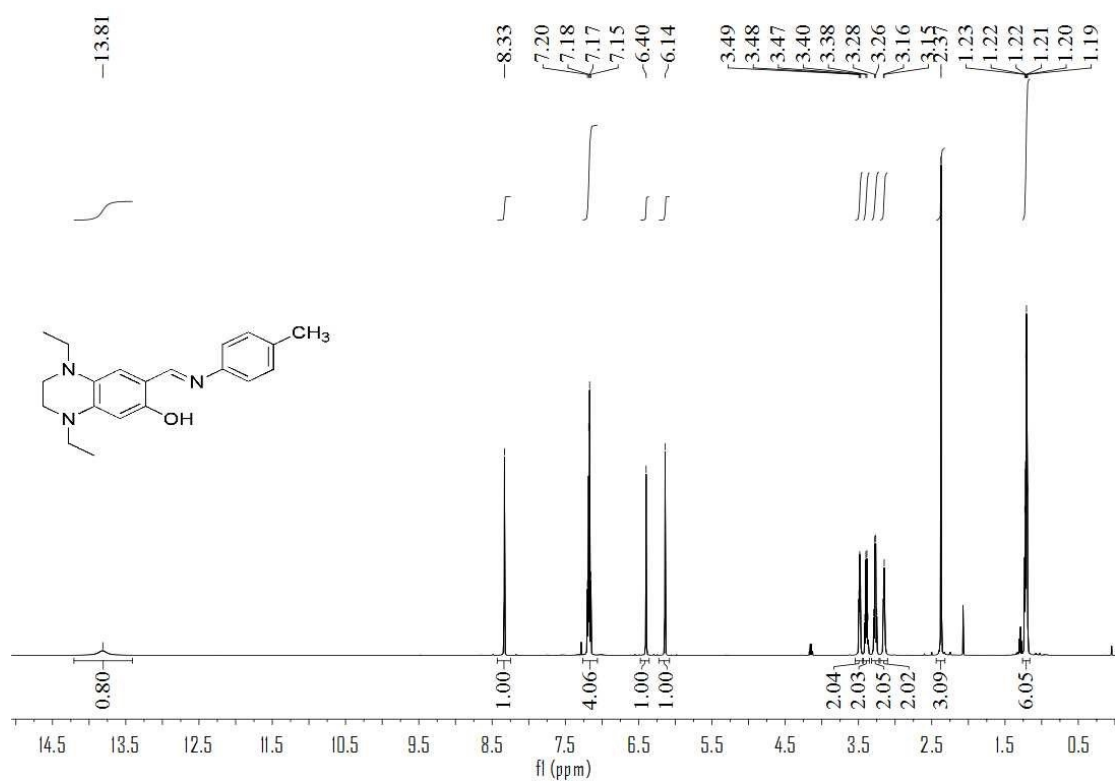


Figure S34. ^1H NMR spectrum of **3** in CDCl_3 .

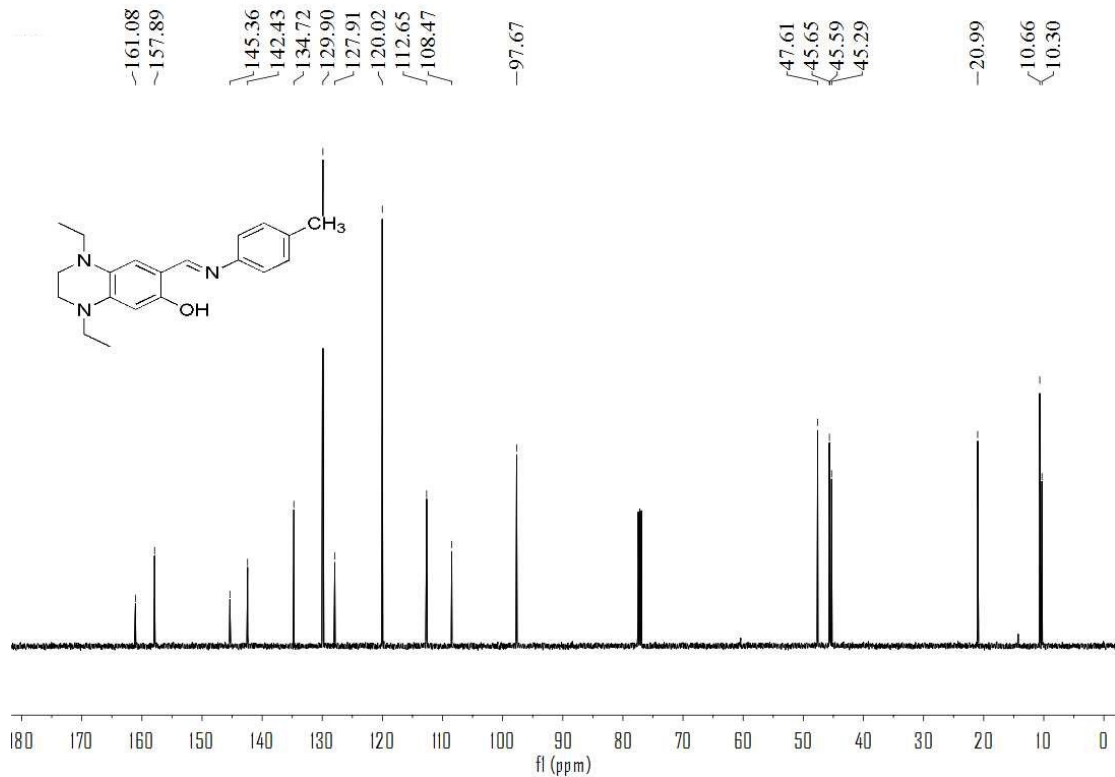


Figure S35. ^{13}C NMR spectrum of **3** in CDCl_3 .

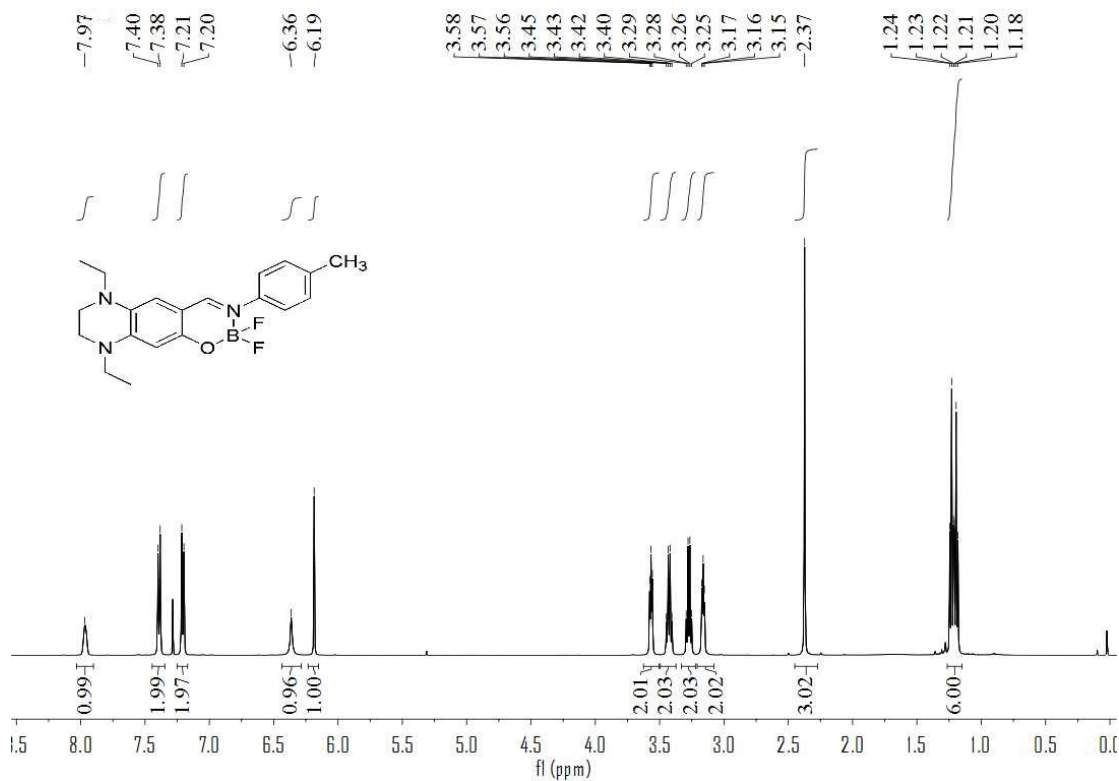


Figure S36. ^1H NMR spectrum of TQ-DFOB-Me in CDCl_3 .

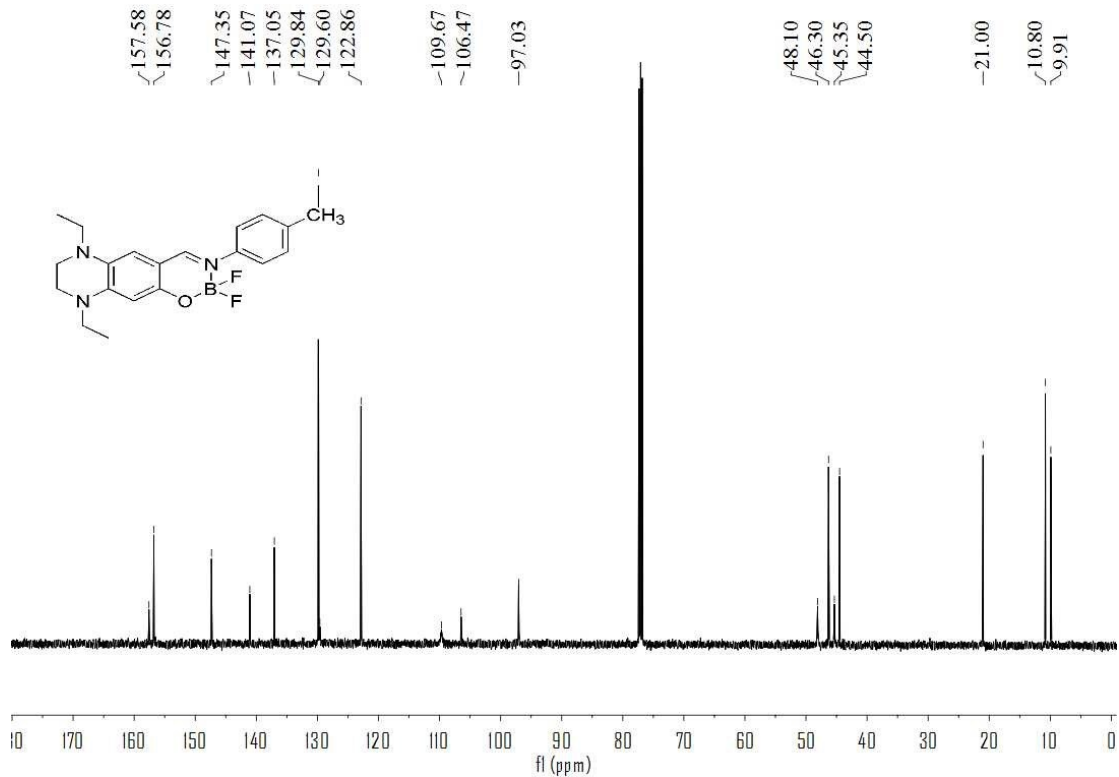


Figure S37. ^{13}C NMR spectrum of TQ-DFOB-Me in CDCl_3 .

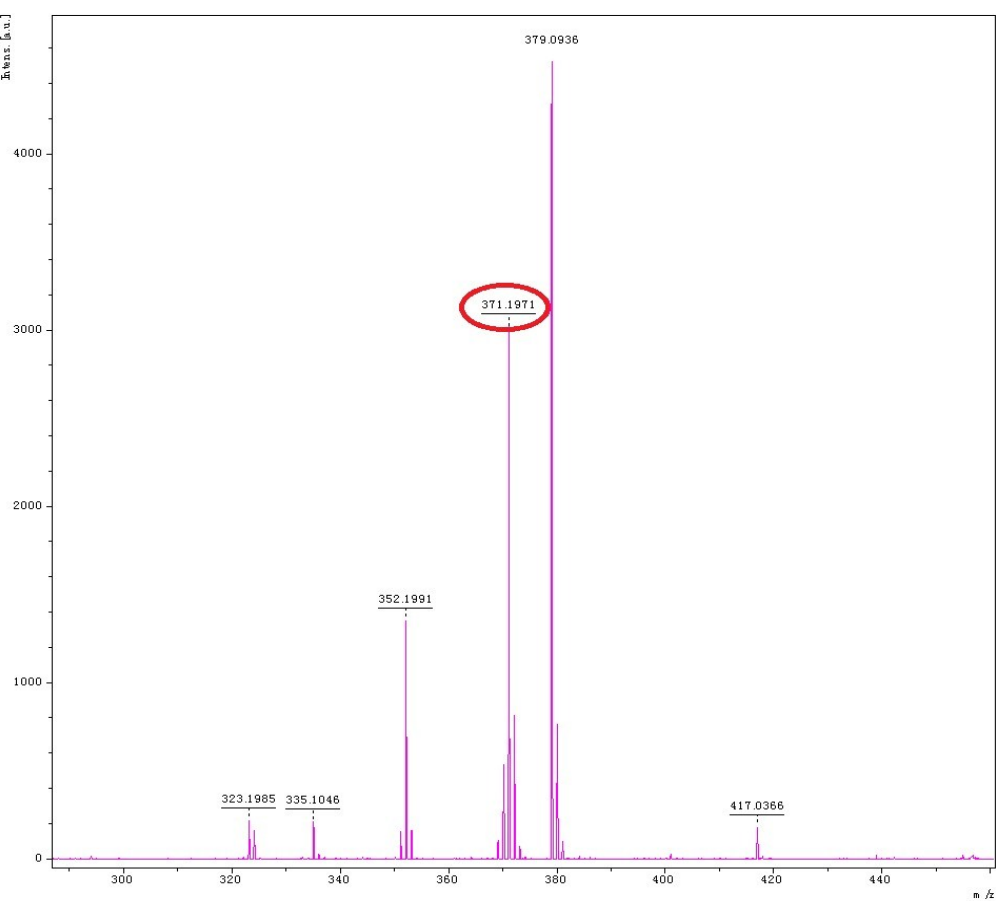


Figure S38. HRMS spectrum of TQ-DFOB-Me.

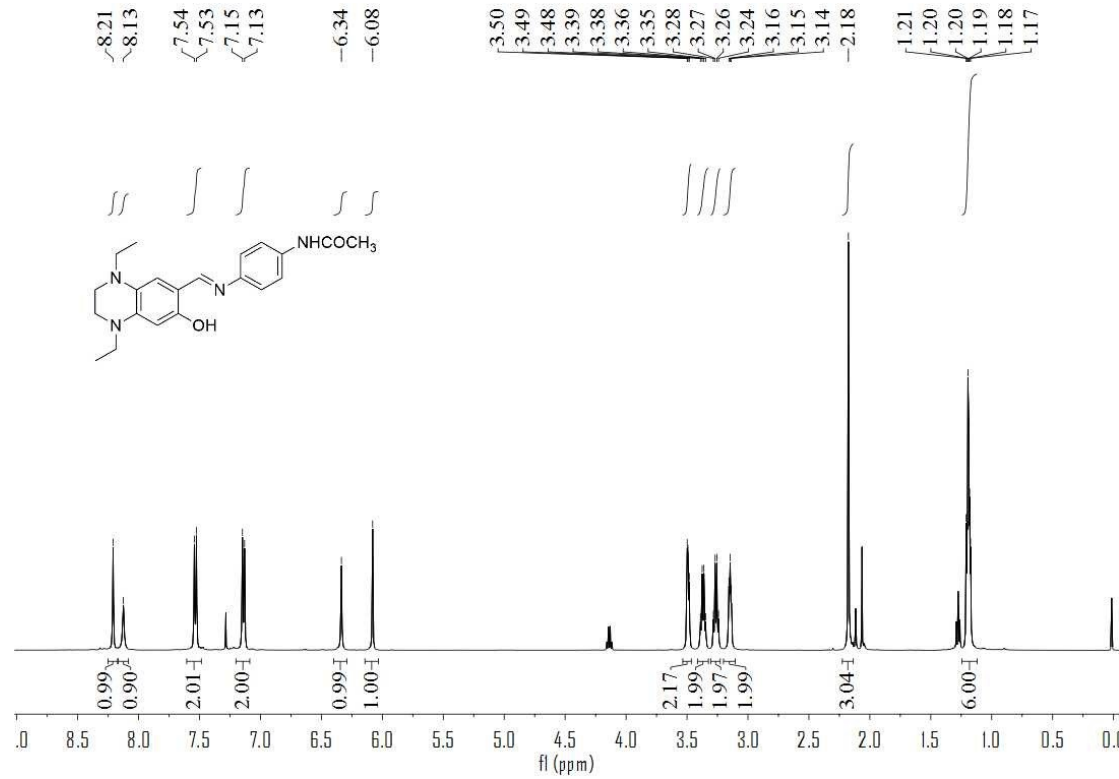


Figure S39. ^1H NMR spectrum of 4 in CDCl_3 .

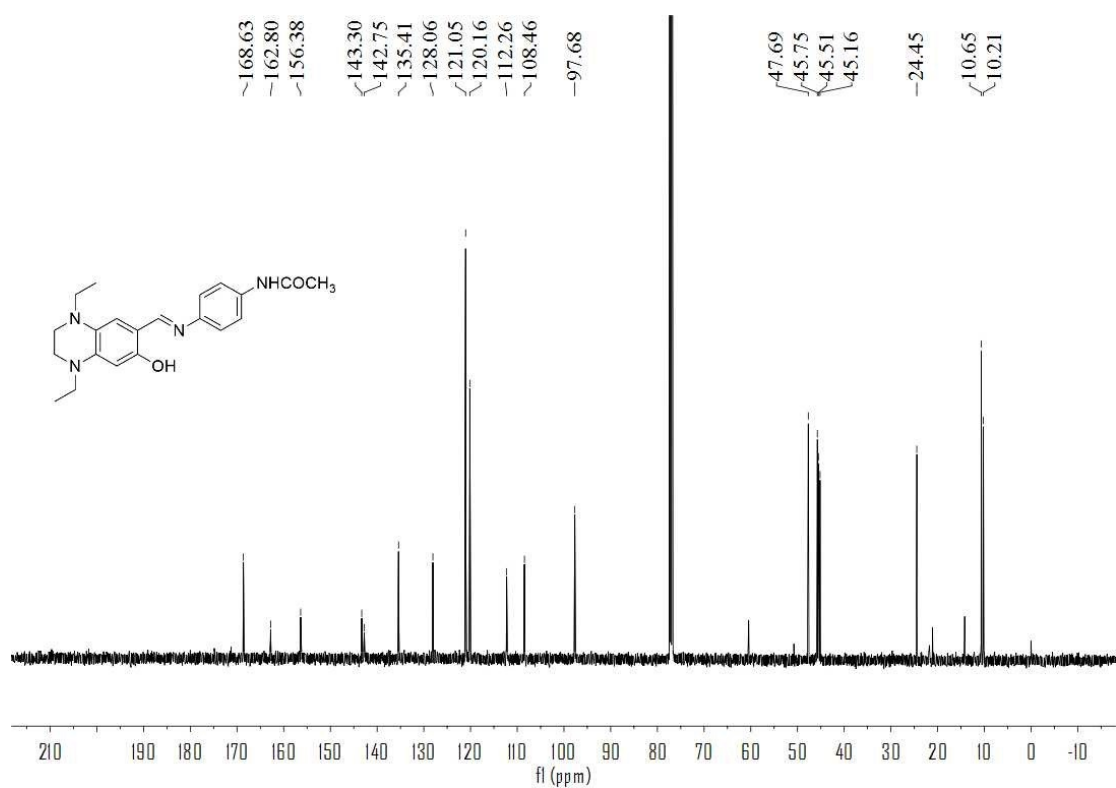


Figure S40. ^{13}C NMR spectrum of **4** in CDCl_3 .

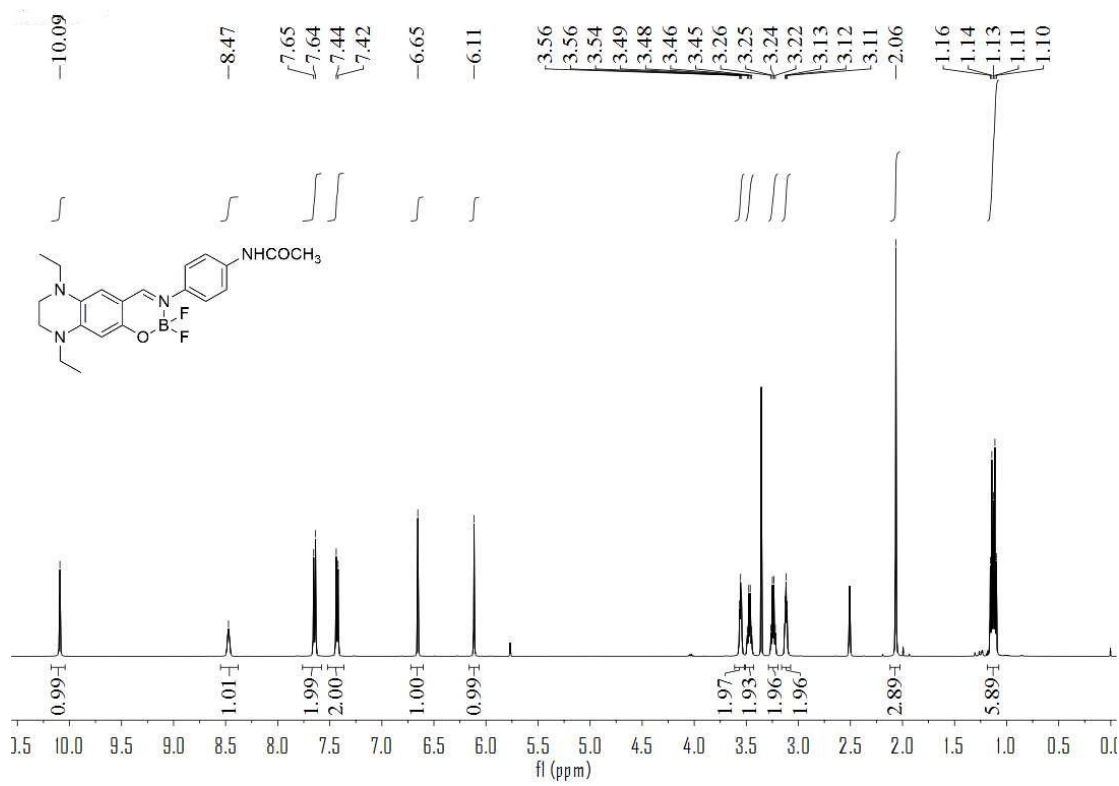


Figure S41. ^1H NMR spectrum of TQ-DFOB-NHCOMe in $\text{DMSO}-d_6$.

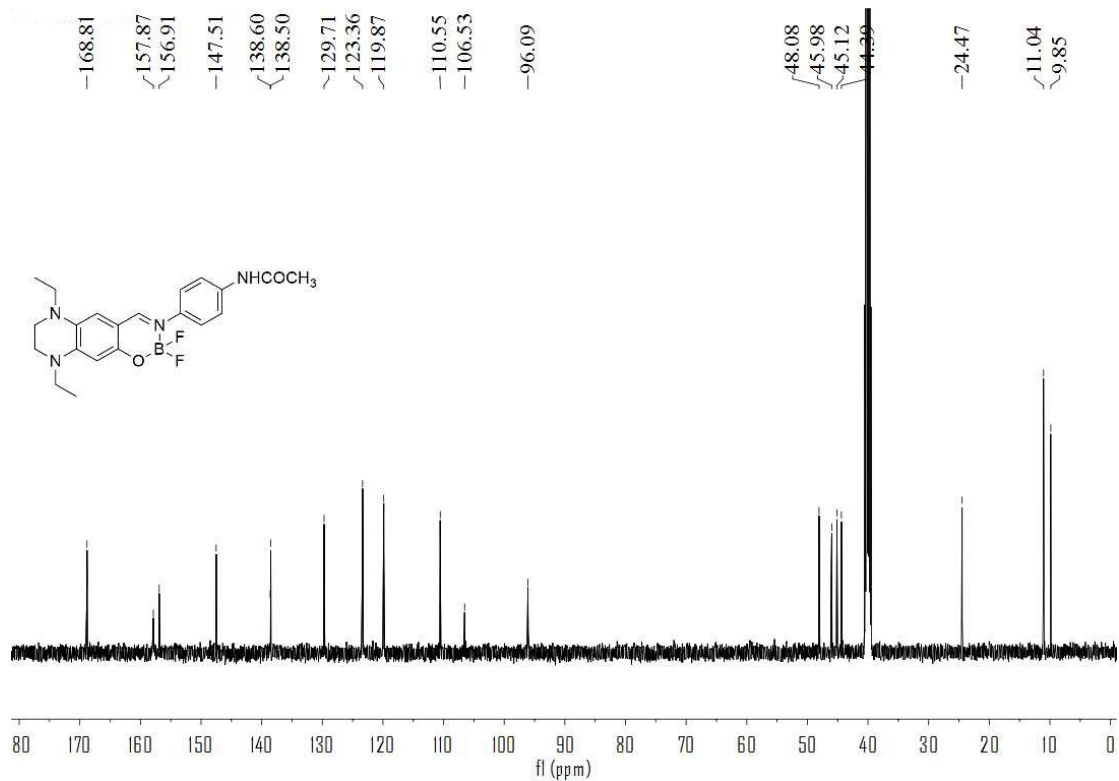


Figure S42. ^{13}C NMR spectrum of TQ-DFOB-NHCOMe in $\text{DMSO}-d_6$.

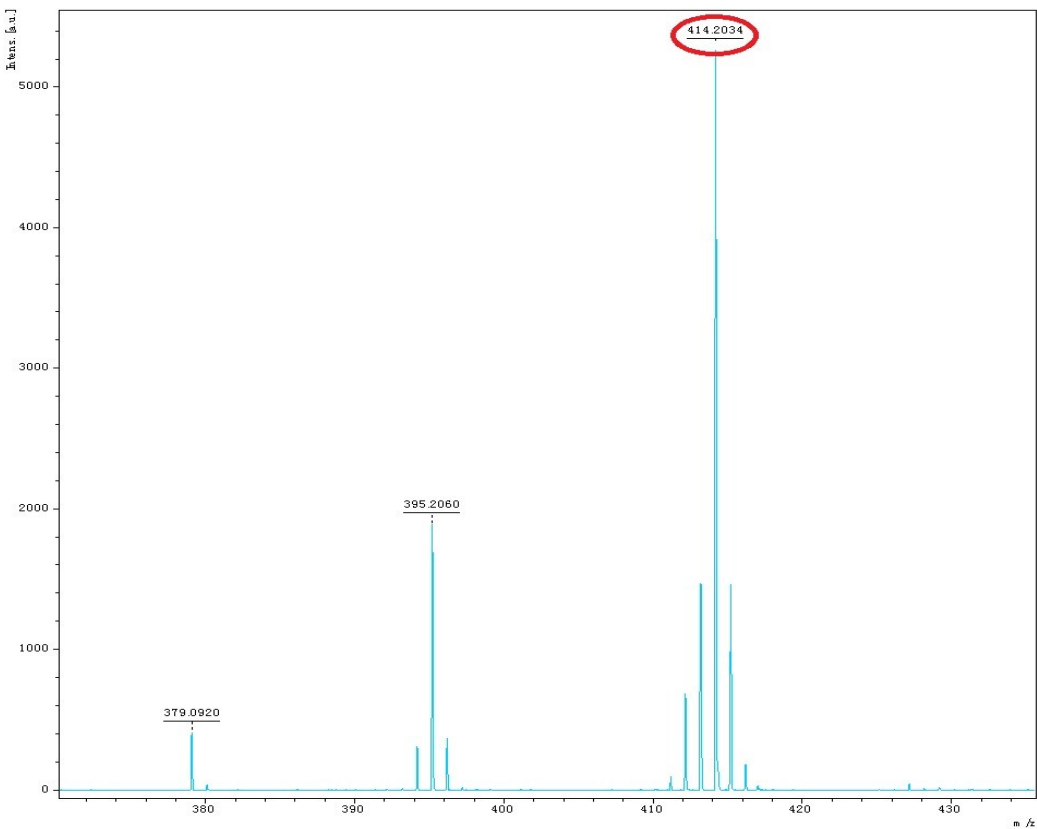


Figure S43. HRMS spectrum of TQ-DFOB-NHCOMe.

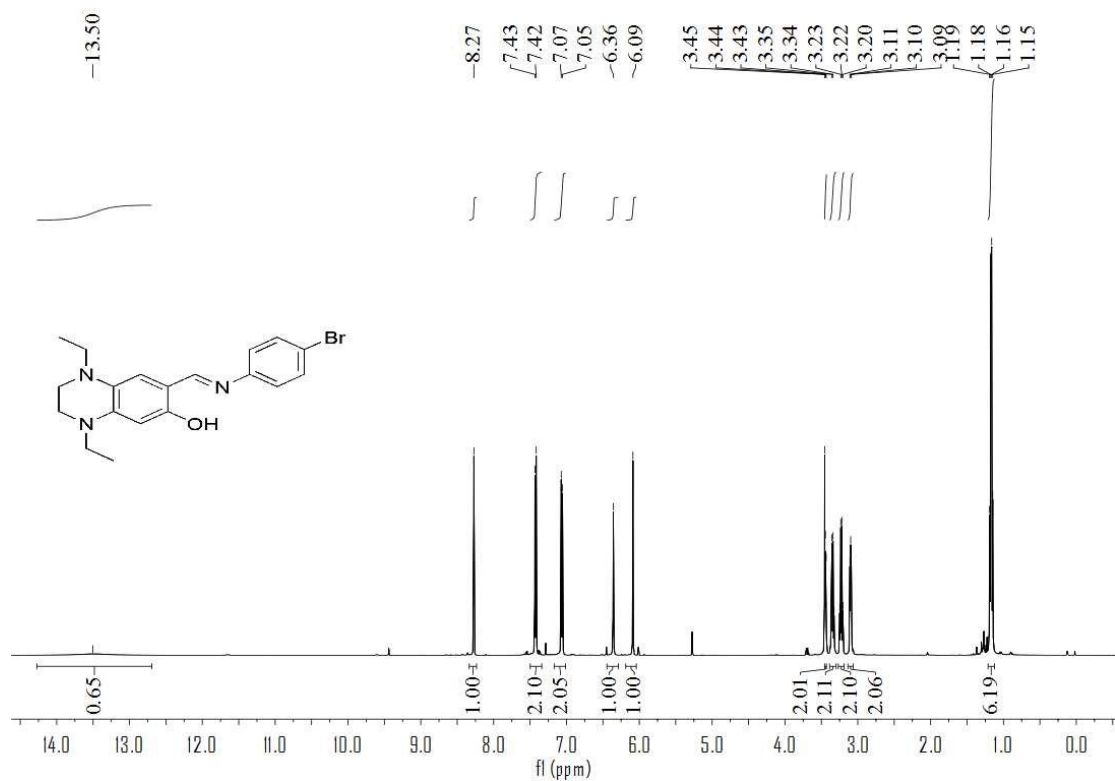


Figure S44. ^1H NMR spectrum of **5** in CDCl_3 .

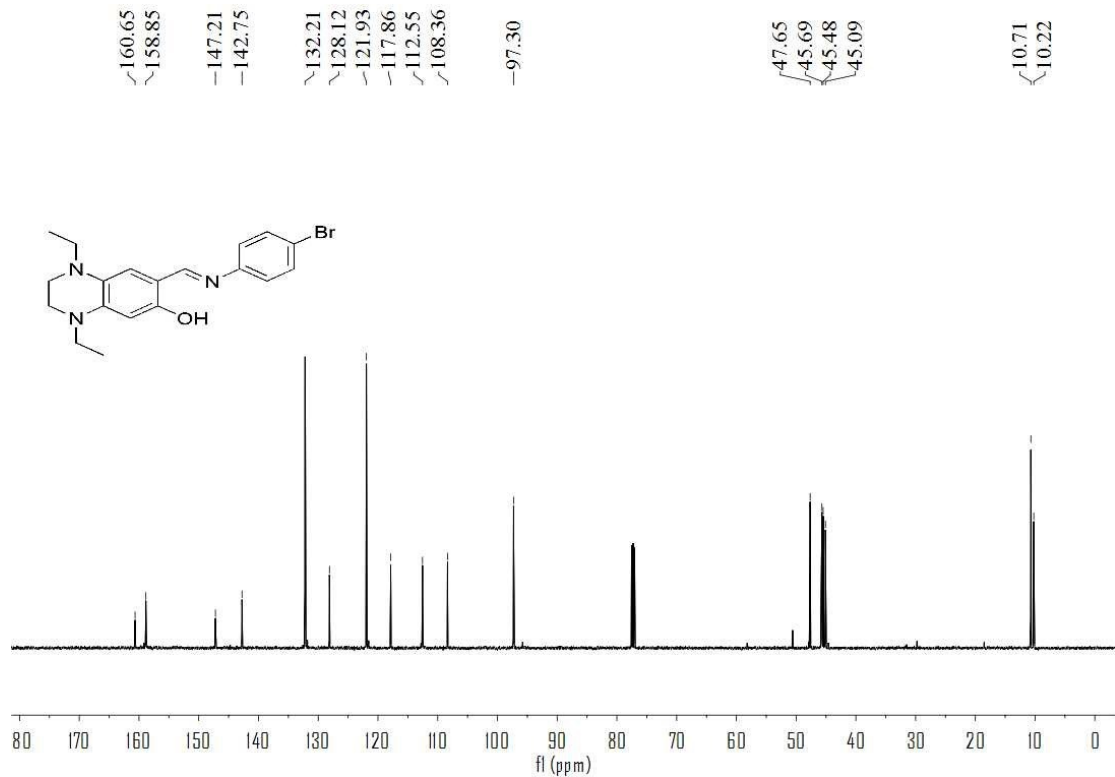


Figure S45. ^{13}C NMR spectrum of **5** in CDCl_3 .

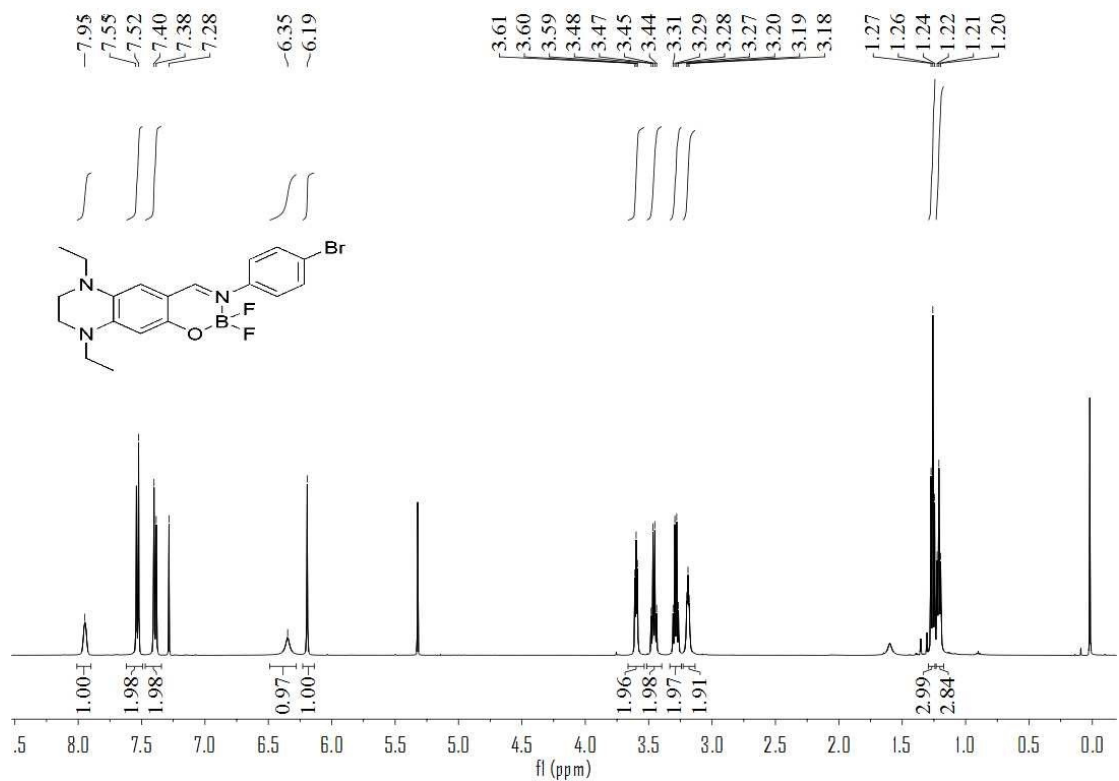


Figure S46. ^1H NMR spectrum of TQ-DFOB-Br in CDCl_3 .

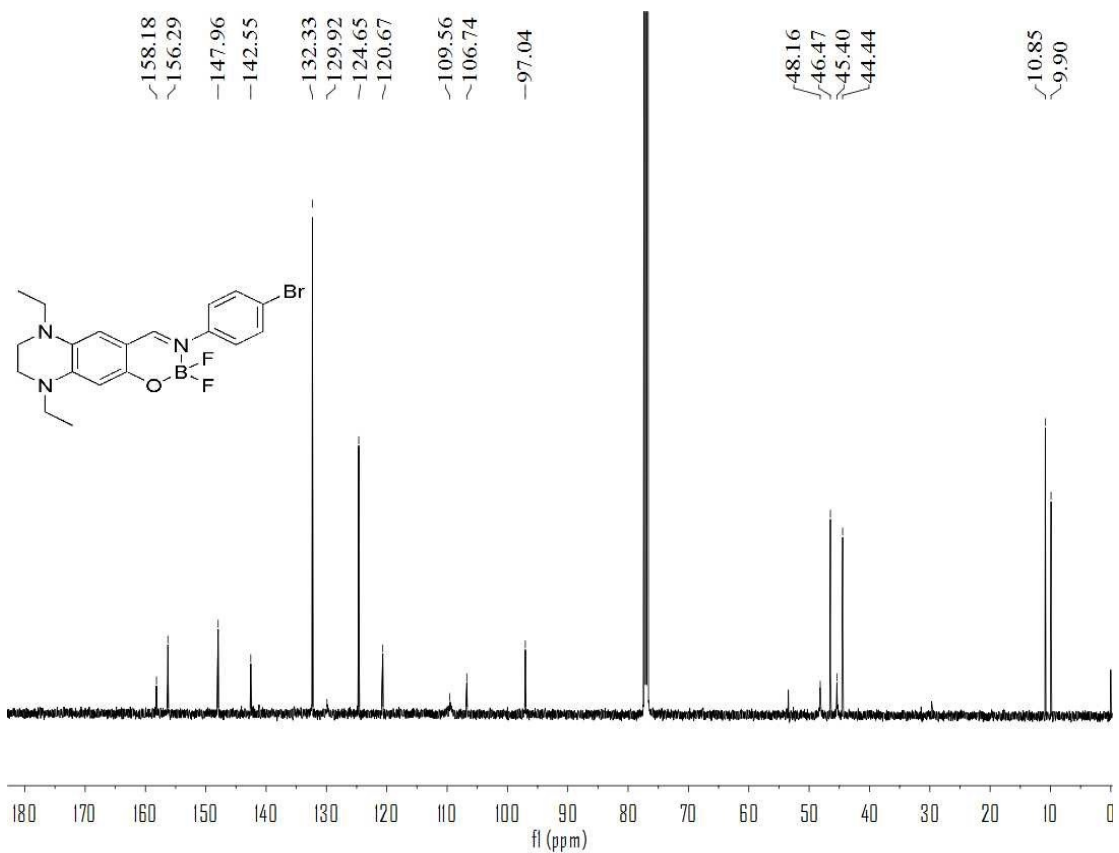


Figure S47. ^{13}C NMR spectrum of TQ-DFOB-Br in CDCl_3 .

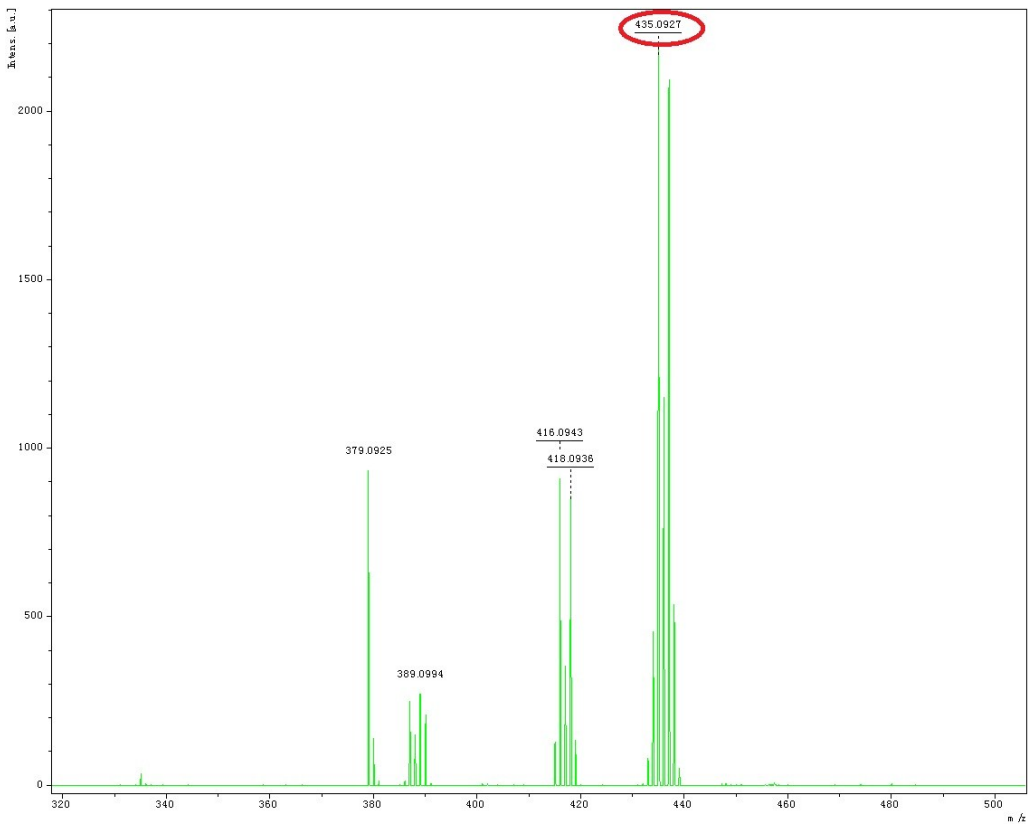


Figure S48. HRMS spectrum of TQ-DFOB-Br.

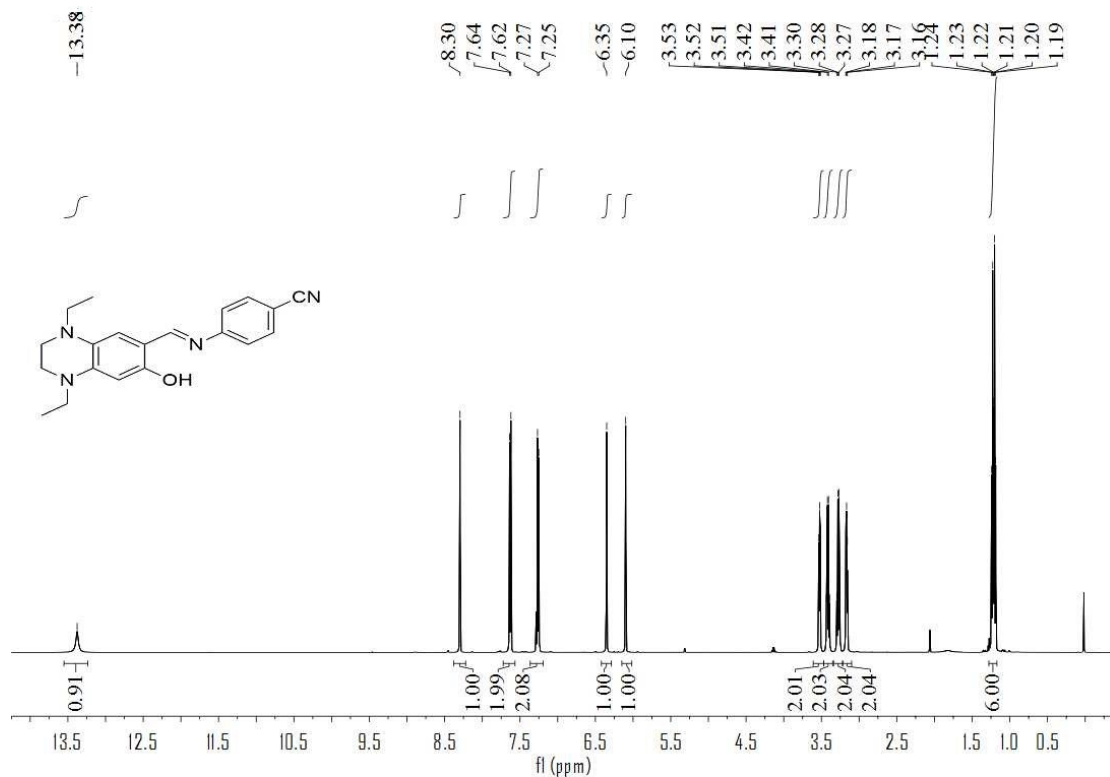


Figure S49. ^1H NMR spectrum of **6** in CDCl_3 .

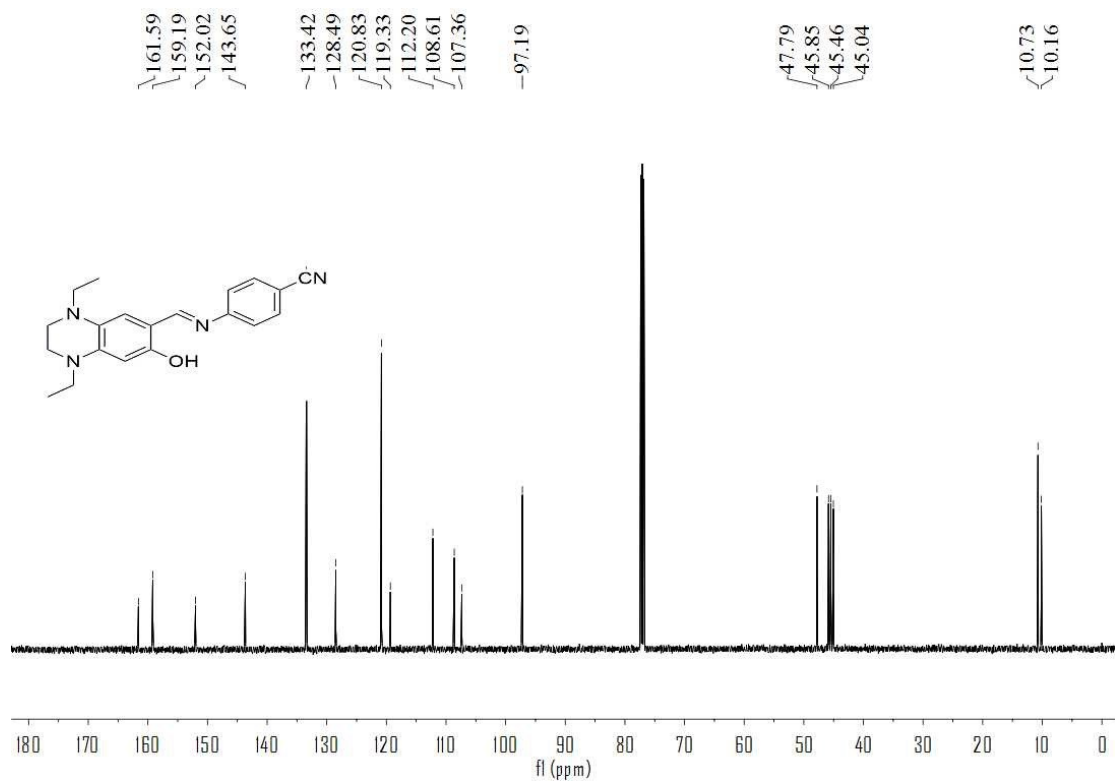


Figure S50. ^{13}C NMR spectrum of **6** in CDCl_3 .

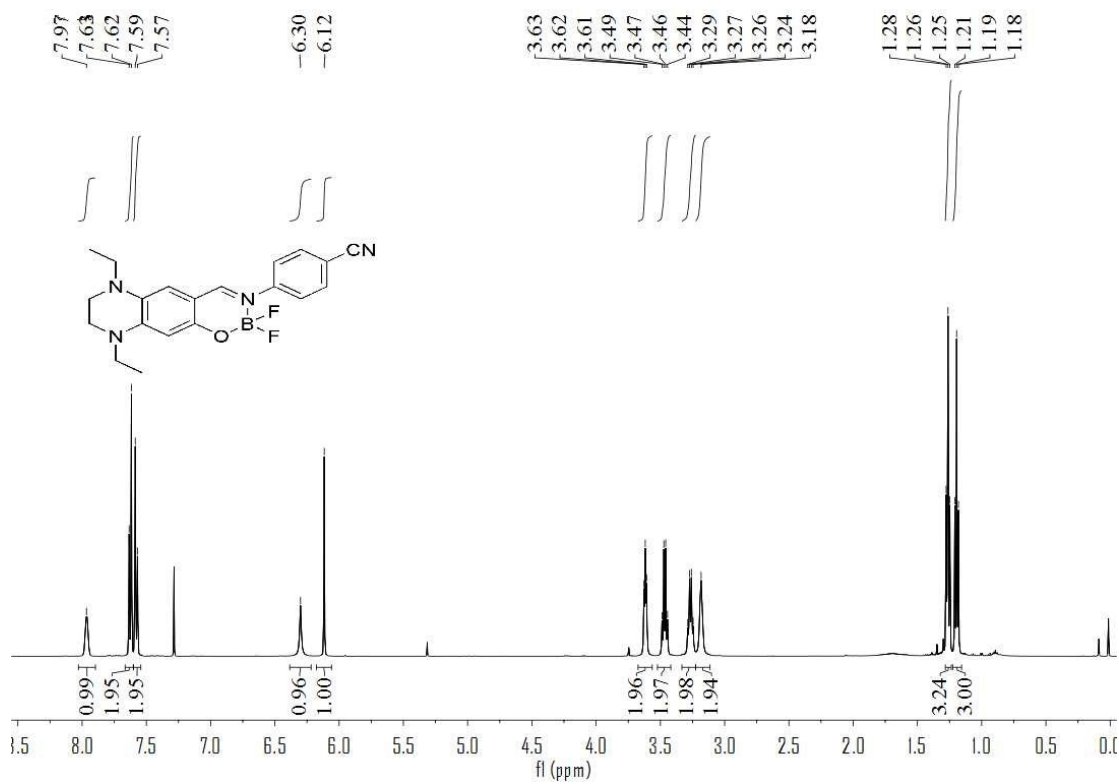


Figure S51. ^1H NMR spectrum of **TQ-DFOB-CN** in CDCl_3 .

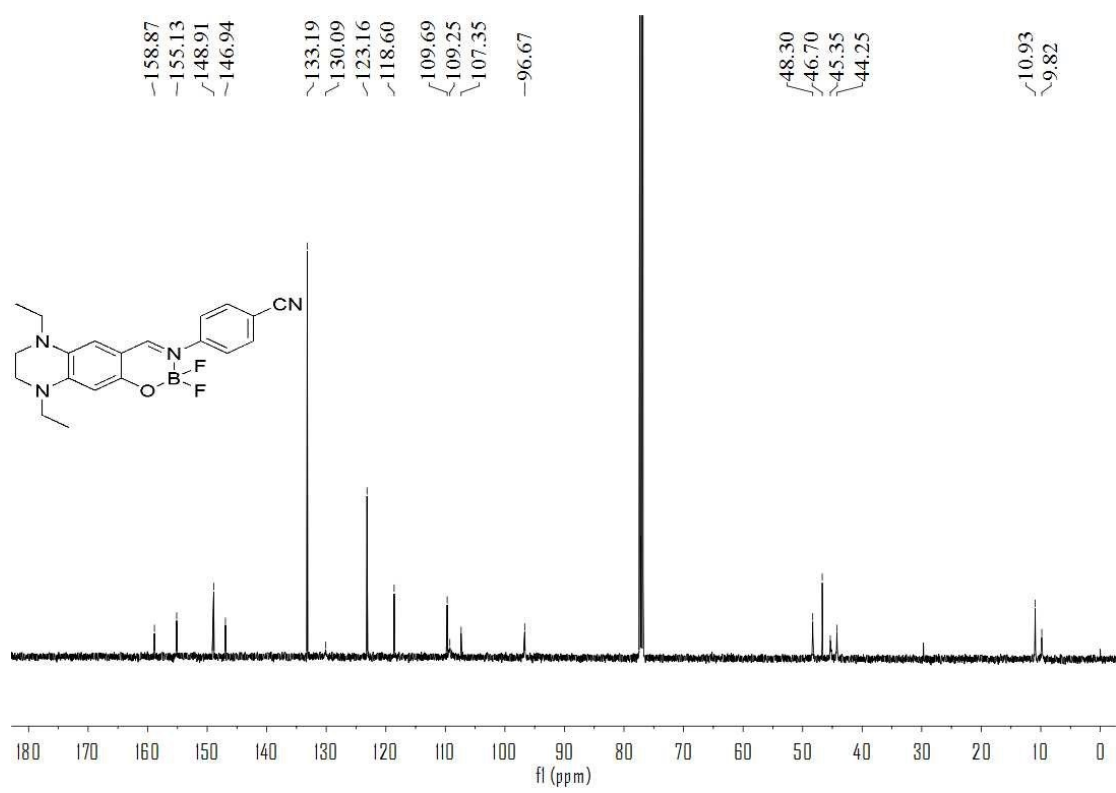


Figure S52. ^{13}C NMR spectrum of TQ-DFOB-CN in CDCl_3 .

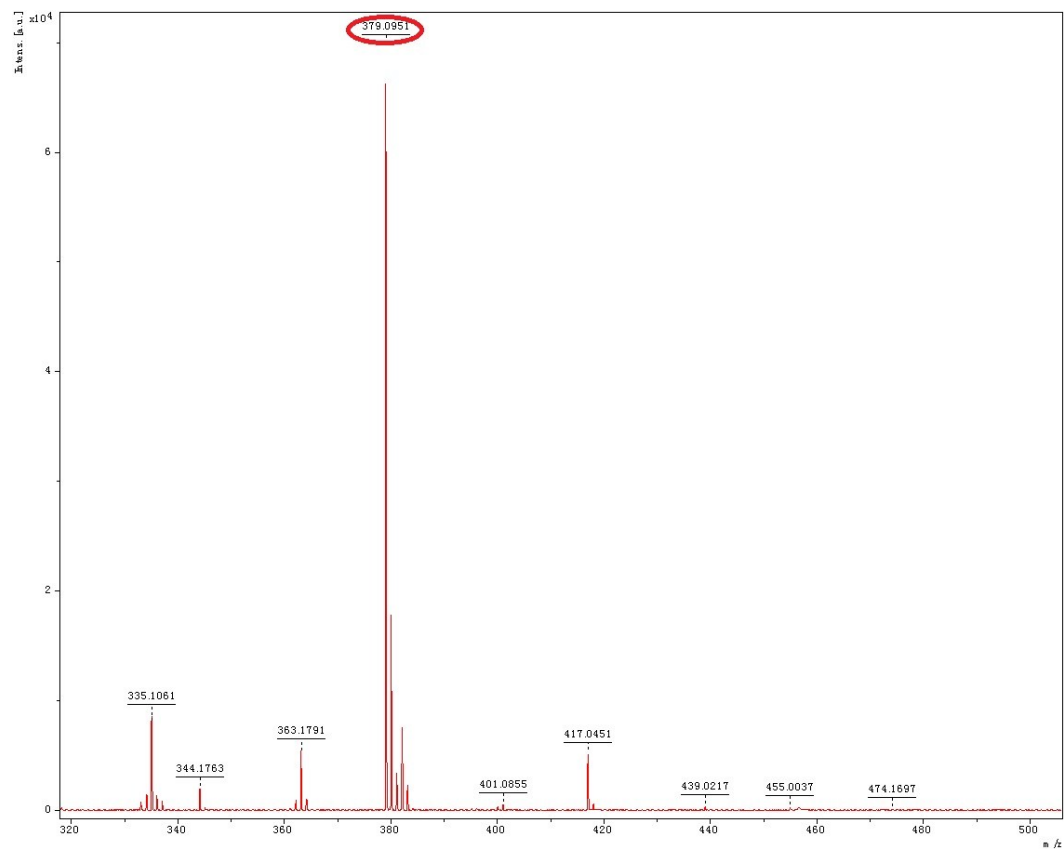


Figure S53. HRMS spectrum of TQ-DFOB-CN.

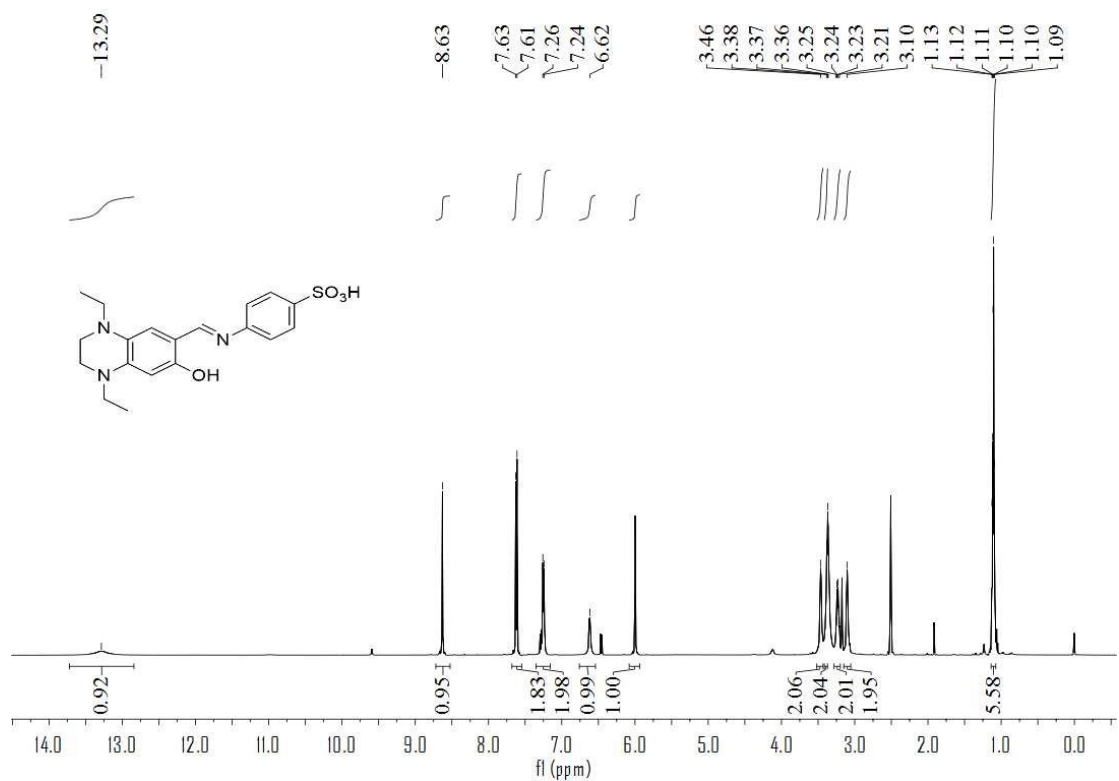


Figure S54. ^1H NMR spectrum of **7** in $\text{DMSO}-d_6$.

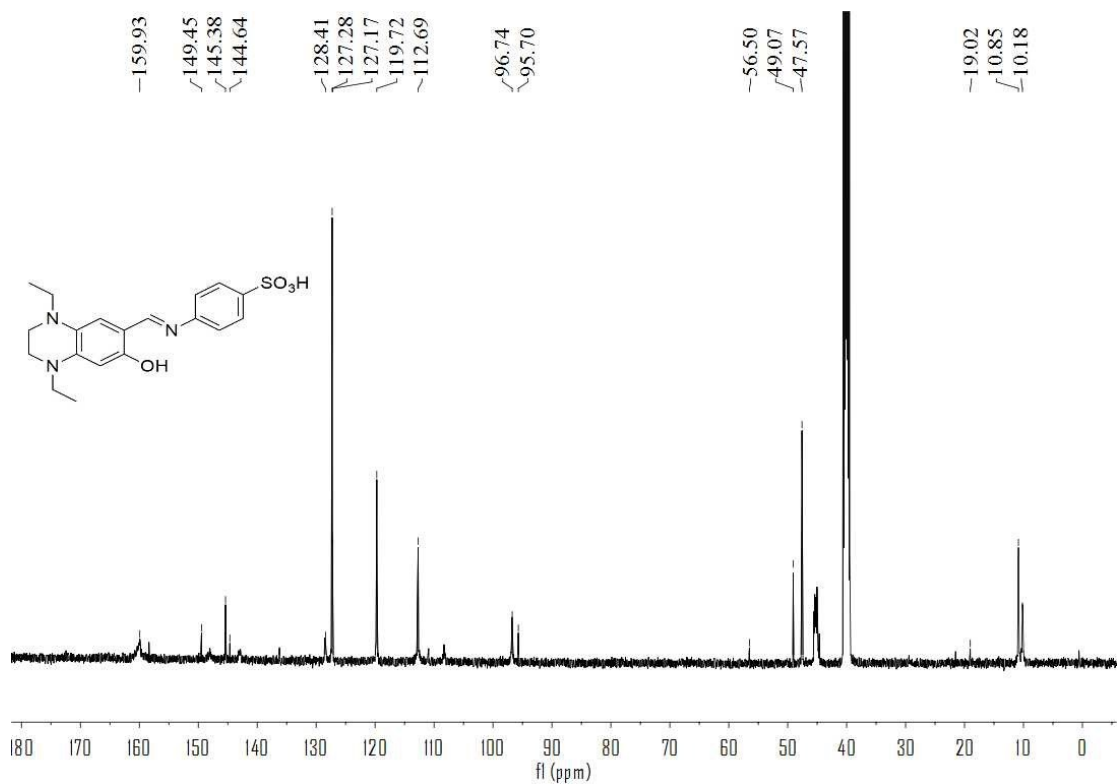


Figure S55. ^{13}C NMR spectrum of **7** in $\text{DMSO}-d_6$.

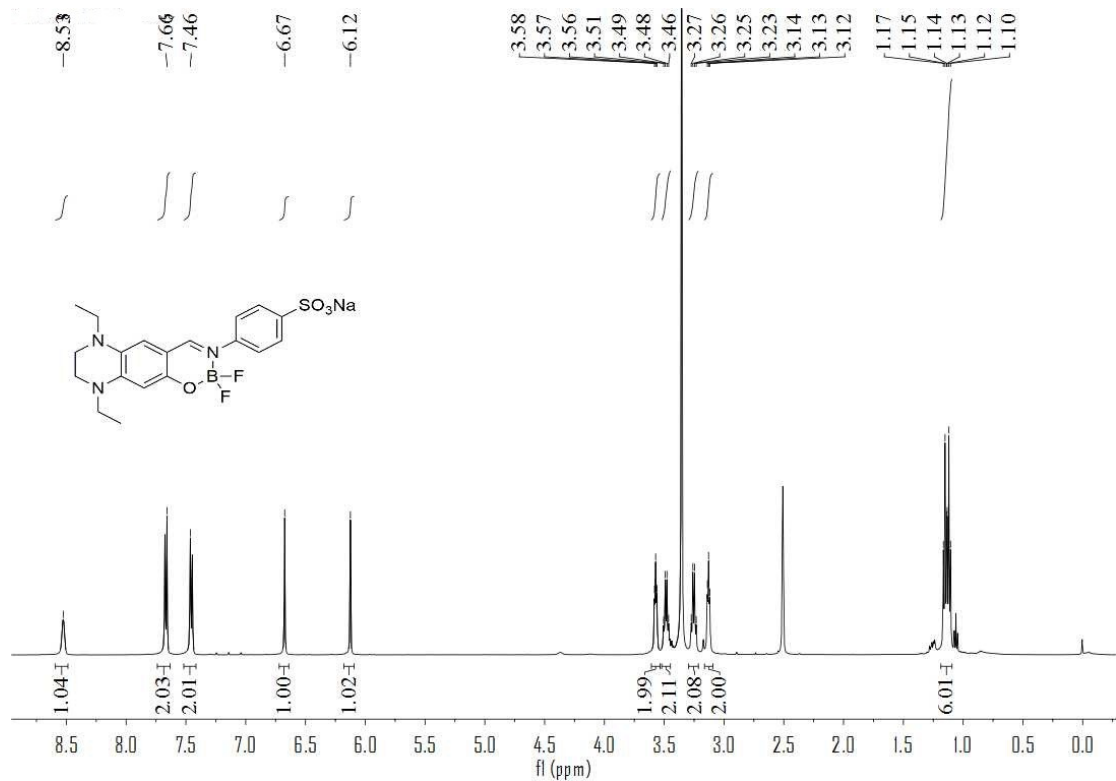


Figure S56. ^1H NMR spectrum of TQ-DFOB- SO_3H in $\text{DMSO}-d_6$.

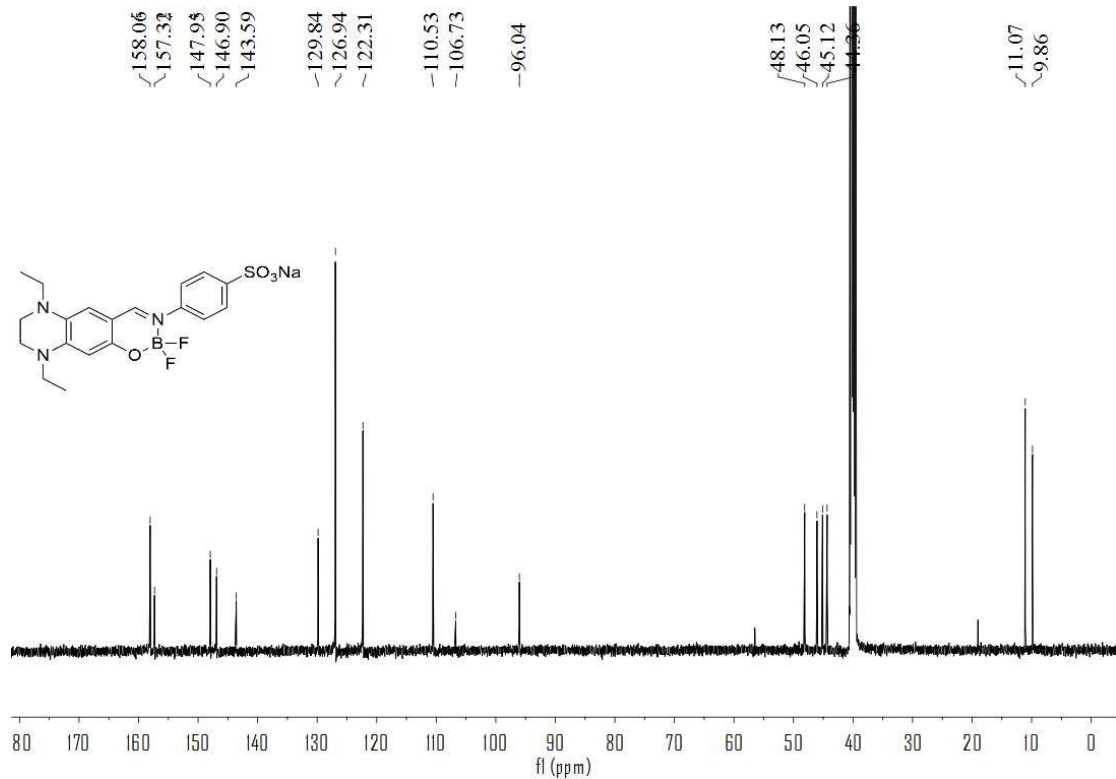


Figure S57. ^{13}C NMR spectrum of TQ-DFOB- SO_3H in $\text{DMSO}-d_6$.

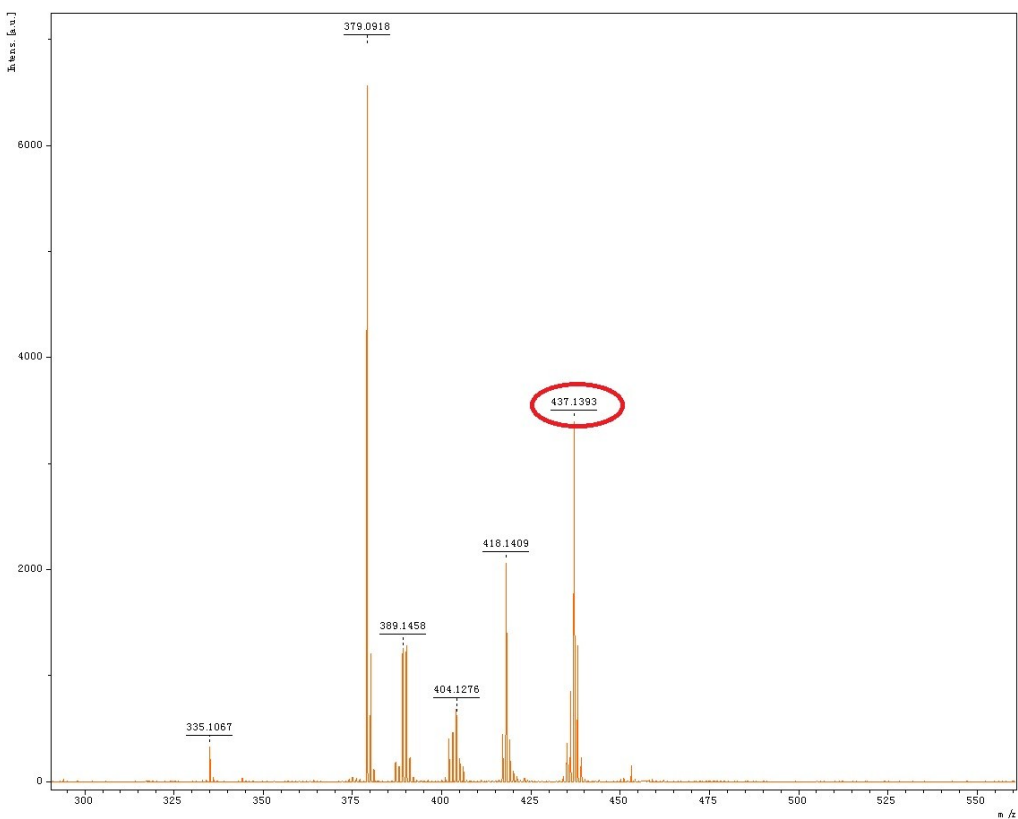
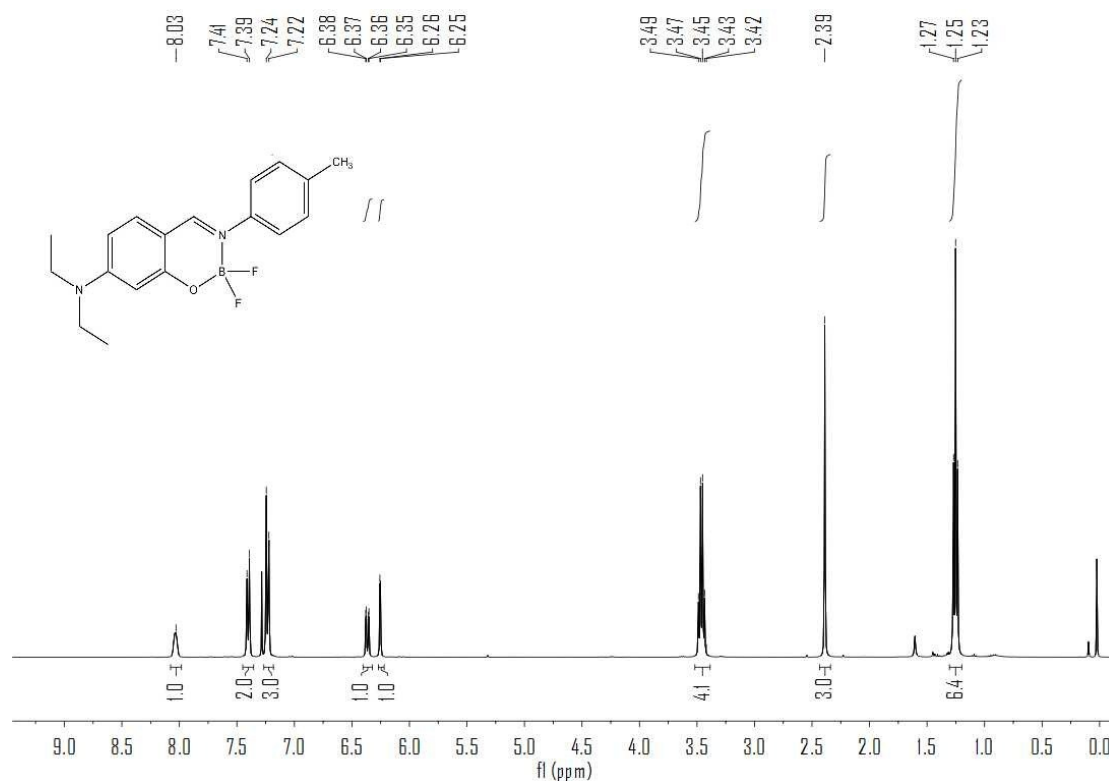


Figure S58. HRMS spectrum of **TQ-DFOB-SO₃H**.



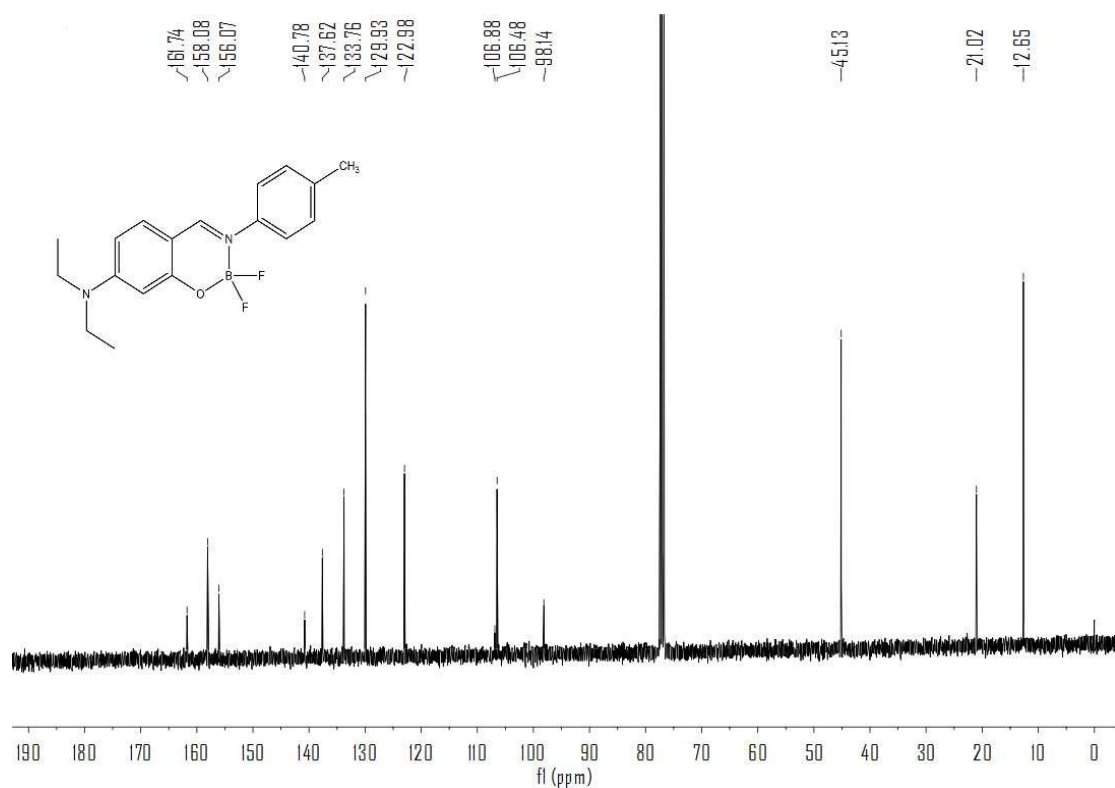


Figure S60. ^{13}C NMR spectrum of **DE-DFOB-Me** in CDCl_3 .

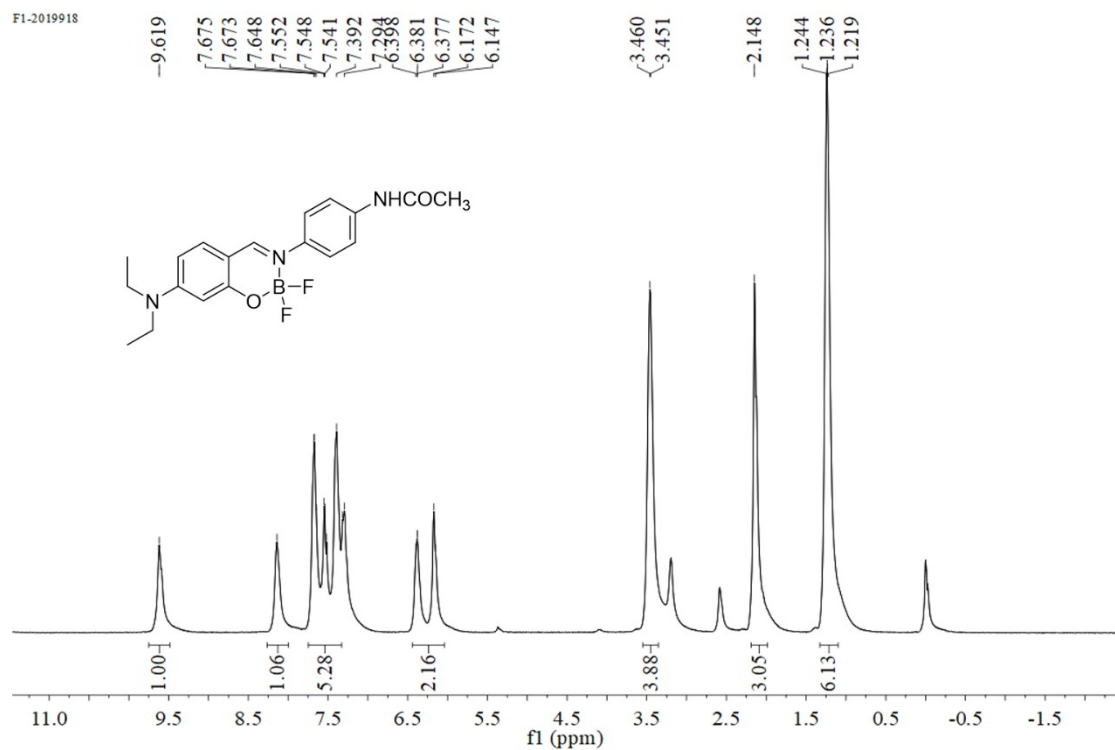


Figure S61. ^1H NMR spectrum of **DE-DFOB-NHCOMe** in CDCl_3 .

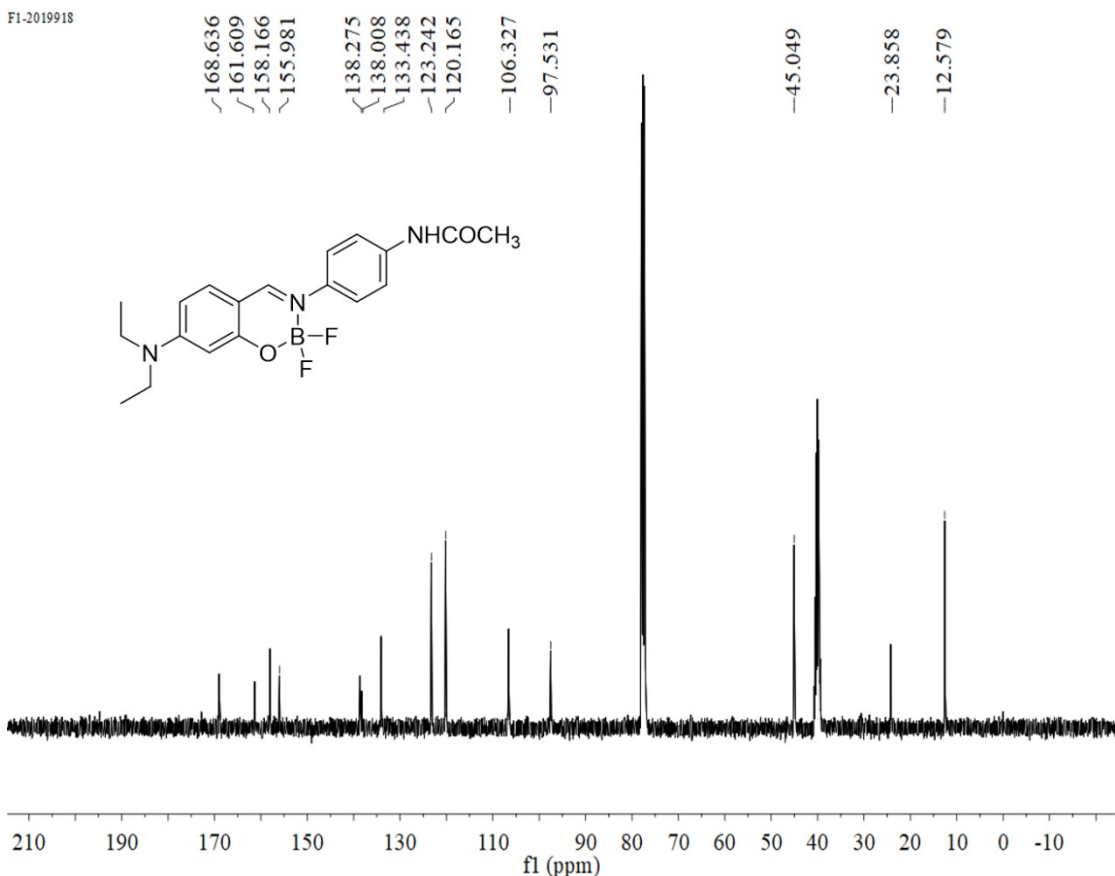


Figure S62. ^{13}C NMR spectrum of **DE-DFOB-NHCOMe** in CDCl_3 .

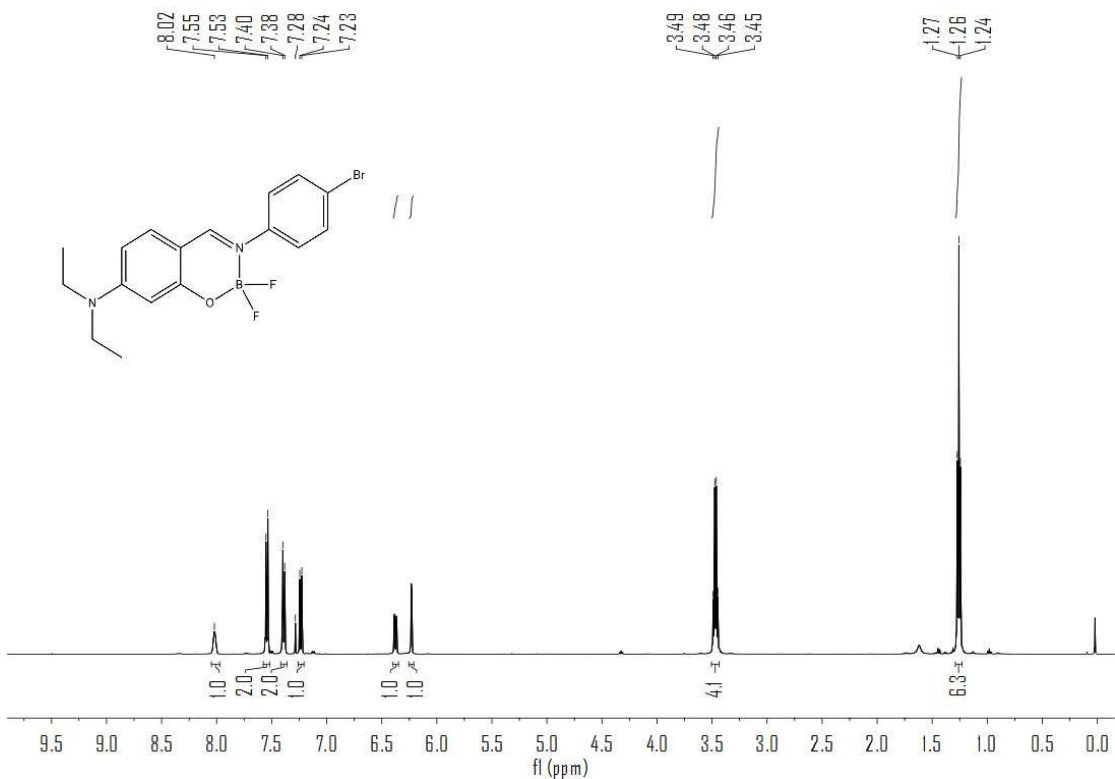


Figure S63. ^1H NMR spectrum of **DE-DFOB-Br** in CDCl_3 .

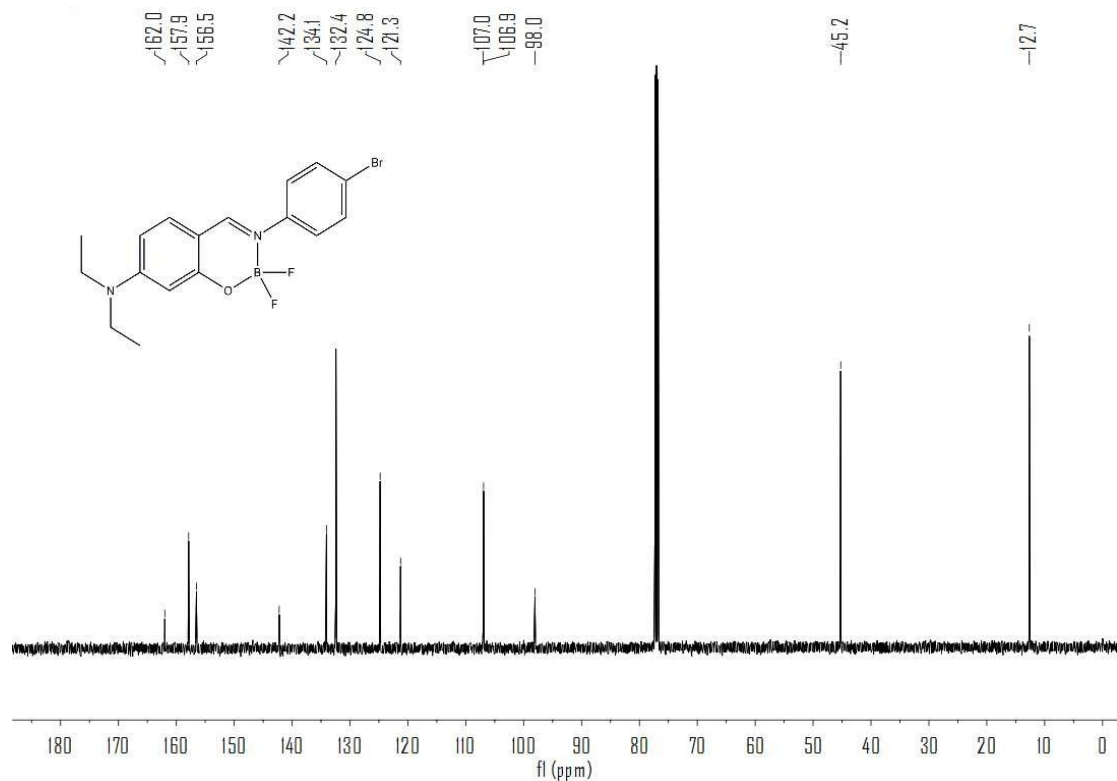


Figure S64. ^{13}C NMR spectrum of **DE-DFOB-Br** in CDCl_3 .

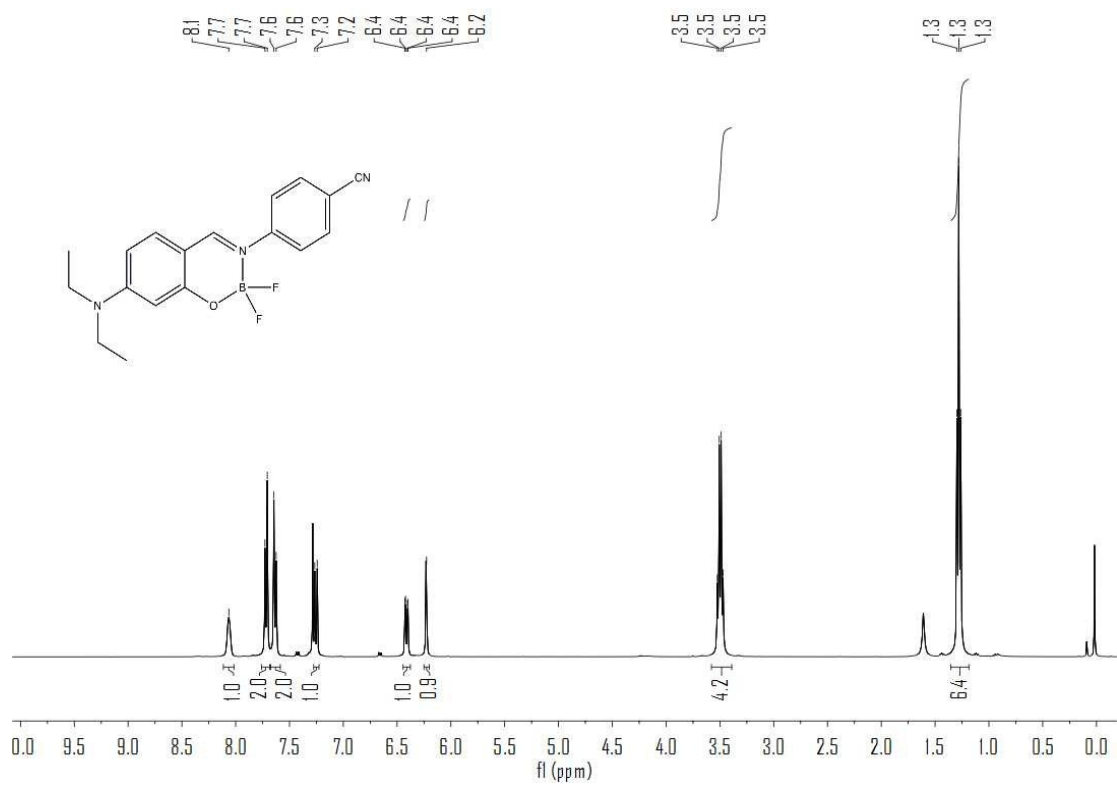


Figure S65. ^1H NMR spectrum of **DE-DFOB-CN** in CDCl_3 .

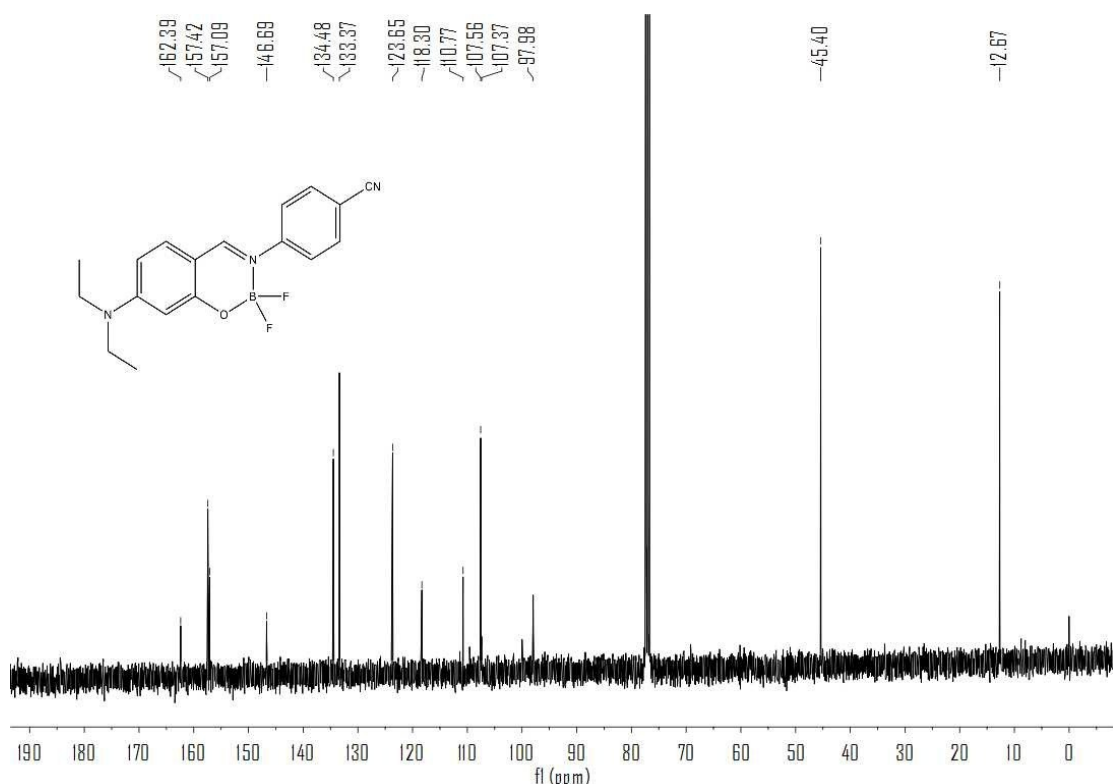


Figure S66. ^{13}C NMR spectrum of **DE-DFOB-CN** in CDCl_3 .

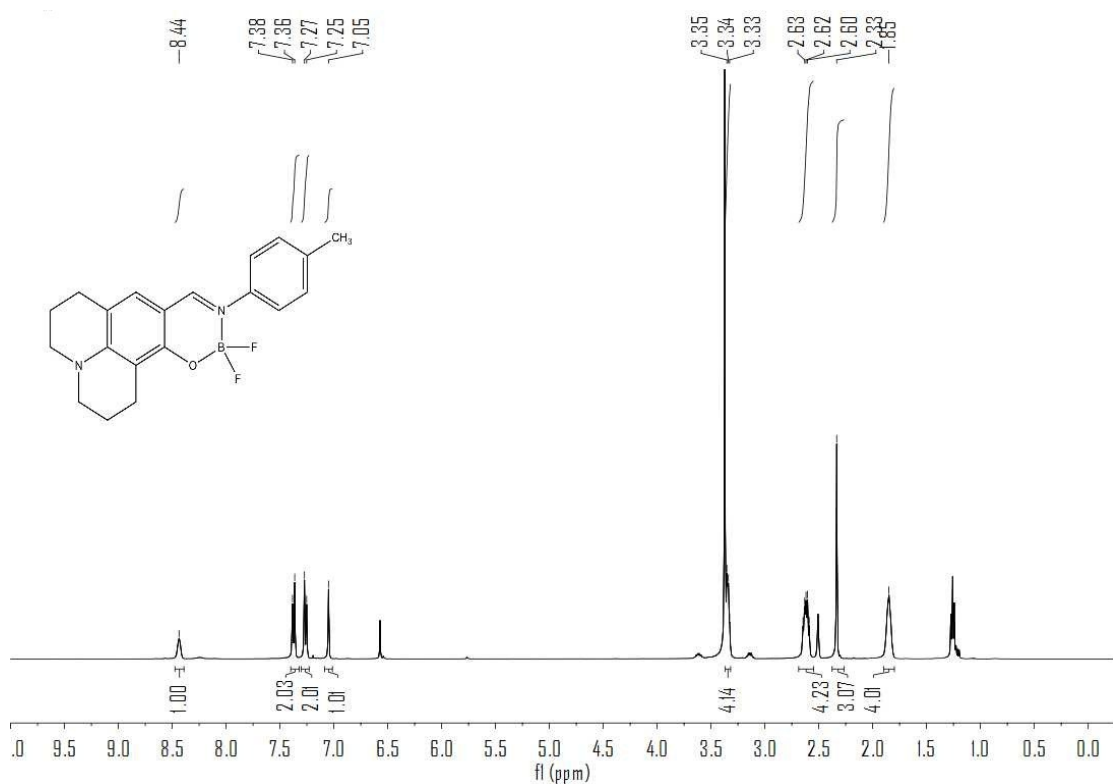


Figure S67. ^1H NMR spectrum of **Julo-DFOB-Me** in DMSO- d_6 .

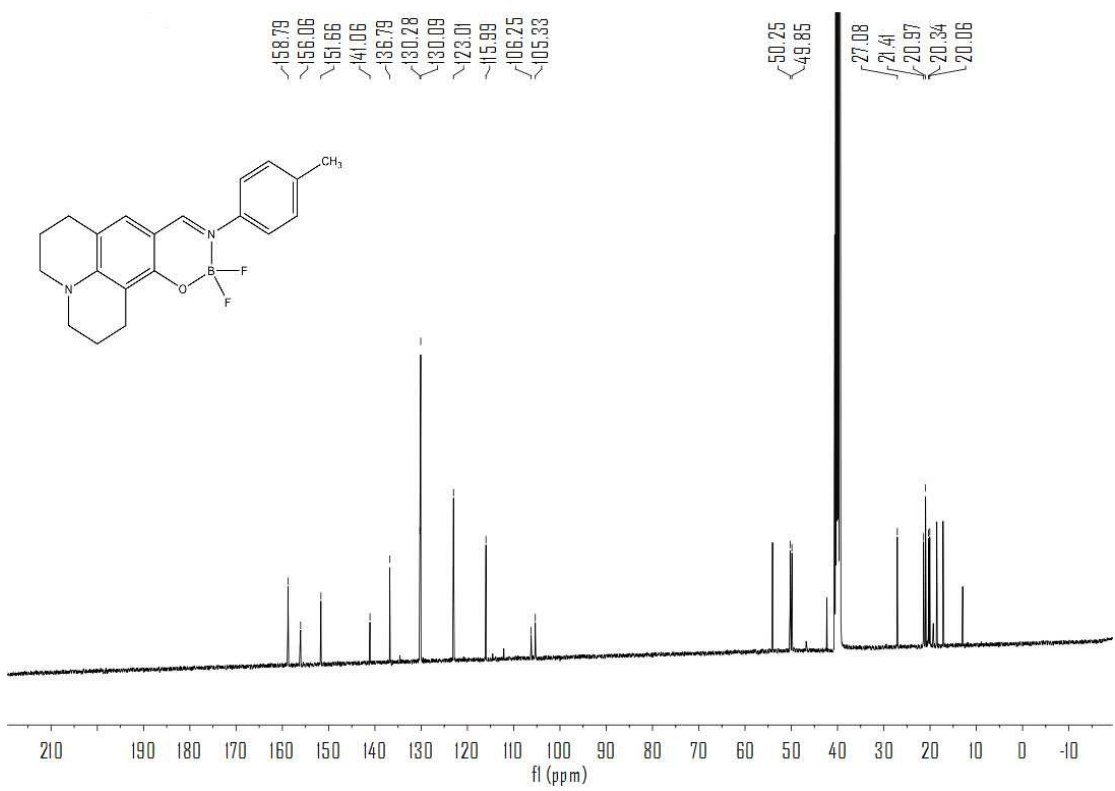


Figure S68. ^{13}C NMR spectrum of Julo-DFOB-Me in $\text{DMSO}-d_6$.